UNCLASSIFIED

AD NUMBER

ADB282244

NEW LIMITATION CHANGE

TO

Approved for public release, distribution unlimited

FROM

Distribution authorized to U.S. Gov't. agencies only; Proprietary Information; Sep 2001. Other requests shall be referred to US Army Medical Research and Materiel Command, 504 Scott Street, Fort Detrick, MD 21702

AUTHORITY

USAMRMC ltr, 26 Nov 2002

THIS PAGE IS UNCLASSIFIED

AD_____

Award Number: DAMD17-99-1-9004

TITLE: A Unifying Theory of Prostate Cancer

PRINCIPAL INVESTIGATOR: Donna Peehl, Ph.D.

CONTRACTING ORGANIZATION: Stanford University
Stanford, California 94305-5401

REPORT DATE: September 2001

TYPE OF REPORT: Final

PREPARED FOR: U.S. Army Medical Research and Materiel Command
Fort Detrick, Maryland 21702-5012

DISTRIBUTION STATEMENT: Distribution authorized to U.S. Government agencies only (proprietary information, Sep 01). Other requests for this document shall be referred to U.S. Army Medical Research and Materiel Command, 504 Scott Street, Fort Detrick, Maryland 21702-5012.

The views, opinions and/or findings contained in this report are those of the author(s) and should not be construed as an official Department of the Army position, policy or decision unless so designated by other documentation.

20020909 031

NOTICE

USING GOVERNMENT DRAWINGS, SPECIFICATIONS, OR OTHER DATA INCLUDED IN THIS DOCUMENT FOR ANY PURPOSE OTHER THAN GOVERNMENT PROCUREMENT DOES NOT IN ANY WAY OBLIGATE THE U.S. GOVERNMENT. THE FACT THAT THE GOVERNMENT FORMULATED OR SUPPLIED THE DRAWINGS, SPECIFICATIONS, OR OTHER DATA DOES NOT LICENSE THE HOLDER OR ANY OTHER PERSON OR CORPORATION; OR CONVEY ANY RIGHTS OR PERMISSION TO MANUFACTURE, USE, OR SELL ANY PATENTED INVENTION THAT MAY RELATE TO THEM.

LIMITED RIGHTS LEGEND

Award Number: DAMD17-99-1-9004
Organization: Stanford University

Those portions of the technical data contained in this report marked as limited rights data shall not, without the written permission of the above contractor, be (a) released or disclosed outside the government, (b) used by the Government for manufacture or, in the case of computer software documentation, for preparing the same or similar computer software, or (c) used by a party other than the Government, except that the Government may release or disclose technical data to persons outside the Government, or permit the use of technical data by such persons, if (i) such release, disclosure, or use is necessary for emergency repair or overhaul or (ii) is a release or disclosure of technical data (other than detailed manufacturing or process data) to, or use of such data by, a foreign government that is in the interest of the Government and is required for evaluational or informational purposes, provided in either case that such release, disclosure or use is made subject to a prohibition that the person to whom the data is released or disclosed may not further use, release or disclose such data, and the contractor or subcontractor or subcontractor asserting the restriction is notified of such release, disclosure or use. This legend, together with the indications of the portions of this data which are subject to such limitations, shall be included on any reproduction hereof which includes any part of the portions subject to such limitations.

THIS TECHNICAL REPORT HAS BEEN REVIEWED AND IS APPROVED FOR PUBLICATION.

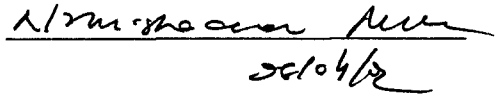

_____

_____

_____

REPORT DOCUMENTATION PAGE

Form Approved
OMB No. 074-0188

Public reporting burden for this collection of information is estimated to average 1 hour per response, including the time for reviewing instructions, searching existing data sources, gathering and maintaining the data needed, and completing and reviewing this collection of information. Send comments regarding this burden estimate or any other aspect of this collection of information, including suggestions for reducing this burden to Washington Headquarters Services, Directorate for Information Operations and Reports, 1215 Jefferson Davis Highway, Suite 1204, Arlington, VA 22202-4302, and to the Office of Management and Budget, Paperwork Reduction Project (0704-0188), Washington, DC 20503

1. AGENCY USE ONLY (Leave blank)	2. REPORT DATE	3. REPORT TYPE AND DATES COVERED
	September 2001	Final (15 Feb 99 - 14 Aug 01)

4. TITLE AND SUBTITLE
A Unifying Theory of Prostate Cancer

5. FUNDING NUMBERS
DAMD17-99-1-9004

6. AUTHOR(S)
Donna Peehl, Ph.D.

7. PERFORMING ORGANIZATION NAME(S) AND ADDRESS(ES)
Stanford University
Stanford, California 94305-5401

E-Mail: dpeehl@stanford.edu

8. PERFORMING ORGANIZATION REPORT NUMBER

9. SPONSORING / MONITORING AGENCY NAME(S) AND ADDRESS(ES)
U.S. Army Medical Research and Materiel Command
Fort Detrick, Maryland 21702-5012

10. SPONSORING / MONITORING AGENCY REPORT NUMBER

11. SUPPLEMENTARY NOTES

12a. DISTRIBUTION / AVAILABILITY STATEMENT
Distribution authorized to U.S. Government agencies only (proprietary information, Sep 01). Other requests for this document shall be referred to U.S. Army Medical Research and Materiel Command, 504 Scott Street, Fort Detrick, Maryland 21702-5012.

12b. DISTRIBUTION CODE

13. ABSTRACT *(Maximum 200 Words)*

The goal of this project was to investigate the biological behavior of p53 in primary cultures of human prostatic epithelial cells. Previous studies had revealed that p53 was not activated in these cells by agents that cause double-stranded DNA breaks, such as gamma-irradiation, suggesting that p53, albeit wild-type, was dysfunctional. Since p53 is a key tumor suppressor gene that protects the genome from damage, we hypothesized that dysfunctional p53 is relevant to the high incidence of cancer in the prostate. In order to determine whether p53 was irreversibly nonfunctional in prostate cells, we inhibited RNA transcription or nuclear protein export. In response, p53 protein accumulated and was functional, as evidenced by transactivation of downstream targets and cell cycle arrest. Therefore, mechanisms responsible for upregulation and activation of p53 are intact in prostatic epithelial cells. We also determined that p53 was activated by ultraviolet radiation, which creates bulky DNA adducts, and by triptolide, a drug whose mechanism of action has not yet been elucidated. These findings show that certain pathways of p53 activation are functional in prostate cells, and that the defect lies in a specific inability of the cells to protect themselves from double-stranded DNA breaks. This finding is relevant to the initiation, progression and therapy of prostate cancer.

14. SUBJECT TERMS	15. NUMBER OF PAGES
prostate cancer. P53, carcinogenesis	136
	16. PRICE CODE

17. SECURITY CLASSIFICATION OF REPORT	18. SECURITY CLASSIFICATION OF THIS PAGE	19. SECURITY CLASSIFICATION OF ABSTRACT	20. LIMITATION OF ABSTRACT
Unclassified	Unclassified	Unclassified	Unlimited

Table of Contents

INTRODUCTION

Prostate cancer is characterized by a number of unique features, including high incidence, multifocal origin, zonal specificity, limited response to androgen ablation, and resistance to chemotherapy (Abbas and Scardino, 1997). Our goal is to determine the biological basis of these properties. Preliminary studies led us to propose that at least some of these characteristics are the result of dysregulated, albeit wild-type, p53 in normal human prostatic epithelial cells and in a majority of prostatic adenocarcinomas. We had noted that p53 was not induced in primary cultures of prostatic epithelial cells in response to DNA-damaging agents such as γ-irradiation (Girinsky et al., 1995). The p53 protein is known to be a key regulator of cell cycle arrest and/or apoptosis (Wiman, 1997). Therefore, in the absence of p53 induction, cell cycle arrest or apoptosis did not occur and DNA damage presumably accumulated. Induction of growth arrest or apoptosis by p53 in response to DNA damage is considered to contribute to the ability of p53 to function as a tumor suppressor gene. Therefore, dysregulated p53 would lead to genetic instability. Our proposed research addressesd two questions: what is the basis of dysregulated p53 in human prostatic epithelial cells, and, can p53-mediated cell arrest or apoptosis be restored in these cells?

BODY

Our first designated task was to determine the biological consequences of lack of p53-mediated, G1-cell cycle arrest in prostatic epithelial cells. As part of this task, one of our first projects was to expand our studies to include a series of epithelial cell strains derived from the normal central zone of the adult prostate. Our previous studies had focused primarily on normal epithelial cells derived from the peripheral zone of the prostate. The peripheral zone is the site of origin of the majority of cancers that occur in the prostate, whereas the occurrence of cancers in the central zone is quite rare (McNeal, 1969).

In our prior work, we had reported that none of the cell strains derived from the normal peripheral zones of 7 separate individuals had showed significant induction of p53 in response to DNA-damaging agents (γ-irradiation, hypoxia, or chemicals) (Girinsky et al., 1995). Our initial studies with cell strains derived from the normal central zone were limited, but we had observed that 2 of the 5 cell strains of this type appeared to show some induction of p53 in response to DNA-damaging agents (Girinsky et al., 1995). We wondered whether central zone cells, unlike peripheral zone cells, retained functional p53; was this the basis for the relative resistance of the central zone to the development of cancer?

We established 8 additional primary cultures of epithelial cells derived from the central zone and exposed them to 6 Gy of γ-irradiation. Levels of p53 protein after irradiation were evaluated by immunoblot analysis. None of the cell strains derived from the central zone showed an induction of p53 protein in response to γ-irradiation. These results, then, were similar to those that we had previously found with cells derived from the peripheral zone. We concluded that p53 was

dysfunctional in the central zone as well as in the peripheral zone, and that differences in p53 activity therefore could not explain the differential susceptibilities of the two zones to the development of cancer. However, it is worth noting that prostatic intraepithelial neoplasia (PIN), considered to be the premalignant precursor of invasive cancer in the prostate, occurs at equivalent frequencies in the central and peripheral zones (McNeal and Bostwick, 1986). Lack of p53 activity might therefore relate to the high rate of PIN in both the central and peripheral zones of the prostate, while other unknown factors limit progression of PIN to invasive cancer in the central but not the peripheral zone.

Another element of task 1 was to investigate the effects of cellular differentiation on p53 induction. Other investigators have reported that the differentiated status of several cell types, such as keratinocytes, affects levels of p53 and ability to repair DNA damage (Li et al., 1997). There are three recognized subtypes of cells in the prostatic epithelium: basal cells, secretory cells and neuroendocrine cells. Each of these subtypes is characterized by expression of a particular pattern of markers. Examples include expression of keratin 5 in the basal cells, keratin 18 and prostate-specific antigen (PSA) in secretory cells, and chromogranin A in neuroendocrine cells. The exact relationship of these cells is not worked out, but the current popular view is that basal cells include the progenitor (stem?) cells that give rise to either secretory or neuroendocrine cells by alternate pathways of differentiation, presumably triggered by different stimuli (Bonkhoff et al., 1994).

Methods to isolate, promote or maintain these different lineages of prostatic cells in vitro are not well worked out. Specific factors or conditions to maintain basal, secretory or neuroendocrine cell populations are not clearly identified, and markers to distinguish the lineages have not been plentiful. However, we believe that our primary cultures of normal prostatic cells most closely resemble basal cells when grown in our standard culture conditions. Treatment with retinoic acid promotes a phenotype that more closely resembles secretory epithelial cells (Peehl et al., 1993).

Accordingly, we treated primary cultures of prostatic epithelial cells with factors that we believe may change the differentiated status of the cells. These included the deletion of epidermal growth factor (EGF) from the culture medium, or the addition of retinoic acid or vitamin D. Deletion of EGF stops proliferation and cellular migration, and causes the cells to form acinar-like arrangements in two-dimensions. Retinoic acid and vitamin D also inhibit growth and induce morphological changes (Peehl et al., 1993 and 1994) . Previously, we reported that treatment with retinoic acid increased the expression of keratins 8 and 18 in these cells, giving a hint of the induction of a secretory-like phenotype. We maintained cells for three days with retinoic acid or vitamin D, or without EGF, then exposed the cells to 6 Gy of γ-irradiation. Relative levels of p53 protein were measured by immunoblot analysis after irradiation. Treatment of cells with retinoic acid or vitamin D alone, or deletion of EGF, did not induce p53. Irradiation of cells treated with either retinoic acid or vitamin D also did not increase levels of p53 protein. However, cells maintained without EGF showed greater accumulation of p53 protein after irradiation than cells in medium with EGF. This is a potentially important finding that we will pursue in future studies. Since anti-EGF therapy is being tested in clinical trials against prostate

and other cancers, the relationship of EGF and p53 is very relevant to developing more effective protocols to treat prostate cancer.

Other studies that we performed were related to the goal of task 1 to determine the biological consequences of lack of p53-mediated, G1-cell cycle checkpoint in prostatic epithelial cells. We suggested that, if prostatic cancer cells are incapable of undergoing p53-mediated cell cycle arrest or apoptosis, then drugs that would be expected to be effective against prostate cancer would be those that induce apoptosis via p53-independent mechanisms. Our studies so far bear this out. We tested a number of agents that have been reported to induce p53-mediated apoptosis in certain other types of cells, and found that none induced p53 or apoptosis. In contrast, the compound brefeldin A (BFA), reported to induce apoptosis in cells by p53-independent pathways (Shao et al., 1996), was a potent inducer of apoptosis in primary cultures of prostatic cancer cells (Wallen et al., 2000, see appendix). Development of this or related compounds, or identification of other agents that induce p53-independent death, might be anticipated to be quite effective for chemotherapy of prostate cancer.

Of interest are our findings with another compound, triptolide, that was reported to induce p53-independent apoptosis in various types of cancer cells. Triptolide is extracted from a Chinese herb that has been used to treat arthritis for centruries; recently, activities consistent with anti-tumor activity have been noted. Since we believed that drugs with the ability to induce p53-independent apoptosis would be effective against prostate cancer cells, we tested triptolide on primary cultures of normal and malignant prostate cells (Kiviharju et al., submitted for publication, see appendix). Indeed, triptolide induced apoptosis in these cells. Surprisingly, however, induction of apoptosis was proceeded by a robust upregulation of p53 protein. Downstream gene targets of p53 were also induced, suggesting that p53 was functional. Thus we identified an functional signaling pathway leading not only to p53 induction but to p53-mediated apoptosis as well. The molecular basis of triptolide's action remains to be elucidated, but we suggest that triptolide may be a promising candidate for therapy of prostate cancer.

While triptolide at concentrations higher than 15 μg/ml induced apoptosis, lower concentrations inhibited growth but did not induce apoptosis. These lower concentrations of triptolide also did not upregulate p53. We hypothesized that triptolide might inhibit growth by inducing premature senescence of prostate cells. We had previously showed that the marker senescence-associated β-galactosidase corresponds with the development of senescence in serially-passaged cultures of prostatic epithelial cells (Choi et al., 2000). Then, in collaboration with the laboratory of Dr. Joyce Slingerland, we examined the molecular pathways involved in the development of the senescent phenotype (Sandhu et al., 2000, see appendix). As has been found in other types of cells, $p16^{INK4A}$ was increased in conjunction with senescence. Interestingly, neither p53 nor p21 increased in senescent prostatic epithelial cells, in contrast to the increase in these proteins seen in senescent fibroblasts. Here, then, is yet another instance of the lack of participation of p53 in a critical growth-regulatory process in prostatic epithelial cells. When we examined the growth-inhibited phenotype of prostate cells induced by low concentrations of triptolide, we indeed found that triptolide induced premature senescence by a p53-independent mechanism. We

suggest that triptolide should be further investigated as a chemopreventive agent against prostate cancer based on its activities on primary cultures.

Task 2 of our proposed work was to attempt to restore p53 activity and the G1-checkpoint to prostatic epithelial cells. We have achieved this goal by using three diverse approaches:

Treatment with inhibitors of RNA transcription

The first approach involved treating prostatic epithelial cells with actinomycin D, a well-known inhibitor of RNA transcription. The rational was to inhibit the transcription of the mdm2 gene, whose product binds the p53 protein and targets p53 for ubiquitin-mediated degradation (Prives, 1998). This process is considered to be the key mechanism causing the rapid turnover of the p53 protein, keeping its levels low in the absence of stress. Whereas p53 levels are mainly regulated by this post-transcriptional mechanism, levels of mdm2 are mainly regulated at the transcriptional level (An et al., 1998).

We found that p53 protein levels were indeed upregulated by exposure of prostatic epithelial cells to actinomycin D (Lecane et al., in preparation, see appendix). This finding demonstrated for the first time that p53 was capable of being upregulated in prostatic epithelial cells. However, the nature of this approach did not allow us to determine whether p53 was capable of functioning after upregulation. Because p53 is a transcriptional factor, the presence of actinomycin D blocked the transcriptional activation of typical targets of p53 such as p21. Therefore, we sought other approaches that might upregulate p53 and also permit us to investigate its functions and biological effects.

Treatment with leptomycin B

To that end, we tested the effects of leptomycin B (LMB), an anti-fungal agent that has been found to be a unique inhibitor of the cell cycle of mammalian cells. Recently, LMB was found to inhibit specific protein and RNA export from the nucleus to the cytoplasm. LMB achieves this by interacting directly with CRM1, a receptor that mediates the export from the nucleus of viral and cellular proteins containing leucine-rich nuclear export signals. Lain et al. (1999) found that addition of LMB to cultures of normal human fibroblasts led to accumulation of p53 and p53-responsive genes in the nuclei of these cells. A nuclear export signal has been described in the mdm2 gene as well as in the p53 gene, suggesting that export of p53 from the nucleus is mediated by the CRM1 exportin. Presumably, LMB upregulates nuclear p53 protein by preventing mdm2- mediated transport of p53 to the cytoplasm for ubiquitin-mediated degradation.

We treated prostatic epithelial cells with LMB for 4 hours and measured cellular levels of p53 protein by immunoblot analysis (Lecane et al., in preparation, see appendix). In untreated cells or cells exposed to γ-irradiation, p53 protein levels remained low. In contrast, p53 levels were significantly elevated by treatment with LMB at 20 nM, or the proteasome inhibitor MG132 at

25 μM. By immunocytochemistry, we also demonstrated the nuclear accumulation of p53 in the presence of LMB.

In additional studies, we found that short-term exposure (2 to 4 hours) of cells to LMB induced long-term elevation of p53. Studies were performed to test the biological effects of this long-term elevation of p53 (Lecane et al., in preparation, see appendix). Cell-cycle analysis by flow cytometry demonstrated a G1-arrest after treatment with LMB. Results from growth assays further demonstrated that exposure to LMB caused proliferative arrest. We treated prostatic epithelial cells for 4 hours with LMB (at which time p53 was determined to be upregulated), then washed away the LMB and tested the ability of the cells to proliferate in clonal growth assays. Treatment with as little as 0.25 ng/ml of LMB for 4 hours resulted in a 40% decrease in clonal growth ability, and treatment with 0.5 ng/ml of LMB completely abrogated subsequent proliferative potential. Additional experiments indicated that the effects of LMB were irreversible. When cells were treated with 0.25 ng/ml of LMB for 4 hours, then were permitted to recover for 24 hours in LMB-free medium before testing for proliferative potential, clonal growth was reduced even further.

LMB, then, like actinomycin D, caused an accumulation of cellular p53 in prostatic epithelial cells. Based on the mechanism of action of LMB, we expected that p53 accumulation in response to LMB would occur as a result of an increase in the half-life of the p53 protein. This indeed was the case. In untreated prostatic epithelial cells, the half-life of p53 was between 30 and 60 minutes. In LMB-treated cells, the half-life was 60 to 120 minutes.

Use of LMB, rather than the transcriptional inhibitors, gave us the opportunity to investigate the functional effects of p53 upregulation. We examined the effects of upregulation of p53 on the p21 and mdm2 genes, well-known targets of p53's transcriptional activation. Immunoblot analysis revealed that p21 and mdm2 were upregulated in correspondence with an increase in p53 levels. This suggested that upregulation of p53 by LMB resulted in active p53, as indicated by an increase in p53's targets, p21 and mdm2.

In other types of cells, upregulation of p53 and p21 result in cell cycle arrest and/or apoptosis. Our experiments to evaluate these possibilities in primary cultures of prostatic epithelial cells suggest that exposure to LMB and subsequent upregulation of p53 and p21 are not sufficient to induce apoptosis. However, activation of p53 by LMB did result in apoptosis of the prostate cancer cell line, LNCaP (Lecane et al., in preparation, see appendix).

Treatment with ultraviolet irradiation

Ultraviolet irradiation induces p53 in certain cells that are defective in γ-irradiation –induction of p53. We exposed normal prostatic epithelial cells to increasing doses of ultraviolet B (UVB)-irradiation and evaluated p53 levels by immunoblot. It was evident that a robust induction of p53 occurred, with an increase seen at 3 hours and peaking at 8 hours. These same cells showed no induction of p53 in response to γ-irradiation. Furthermore, induction of p53 was

accompanied by upregulation of p21 and mdm2, two targets of p53 transcriptional activation. Thus, the signaling pathway leading to p53 activation in response to DNA damage (bulky adducts) caused by UVB radiation is functional in prostate cells.

Regulation of p53

These results, then, provide us with a key to dissect out the basis for the dysregulation of p53 in prostatic epithelial cells. Both UVB and γ-irradiation induce DNA damage, yet only UVB provides a signal that stabilizes and activates p53 in prostatic epithelial cells. What is the basis of this differential effect? We hypothesize that post-translational changes that modify and stabilize p53 do not occur effectively following γ-irradiation or after exposure to drugs that cause double-stranded DNA breaks. The molecules involved in these post-translational modifications of p53 differ between the pathway triggered by γ-irradiation versus UVB irradiation. In particular, ATM and Chk2 are implicated in phosphorylation of p53 following γ-irradiation, while ATR and Chk1 are activated following UVB irradiation. These genes will be evaluated in future studies of p53 activity in human prostatic epithelial cells.

KEY RESEARCH ACCOMPLISHMENTS

* determined that p53 protein in normal epithelial cells derived from the central zone of the prostate is not induced in response to DNA damage caused by γ-irradiation

* determined that treatment of prostatic epithelial cells with putative differentiation agents (retinoic acid or vitamin D) did not themselves induce p53 protein.

* noted in preliminary studies that absence of EGF signaling possibly sensitized prostate cells to induction of p53 by γ-irradiation

* tested a number of drugs or other compounds and found that only one, brefeldin A, which acts via p53-independent mechanisms, induced apoptosis in prostatic epithelial cells

* confirmed that senescence-associated β-galactosidase and increased levels of p16, but not p53 or p21, are markers of senescence in prostatic epithelial cells

* showed that p53 protein in prostatic epithelial cells was inducible by treatment with an inhibitor of RNA transcription (actinomycin D)

* demonstrated that treatment of prostatic epithelial cells with leptomycin B, an agent that blocks export of proteins from the nucleus to the cytoplasm, leads to upregulation of p53 protein

* found that p53 protein upregulated by leptomycin B in prostatic epithelial cells was active, as demonstrated by an increase in transactivation targets of p53 (mdm2 and p21)

* observed that induction of active p53 by leptomycin B led to G1-cell cycle arrest and irreversible growth inhibition

* discovered that DNA damage caused by ultraviolet B-irradiation, in contrast to that caused by γ-irradiation, induced p53 in prostatic epithelial cells

* identified a drug, triptolide, that activates a functional p53 pathway that culminates in apoptosis of prostatic epithelial cells

REPORTABLE OUTCOMES

Manuscripts

Sandhu, C., Peehl, D.M. and Slingerland, J. $p16^{INK4A}$ mediates Cdk4/6 inhibition in senescent prostatic epithelial cells. Cancer Research 60:2616-2622, 2000.

Wallen, E., Sellers, R.G. and Peehl, D.M. Brefeldin A induces p53-independent apoptosis in primary cultures of human prostatic cancer cells. Journal of Urology 164:836-841, 2000.

Armstrong, J.S., Steinauer, K.K., Hornung, B., Irish, J.M., Lecane, P., Birrell, G., Peehl, D.M. and Knox, S.J. Role of glutathione depletion and reactive species generation in apoptotic signaling in a human B lymphoma cell line. Cell Death & Differentiation, in press.

Kiviharju, T.M., Lecane, P.S., Sellers, R.G. and Peehl, D.M. Antiproliferative and proapoptotic activity of triptolide on human prostatic epithelial cells. Submitted to European Journal of Cancer.

Lecane, P.S., Hammond, E.M., Kiviharju, T.M., Sellers, R.G., Giaccia, A.J. and Peehl, D.M. Leptomycin B stabilizes and activates p53 in primary prostatic epithelial cells and induces apoptosis in the LNCaP cell line. In preparation.

CONCLUSIONS

DNA damage induced by γ-irradiation and chemicals that cause double-strand DNA breaks does not activate wild-type p53 in primary cultures of normal human prostatic epithelial cells or prostatic cancer cells. This lack of p53 induction, and therefore lack of cell cycle arrest or apoptosis, may lead to genomic instability and the development of cancer.

One of our goals was to determine whether p53 was irreversibly nonfunctional in prostatic epithelial cells. The experiments that we performed during this period have shown that this is not the case. Treatment of cells with inhibitors of RNA transcription resulted in elevated levels of p53 protein. This was presumably due to the inhibition of transcription of mdm2, the protein which regulates the degradation of p53 protein and whose own levels are regulated by transcription. While these experiments showed that p53 protein could be upregulated in prostatic epithelial cells, the question of whether this elevated p53 protein was functional could not be addressed because inhibitors of transcription block the transactivation properties of p53. Therefore, we tested an alternate means of elevating p53 by treating cells with leptomycin B (LMB), an inhibitor of nuclear transport. Since p53 levels are normally kept low by translocation from the nucleus to the cytoplasm for ubiquitin-mediated degradation, inhibition of nuclear transport should elevate levels of p53 protein. We showed that this indeed occurred in prostatic epithelial cells. Furthermore, this p53 protein was active, as shown by a concomitant increase in p21 and mdm2, two of p53's transcriptional targets. LMB-mediated activation of p53 caused arrest in the G1-phase of the cell cycle, and irreversible loss of proliferative potential.

Other agents also activated p53 in prostatic epithelial cells. Triptolide, a compound extracted from a Chinese herb, dramatically upregulated p53 and induced apoptosis. Ultraviolet (UV) irradiation, in contrast to γ-irradiation, also induced p53 that led to growth arrest.

In conclusion, we now know that certain signaling pathways leading to the upregulation of p53 protein and activation are intact in prostatic epithelial cells. These pathways can be exploited for new chemopreventive or therapeutic strategies. The specific p53 dysfunction lies in the inability of the cells to respond to signals generated by agents that cause DNA double-stranded breaks. Such agents are considered to be the most prevalent factors that initiate cancer. Future studies will focus on molecules such as ATM and Chk2 that are mediators of p53 activation in response to double-strand DNA breaks.

REFERENCES

Abbas, F. and P. T. Scardino (1997). "The natural history of clinical prostate carcinoma [editorial; comment]." Cancer **80**: 827-33.

An, W. G., Y. Chuman, et al. (1998). "Inhibitors of transcription, proteasome inhibitors, and DNA-damaging drugs differentially affect feedback of p53 degradation." Exp Cell Res **244**: 54-60.

Choi, J., I. Shendrik, et al. (2000). "The expression of senescence-associated b-galactosidase (SA b-gal) in enlarged prostates from men with benign prostatic hypertrophy." Urology **56**: 160-66.

Girinsky, T., C. Koumenis, et al. (1995). "Attenuated response of p53 and p21 in primary cultures of human prostatic epithelial cells exposed to DNA-damaging agents." Cancer Res **55**: 3726-31.

Lain, S., D. Xirodimas, et al. (1999). "Accumulating active p53 in the nucleus by inhibition of nuclear export: a novel strategy to promote the p53 tumor suppressor function." Exp Cell Res **253**: 315-24.

Li, G., V. C. Ho, et al. (1997). "Differentiation-dependent p53 regulation of nucleotide excision repair in keratinocytes." Am J Pathol **150**: 1457-64.

McNeal, J. E. (1969). "Origin and development of carcinoma in the prostate." Cancer **23**: 24-34.

McNeal, J. E. and D. G. Bostwick (1986). "Intraductal dysplasia: a premalignant lesion of the prostate." Hum Pathol **17**: 64-71.

Peehl, D. M., R. J. Skowronski, et al. (1994). "Antiproliferative effects of 1,25-dihydroxyvitamin D3 on primary cultures of human prostatic cells." Cancer Res **54**: 805-10.

Peehl, D. M., S. T. Wong, et al. (1993). "Vitamin A regulates proliferation and differentiation of human prostatic epithelial cells." Prostate **23**: 69-78.

Prives, C. (1998). "Signaling to p53: breaking the MDM2-p53 circuit." Cell **95**: 5-8.

Shao, R. G., T. Shimizu, et al. (1996). "Brefeldin A is a potent inducer of apoptosis in human cancer cells independently of p53." Exp Cell Res **227**: 190-6.

Wiman, K. G. (1997). "p53: emergency brake and target for cancer therapy." Exp Cell Res **237**: 14-8.

[CANCER RESEARCH 60, 2616–2622, May 15, 2000]

$p16^{INK4A}$ Mediates Cyclin Dependent Kinase 4 and 6 Inhibition in Senescent Prostatic Epithelial Cells[1]

Charanjit Sandhu, Donna M. Peehl, and Joyce Slingerland[2]

Division of Cancer Biology Research, Sunnybrook Health and Women's Science Centre, Toronto, Ontario M4N 3M5, Canada [C. S., J. S.], and Department of Urology, Stanford University, Stanford, California 94305-5118 [D. M. P.]

ABSTRACT

The senescence checkpoint constrains the proliferative potential of normal cells in culture to a finite number of cell doublings. In this study, we investigated the mechanism of cyclin dependent kinase (cdk) inhibition in senescent human prostatic epithelial cells (HPECs). Progression of HPECs from early passage to senescence was accompanied by a gradual loss of cells in S phase and an accumulation of cells containing 2N DNA. Furthermore, G_1-S phase-associated kinase activities progressively diminished with increasing cell passage. In senescent HPECs, cdk4 and cyclin E1- and A-associated kinases were catalytically inactive. In contrast to observations in senescent fibroblasts, levels of the kinase inhibitor protein (KIP) inhibitor $p21^{CIP1}$ diminished over the proliferative life span of HPECs. $p27^{KIP1}$ levels fell as cells approached senescence, and the association of both $p21^{CIP1}$ and $p27^{KIP1}$ with cdk4/6 complexes was decreased. However, the level of cyclin E1-associated KIP molecules was unaltered as cells progressed into senescence. Progression to senescence was accompanied by a progressive increase in both the level of $p16^{INK4A}$ and in its association with cdk4 and cdk6. As HPECs approached senescence, cdk4- and cdk6-bound $p16^{INK4A}$ showed a shift to a slower mobility due to a change in its phosphorylation profile. As $p16^{INK4A}$ increased in cdk4 and cdk6 complexes, there was a loss of cyclin D1 binding. The altered phosphorylation of $p16^{INK4A}$ in senescent prostatic epithelial cells may facilitate its association with cdk4 and cdk6 and play a role in the inactivation of these kinases.

INTRODUCTION

The eventual growth arrest that defines the termination of cellular proliferation of normal cells in culture is referred to as cellular senescence (1). Normal cells can undergo a finite number of population doublings in culture before they stop proliferation at senescence (1, 2). Fibroblasts arrested at senescence have predominantly 2N DNA, reflecting arrest during the G_1 phase of the cell cycle (2). Several lines of evidence suggest that the mechanisms regulating cell cycle arrest at senescence are genetically programmed and reflect processes relevant to aging within the organism (3–5). It has been postulated that the senescence checkpoint may function as a critical tumor suppression checkpoint *in vivo*. Estimations of cellular proliferation have suggested that tumor growth beyond a volume of 1 cm^3 requires abrogation of the senescence arrest (6).

Most previous studies investigating senescence have used fibroblasts. The high incidence of prostatic cancer in adult males and our limited understanding of prostatic oncogenesis motivated our study of prostatic epithelial cell senescence. Primary prostatic cancers frequently show telomerase activation (7–10), and it is possible to establish immortal lines from primary prostate cancers (11–13). Thus prostate cancer development may be associated with loss of the senescence checkpoint. An understanding of the molecular mechanisms whereby the senescence checkpoint is lost in cancers requires an assessment of this checkpoint in normal HPECs.[3] In the present study, we investigated the mechanisms of cdk inhibition in HPEC senescence.

Transition from one phase of the cell cycle to the next requires the orderly activation and inactivation of a family of related cdks, cdk1–7 [reviewed by Sherr (14) and Morgan (15)]. Cdks are activated by cyclin binding (14) and regulated by phosphorylation (16). G_1 phase to S phase progression requires phosphorylation of pRb, which is mediated primarily by cyclin D1-associated cdk4 or cdk6, and also by cyclin E-cdk2 (17, 18).

Two families of cdk inhibitors, the INK4 and KIP families, regulate cdk activity [reviewed by Sherr and Roberts (19, 20)]. The KIP family consists of three broadly acting inhibitors: $p21^{CIP1}$, $p27^{KIP1}$, and $p57^{KIP2}$. KIP family members bind to and inhibit the cyclin-cdk complexes. Recent *in vitro* experiments demonstrated that a single KIP molecule is sufficient to inhibit cyclin/cdk kinase activity (21). In contrast to the KIP inhibitors, members of the INK4 family ($p15^{INK4B}$, $p16^{INK4A}$, $p18^{INK4C}$, and $p19^{INK4D}$) bind specifically cdk4 and cdk6, with resulting loss of cyclin D binding and catalytic inactivation.

Cell culture models have identified a role for the cdk inhibitors in senescence. An increased expression of p21 and/or p16 at senescence has been identified in human and murine fibroblasts and melanocytes (22–26). The induction of p21 in senescent fibroblasts led to the initial identification and cloning of this gene by Noda *et al.* (27). The elevated expression of p16 and/or p21 at senescence is associated with their increased binding and inhibition of G_1-S phase cdks. Elimination of *p21* expression through homologous recombination extended the life span of human diploid fibroblasts in culture (28). Thus, the loss of p21 expression, although itself not sufficient to abrogate senescence arrest, may represent a key step in the immortalization of cells of fibroblastic lineage. The loss of *p21* and *p16* expression in human cancers suggests that *in vivo*, these inhibitors may contribute to the senescence checkpoint and limit tumor development (29, 30).

In human prostatic tumors, although *p16* is rarely mutated (31, 32), loss of expression occurs frequently through hypermethylation or deletion (29, 33, 34). Furthermore, loss of p16 expression in human prostatic tumors may have prognostic implications (30). Together, these results suggest that p16 may play an important tumor suppressor role in prostatic epithelial cells. In this study, we show that the progression toward HPEC senescence was associated with an increase in p16 levels. Novel phosphorylated forms of p16 showed increased association with the target cdk complexes, cdk4 and cdk6. In contrast to senescence in fibroblasts, neither the expression of p21 nor its association with target cdk complexes was increased. Phosphorylation

Received 8/2/99; accepted 3/20/00.

The costs of publication of this article were defrayed in part by the payment of page charges. This article must therefore be hereby marked *advertisement* in accordance with 18 U.S.C. Section 1734 solely to indicate this fact.

[1] J. Slingerland is a physician scientist supported by Cancer Care Ontario and by career awards from the United States Army Breast Cancer Program, and by the Burrough's Welcome Fund. This work was supported by grants from the United States Army Prostate Cancer Research Program and the Canadian Breast Cancer Research Initiative of the National Cancer Institute of Canada (to J. M. S.) and from the United States Army Prostate Cancer Program (to D. M. P.).

[2] To whom requests for reprints should be addressed, at Division of Cancer Biology Research, Sunnybrook Health and Women's Science Centre, S-218, 2075 Bayview Avenue, Toronto, ON M4N 3M5, Canada. Phone: (416) 480-6100, Ext. 3494; Fax (416) 480-5703; E-mail: joyce.slingerland@utoronto.ca.

[3] The abbreviations used are: HPEC, human prostatic epithelial cell; cdk, cyclin dependent kinase; pRb, retinoblastoma protein; INK4, inhibitors of cdk4; KIP, kinase inhibitor protein; BrdUrd, bromodeoxyuridine; mAb, monoclonal antibody; PAP, potato acid phosphatase; 2D IEF, two-dimensional isoelectric focusing.

of p16 may represent a novel regulatory pathway for p16 inhibitory activity.

MATERIALS AND METHODS

Cell Culture. Cell cultures were established as follows: Cell strains E-PZ-16 and E-PZ-22 were obtained from men 60 and 61 years of age, respectively, undergoing radical prostatectomy to treat prostate cancer. Neither patient had received previous therapy. Prostatic specimens were transferred to the laboratory within 1 h after surgery. A small wedge of tissue was dissected from the peripheral zone of each specimen, and primary cultures were established as described previously (35). Briefly, tissues were minced and digested overnight with collagenase. The digested tissues were inoculated into dishes coated with collagen type I and containing PFMR-4A medium supplemented with 10 ng/ml cholera toxin, 10 ng/ml epidermal growth factor, 40 μg/ml bovine pituitary extract, 4 μg/ml insulin, 1 μg/ml hydrocortisone, 100 μg/ml gentamicin, 0.1 mM phosphoethanolamine, 3 nM selenous acid, 2.3 μM α-tocopherol, and 0.03 nM all-*trans* retinoic acid (35). Cells that grew out in primary culture were aliquoted and stored frozen in liquid nitrogen. The epithelial nature of these cells was verified by immunocytochemical staining for cytokeratins (35). To verify the histology of origin, the prostatic specimens were inked after dissection, fixed, and serially sectioned (36). The histology of tissues immediately adjacent to and surrounding the portion removed for culture was reviewed. Neither cancer nor benign prostatic hyperplasia was present in the areas of tissue from which the cell strains were derived.

Cells were serially passaged as follows: Cells were thawed and inoculated into collagen-coated dishes containing MCDB 105 (Sigma, St. Louis, MO) supplemented as described for PFMR-4A except with 10 rather than 40 μg/ml pituitary extract. When ~50% confluent, a portion of the cells was harvested for analysis of cell cycle regulators at "passage 1." The remainder of the cells (~10 or 20%) were passaged after trypsinization into 40 dishes and again grown to ~50% confluency, at which time cells were again either harvested ("passage 2") or passaged. This process was repeated twice more (passages 3 and 4) until the cells ceased proliferation.

Flow Cytometric Analysis. At different passages, cells were pulse labeled with 10 μM BrdUrd for 2 h. Cells were then harvested, fixed with 70% ethanol, treated with 0.1 N HCl, and heated for 10 min at 90°C to expose the labeled DNA. Cells were then stained with anti-BrdUrd-conjugated FITC (Becton Dickinson, Bedford, MA) and propidium iodide. Cell cycle analysis was carried out on a Becton Dickinson FACScan, using Cell Quest software.

Antibodies. Antibodies to pRb, cdk2, cyclins A and D1, and p21 were obtained from PharMingen (San Diego, CA) or Santa Cruz Biotechnology (Santa Cruz, CA). Cyclin E1-specific antibodies (mAbs E12 and E172; Refs. 37, 38) were from E. Lees and E. Harlow (Massachusetts General Hospital, Boston, MA). Monoclonal PSTAIRE antibody (39) was a gift from S. Reed (The Scripps Research Institute, La Jolla, CA), and cyclin D1 antibody, DCS-11, was purchased from Neomarkers (Fremont, CA). Cyclin A mAb E67 was provided by J. Gannon and T. Hunt (ICRF, London, United Kingdom). Monoclonal p27 antibody was purchased from Transduction Labs (Lexington, KY). Cdk4 and cdk6 polyclonal sera were provided by G. Hannon and D. Beach (CSH Labs, Cold Spring Harbor, NY). The JC-6 monoclonal, provided by J. Koh and E. Harlow (Massachusetts General Hospital; Ref. 40), and p16 polyclonal antibody, purchased from Santa Cruz, were used for immunoblotting of p16 in these studies. β-actin antibody was purchased from Sigma. Monoclonal p19 antibody was obtained from Neomarkers. Polyclonal p18 antibody was kindly provided by Y. Xiong (University of North Carolina, Chapel Hill, NC).

Immunoblotting. Cells were lysed in ice-cold NP40 lysis buffer [0.1% NP40, 50 mM Tris (pH 7.5), 150 mM NaCl, 1 mM phenylmethylsulfonyl fluoride, and 0.02 mg/ml each of aprotinin, leupeptin, and pepstatin]. Lysates were sonicated and clarified by centrifugation.

Protein was quantitated by Bradford analysis. Twenty or 50 μg of protein were loaded in each lane and resolved by SDS-PAGE. Transfer and blotting were as described (41). Equal loading of the lanes was verified using a β-actin antibody. For detection of cdk4-associated proteins by immunoprecipitation/Western analysis, cdk4 was immunoprecipitated from 200 μg of protein lysate, complexes were resolved and blotted, and the blot was reacted with cdk4, cyclin D1, p16, p21, or p27 antibodies. To verify the identity of associated proteins, control cyclin D1, p16, p21, and p27 immunoprecipitations were resolved along side the cdk4 immune complexes (data not shown). Similar methods were used to detect cdk6- and cyclin E1-associated proteins.

Protein Expression in Bacteria. pRb substrate for cyclin D1-associated kinase assays was generated from a pGEX vector containing the COOH terminus of pRb (amino acids 729–928) fused to glutathione *S*-transferase (kindly provided by J. Zhao and E. Harlow, Massachusetts General Hospital). Bacteria were lysed in PBS containing 1% Triton X-100, 1 mg/ml lysozyme, and protease inhibitors, and lysates were clarified by centrifugation at 15,000 rpm for 20 min. The pRb fragment was isolated by incubating bacterial extract with glutathione beads for 1 h. Beads were then washed repeatedly with PBS-1% Triton X-100 and then with PBS alone. The pRb fragment was eluted in 20 mM glutathione in PBS (pH 7.8).

Kinase Assays. For cdk4 kinase assays, cells were lysed in 50 mM HEPES, 150 mM NaCl, 1 mM EDTA (pH 8.0), 2.5 mM EGTA (pH 8.0), 10% glycerol, 10 mM β-glycerophosphate, 1 mM NaF, 0.1% Tween-20, 0.1 mM Na_2VO_4, 1 mM 4-(2-aminoethyl)benzenesulfonyl fluoride, 0.5 mM DTT and 1 mg/ml both leupeptin and aprotinin. Cdk4 kinase assays were performed following the method of LaBaer *et al.* (42), using cdk4 antibody obtained from Santa Cruz for immunoprecipitation and the COOH-terminal fragment of pRb as substrate. Radioactivity was quantified using a Molecular Dynamics PhosphorImager and ImageQuant software. Cyclin E1- and A-associated kinase assays were performed as described (43). Histone H1 substrate was obtained from Boehringer Mannheim (Laval, Quebec). Background levels of kinase activity were determined for each kinase reaction by immunoprecipitating early passage cellular extract with nonspecific mouse mAbs (Fig. 2, *Lane C*).

Phosphatase Assay. Dephosphorylation of p16 was carried out by immunoprecipitating cdk6 complexes from 100 μg of cellular extract. Complexes were washed three times with NP40 lysis buffer and twice with potato acid phosphatase (PAP) buffer [40 mM PIPES (pH 6.0; Sigma), 1 mM DTT, 20 μg/ml aprotinin, and 20 μg/ml leupeptin]. An ammonium sulfate precipitate of PAP (Sigma) was resuspended in 1 ml of PAP buffer and eluted from a desalting column (Pharmacia Nap-5) with 500 μl of PAP buffer. Immunoprecipitated complexes were then incubated with 12 units of PAP for 2 h. The specificity of the phosphatase assay was confirmed by incubating immunoprecipitates with 1 mM Na_2VO_4 and 100 mM β-glycerophosphate in addition to PAP. The complexes were then resolved by SDS-PAGE and immunoblotted for p16.

Two-Dimensional Gel Electrophoresis. Isoeletric focusing of p16 was carried out by immunoprecipitating cdk6 complexes from 1 mg of protein cell extract. The immune complexes were washed three times with NP40 lysis buffer and then once with 20 mM Tris (pH 7.5). The washed complexes were solubilized in 200 μl of rehydration buffer [8 M urea, 2% (w/v) CHAPS, 0.5% (v/v) pH 3–10 IPG (Immobiline Dry Strip Gels) buffer (Amersham Pharmacia Biotech), and 18 mM DTT] and loaded onto IPG strip holders containing pH 3–10 linear IPG strips (Amersham Pharmacia Biotech). The gels were rehydrated with the sample solution for 17 h at 20°C and then focused consecutively for 1 h at 500 V, 1 h at 1000 V, and 2 h at 8000 V in an IPGPHOR Isoelectric Focusing System (Amersham Pharmacia Biotech). The focused gel strips were incubated for 15 min at room temperature in equilibration buffer [50 mM Tris (pH 8.8), 6 M urea, 30% (v/v) glycerol, 2% (w/v) SDS, and 65 mM DTT] prior to loading onto 17.5% SDS-PAGE gels. The electrophoresed gels were then transferred to Immobilon, and p16 was detected by immunoblotting.

RESULTS

Cell Cycle Arrest in Senescence. The cell cycle profile of HPECs was determined by BrdUrd pulse labeling and flow cytometric analysis of cells at early passage and senescence (Fig. 1). At early passage, 22% of asynchronously growing cells were in S phase, 66% contained 2N DNA, and the remaining 12% of cells contained 4N DNA. Cellular proliferation ceased after six passages, which corresponded to ~30 population doublings at senescence. Cells were considered to be senescent after they remained subconfluent for >1 month. Flow cytometry of senescent HPECs demonstrated a cell cycle arrest with <1% of cells in S phase and 85% of the cells with 2N DNA. The remaining 14% of cells had 4N DNA at senescence.

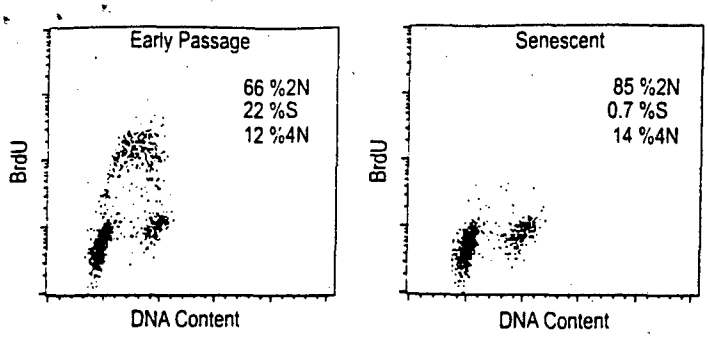

Fig. 1. Cell cycle arrest in senescence. Asynchronously growing and senescent cells were pulse labeled with BrdUrd and counterstained with propidium iodide. BrdUrd incorporation and propidium iodide uptake were plotted for both early passage (*left panel*) and senescent (*right panel*) cells. *S*, cells in S phase.

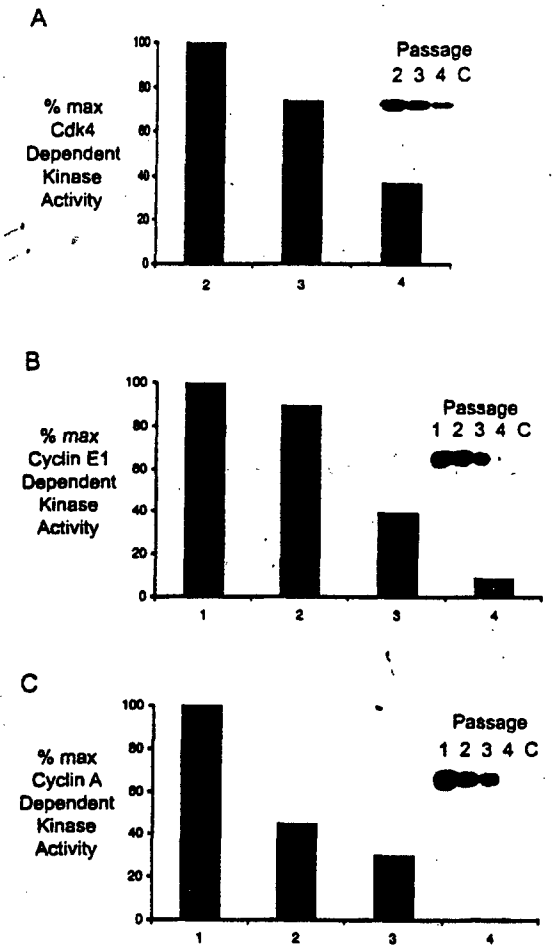

Fig. 2. Cyclin-dependent kinase activities. Kinase activities were assayed in immunoprecipitates recovered from cell lysates from early passage (*passage 1*) to senescence (*passage 4*). Background levels of kinase activity were determined by immunoprecipitation with nonspecific mouse mAbs from early passage cellular extracts (*p Lane C* in *insets*). Reaction products were resolved by SDS-PAGE, dried, and autoradiographed (*insets*). Phosphorylation of substrate was quantitated by phosphorimager, and the results were graphed as a percentage of the maximum early passage kinase activity. *A*, cdk4-associated kinase activity. The COOH-terminal domain of pRb was used as substrate in cdk4-associated kinase assays. *B*, cyclin E1-associated kinase activity. *C*, cyclin A-associated kinase activity. For *B* and *C*, histone H1 kinase activity was assayed in cyclin E or cyclin A immunoprecipitates recovered from increasing passages.

Cdk Activities Decreased Progressively with Increasing Passage. The kinase activities in cyclin E1, cyclin A, and cdk4 immune complexes from cell populations of increasing passage were assayed using either histone H1 (cyclins A and E) or a pRb fragment (cdk4) as substrates. Results are shown in Fig. 2. The activities of cyclin E1- and cyclin A-associated kinases and of cdk4 decreased steadily as cells progressed from early passage to senescence. Senescent cells showed no kinase activities above that in nonspecific immune controls. Furthermore, analysis of cells of increasing passage revealed a progressive loss of pRb phosphorylation, indicative of cell cycle arrest in G_1 (see Fig. 3*A*). Because pRb is phosphorylated by cyclin E1- and D1-associated kinases, loss of pRb phosphorylation provides further evidence of inhibition of these cdks.

Increased p16^{INK4A} Levels in Senescent Prostatic Cells. The levels of cdk inhibitors, cyclins, and cdks associated with the G_1-S transition were assayed as HPECs progressed from early passage toward senescence (Fig. 3*A*). Western analysis revealed no change in cyclin E1 or cyclin D1 levels during the aging of prostatic epithelial cell populations. Cyclin A levels gradually decreased, consistent with the gradual recruitment of cells into G_1 arrest at senescence. The decrease in cyclin A levels was likely the consequence of decreased cyclin E1- and cyclin D1-associated kinase activities, resulting in reduced E2F-mediated transcription of cyclin A. The cdk4 and 6 levels remained unchanged. The loss of cdk2 protein with increasing population doublings was largely due to loss of the CAK-activated, Thr-160 phosphoform (faster migrating cdk2 band).

The levels of the KIP and INK inhibitors were also analyzed in asynchronous prostatic epithelial cells at increasing population doublings and at senescence. There was a steady decrease in the protein levels of p21^{CIP1} and p27^{KIP1}. p18^{INK4C} expression was not detected (data not shown), and p19^{INK4D} levels remained unchanged, whereas p16^{INK4A} levels steadily increased, reaching maximal levels of expression in senescent cells. In addition, longer exposures of the p16 immunoblots revealed the presence of two additional p16-reactive bands of decreased mobility on SDS-PAGE (Fig. 3*B*). These slower mobility bands were detected using two different anti-p16 antibodies (the JC-6 monoclonal and the Santa Cruz polyclonal). The abundance of these two novel p16-related bands increased with increasing population doublings.

KIP Binding to Cyclin E-cdk2 Did Not Increase in Senescent HPECs. The composition of cyclin E1-cdk2 complexes showed no apparent change during the progression of HPECs toward senescence (Fig. 4*A*). The amount of cdk2 bound to cyclin E1 was not reduced.

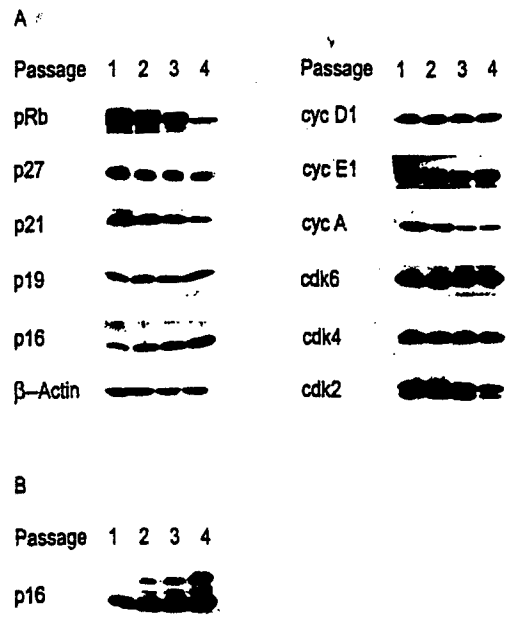

Fig. 3. Steady-state levels of G_1-S-associated cell cycle regulators during the aging of the prostatic epithelial cell population. *A*, lysates were collected from prostatic epithelial cells between early passage (*passage 1*) and senescence (*passage 4*). Cell lysates from the indicated passage numbers were resolved by SDS-PAGE and immunoblotted with the indicated antibodies. *B*, longer exposure of p16 immunoblot from *A*. *cyc*, cyclin.

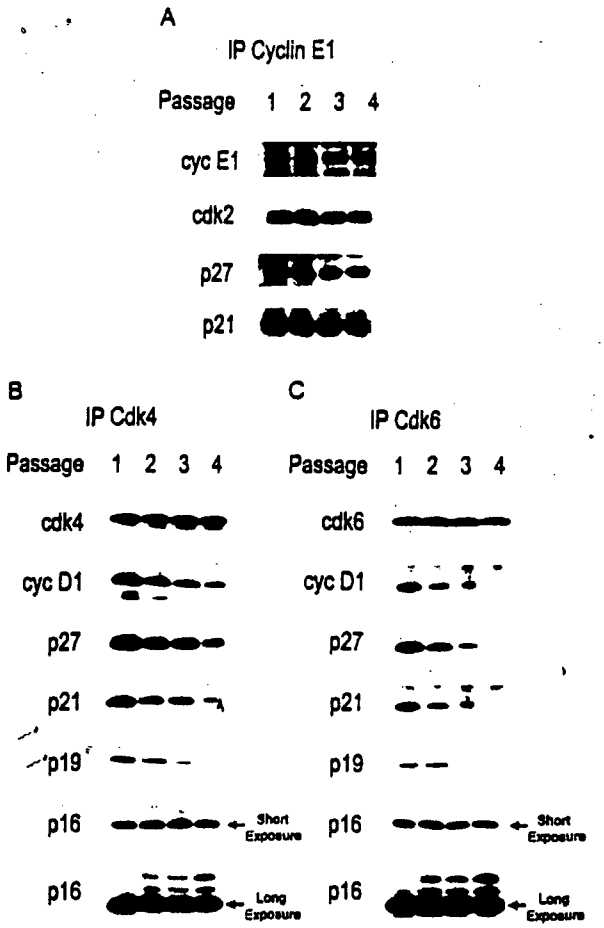

Fig. 4. Cyclin/cdk inhibitor complexes in prostatic epithelial cells from early passage to senescence. Cyclin (*A*) or cdk (*B* and *C*) immunoprecipitations were carried out as described in "Material and Methods." Complexes from the indicated passages were resolved and immunoblotted for associated cdk, cyclin, and cdk inhibitors. *A*, cyclin E1 (*cyc E1*) binding to cdk2 and cdk inhibitors p21 and p27. *B*, cdk4 binding to cyclin D1 (*cyc D1*) and cdk inhibitors p16, p19, p21, and p27. *C*, cdk6 binding to cyclin D1 (*cyc D1*) and cdk inhibitors p16, p19, p21, and p27.

Furthermore, the proportion of Thr-160 phosphorylated cdk2 bound to cyclin E1 remained constant. The levels of cyclin E1-associated p21 and p27 remained constant. Thus, the inhibition of cyclin E1-cdk2 activity could not be attributed to increased KIP binding or to a lack of activating phosphorylation at the Thr-160 residue of cdk2.

p16 Accumulated in cdk4 and cdk6 Complexes as HPECs Approached Senescence. As total $p16^{INK4A}$ levels increased during the aging of the HPEC population, the association of $p16^{INK4A}$ with cdk4 and cdk6 complexes also increased (Fig. 4, *B* and *C*). Although there was no increase in the faster mobility band of p16 in cdk4 and cdk6 complexes (Fig. 4, *B* and *C*, *short exposure*), longer exposures of the cdk-associated p16 immunoblots (Fig. 4, *B* and *C*, *long exposure*) again revealed the existence of two delayed mobility bands that cross-reacted with p16-specific antibodies. The association of these two bands with cdk4 and cdk6 complexes steadily increased with later cell passages. Densitometry showed that association of the slower migrating forms of p16 increased by 2-fold in cdk6 complexes and by 1.5-fold in cdk4 complexes between passage 2 and senescence. The accumulation of these slower mobility p16 bands in cdk4 and cdk6 complexes was correlated with a decrease in the binding of cyclin D1, p27, p21, and p19. None of the anti-p16-reactive bands were cross-reactive with p18 or p19 antibodies.

Altered Phosphorylation of p16 in Senescent Prostatic Epithelial Cells. To determine whether the novel bands of delayed mobility were different phosphoforms of p16, cdk6 complexes were immunoprecipitated from senescent cellular extract (Fig. 5, *Lane 1*) and treated with PAP (Fig. 5, *Lane 2*); immunoblots were reacted with p16 antibodies. PAP treatment of the immunoprecipitates from senescent cells resulted in the loss of the upper two p16 bands visible on long exposures and the formation of two bands of increased mobility (data for senescent cells shown in Fig. 5, *middle* and *bottom panels*). Thus, the slower mobility forms of p16, whose association with both cdk4 and cdk6 complexes increased in senescent HPECs, represented novel phosphoforms of p16. These delayed mobility p16 phosphoforms were not detected, even with prolonged exposure in the early passage HPECs. It is notable that the dominant, faster mobility p16 band, detected in both early passage and senescent cells, also shifted to two faster mobility bands when the phosphatase reaction went to completion, indicating that this dominant band also represents phosphorylated p16 (Fig. 5). There was no loss of any of the p16 reactive bands when PAP was preincubated with phosphatase inhibitors (Fig. 5, *Lane 3*). The formation of two p16-reactive bands of increased mobility after PAP treatment suggested that all of the cellular p16 is phosphorylated, but the pattern of expression of the different phosphoforms differed between early passage and senescent cells.

2D IEF of p16 in cdk6 immunoprecipitates with and without PAP confirmed the existence of multiple p16 phosphoforms (Fig. 6). In early passage cells, the solitary band of p16 seen on one-dimensional Western blots (Fig. 4) resolved on 2D IEF as two forms of p16, which focused to a pH between 5 and 6 (Fig. 6, *arrowhead 3*). In senescent

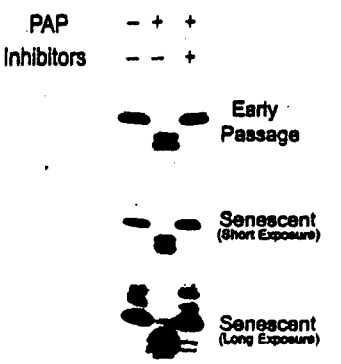

Fig. 5. p16 phosphorylation in senescent cells. Cdk6 complexes from early passage and senescent cellular extracts were immunoprecipitated and treated with PAP in the presence or absence of β-glycerophosphate (*inhibitor*). Complexes were then resolved and immunoblotted for p16. +, present; −, absent.

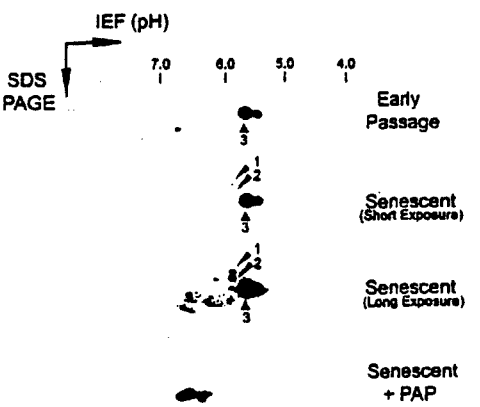

Fig. 6. 2D IEF of cdk6-associated p16. Cdk6 complexes from early passage and senescent extracts were immunoprecipitated and treated (or not) with PAP as indicated. Complexes were resolved in the first dimension by IEF and in the second dimension by SDS-PAGE. Gels were transferred and p16 was immunoblotted. *Arrowhead 1*, isoform 1, found in senescent cells, which showed delayed mobility on SDS-PAGE; *arrowhead 2*, isoform 2, found in senescent cells, which showed delayed mobility on SDS-PAGE; *arrowhead 3*, two forms of p16, found in early passage and senescent cells, which focused to a pH between 5 and 6.

cells, in addition to the two forms of p16 observed in early passage cells, two additional p16 isoforms (Fig. 6, *arrowheads 1* and *2*) were present. These two isoforms showed a delayed mobility on SDS-PAGE (the second dimension) and focused just below pH 6.0. The relative mobilities of isoforms 1 and 2 in the second dimension with respect to the predominant forms of p16 was consistent with these being the two minor p16 bands of delayed mobility that were observed in senescent cells in one-dimensional Western blots in Fig. 4.

With PAP treatment prior to resolution on 2D IEF, all of the p16 isoforms focusing between pH 5.0 and 6.0 were lost. Phosphatase-treated p16 focused at a higher isoelectric point, at approximately pH 6.8, and had increased mobility in the second dimension. These results confirm the results in Fig. 5 and indicate that all three p16 bands detected on Western blotting represent p16 phosphoforms. The pattern differs between early passage and senescence, with isoforms 1 and 2 increasing as cells approach and enter senescence.

DISCUSSION

The senescence checkpoint limits the proliferative capacity of cells in a tissue culture environment. Processes analogous to the senescence checkpoint observed in cultured cells are thought to limit cellular proliferation *in vivo*. A number of observations have suggested that senescence occurs within the organism *in vivo*. The proliferative capacity of cells with a finite life span in culture is inversely related to the donor's age (3). The number of population doublings that fibroblasts undergo in culture is related to the longevity of the donor species (4). The limit imposed by senescence on the proliferative capacity of cells has raised the hypothesis that cellular senescence may indeed represent a natural impediment to malignant degeneration. To date, most studies investigating senescence have used human fibroblasts and rodent cells. Because the incidence of malignancies arising from fibroblasts such as sarcomas is relatively rare in humans, we examined the senescence phenomenon in epithelial cells, which undergo malignant transformation more frequently than fibroblasts. Our investigation of senescence arrest in HPECs and in human mammary epithelial cells[4] demonstrates that epithelial cells differ from fibroblasts in the manner whereby cdk inhibition occurs at senescence.

The identification of key inhibitor(s) of cell cycle progression at senescence could potentially indicate a critical regulator whose expression or activity would need to be down-regulated for tumor progression to proceed. Investigations of senescence in fibroblasts suggest important roles for p21 and p16. Here we have demonstrated an increase in p16 and the appearance of novel phosphorylated forms of p16 that bind and inhibit cdk4 and cdk6 activity in senescent HPECs.

The prostatic epithelial cell cultures used in this study moved from a proliferatively active state to a senescent state within six passages or ~30 population doublings. Senescent HPECs showed predominantly 2N DNA. A small proportion of cells had 4N DNA at senescence. We and others have observed an increase in tetraploidy as cultured cells approach senescence[4] (44). Thus, cells with 4N DNA are most likely tetraploid cells arrested prior to S phase entrance at the senescence checkpoint, as opposed to cells arrested at the G_2-M transition. The catalytic activity of the cdks associated with the G_1-S transition underwent a steady decrease from early passage to senescence. The steady loss of kinase activity implies that the entry of cells into senescence does not occur in a synchronized manner. Rather, there appears to be some heterogeneity with regard to the passage at which epithelial cells enter senescence. Early studies of senescence identified this phenomenon by the progressive reduction of tritiated thymidine incorporation that occurred during the serial passaging of fibroblasts (45). The established relationship between telomere length and the proliferative capacity of cells suggests that variations in telomere length within a population of cells may account for the apparently stochastic manner whereby cells enter senescence (46). The heterogeneity in telomere length may reflect variations in the proliferation of epithelial stem cell populations *in vivo*.

To investigate the cause of cdk inhibition in senescent HPECs, we examined the steady-state levels of G_1-S-associated cell cycle regulators. Of the cyclins examined, only cyclin A diminished with increasing passage, accounting for the corresponding loss of cyclin A-associated kinase activity. The loss of cyclin A in senescent HPECs is likely a consequence of the cells arresting at a point within the cell cycle prior to cyclin A induction. Studies in human fibroblasts have shown that entrance into senescence is similarly associated with a loss of cyclin A (47). However, in senescent fibroblasts there is a significant increase in the expression of cyclins D1 and E1 (48, 49). The levels of cdk4 and cdk6 were unaffected by increasing passage in HPECs, whereas loss of cdk2 was largely due to loss of the Thr-160 phosphorylated form of cdk2. Fibroblasts have a similar loss of the Thr-160 form of cdk2 during senescence (48, 50), and in addition, studies of fibroblast senescence have revealed a reduction in cdk4 levels (49). Thus, it appears that the regulation of both cyclin and cdk expression differs between senescent fibroblasts and prostatic epithelial cells.

In contrast to reports in cells of fibroblastic and melanocytic lineage, the steady-state levels of both p21 and p27 proteins decreased as HPECs moved toward senescence (22, 27, 51). Furthermore, there was no increase in the binding of p21 and p27 to cyclin E1-associated complexes in senescent HPEC extracts. These KIP molecules were also lost from cdk4 and cdk6 complexes during the progression toward senescence. These results contrast with previous findings in senescent human fibroblasts and keratinocytes, where p21 was shown to be induced at senescence and its binding to G_1-S-associated cdks was increased (28, 51, 52). Our findings in senescent HPECs and human mammary epithelial cells,[4] indicate that p21 does not appear to mediate cdk inhibition in all senescent epithelial cells. The lack of p21 induction in senescent prostatic and mammary epithelial cells may represent a fundamental difference between these epithelial cell types and keratinocytes and fibroblasts at senescence.

Investigations of senescence in fibroblasts, lymphocytes, and uroepithelial cells have implicated p16 in the inhibition of cyclin D1-dependent kinases (22, 26, 53). The high incidence of *p16* inactivation in prostatic tumors suggests that p16 may play a role in arresting HPECs at senescence both *in vivo* and *in vitro* (29, 33). The present study and the recent report of Jarrard *et al.* (54) establish that there is an increase in p16 levels in senescent prostatic epithelial cells. Immortal HPEC derivatives, generated by the introduction of human papilloma virus E6 and/or E7, were associated with a loss of p16 or pRb expression (54). We have identified two novel p16-related bands of delayed mobility that accumulate in senescent HPECs. Resolution on both one-dimensional gels and by 2D IEF after treatment with PAP demonstrates that the two novel p16 bands of delayed mobility observed in one-dimensional Western blots were p16 phosphoforms. In both early and late passage cell extracts, PAP treatment also shifted the most abundant (faster mobility) p16 band on the one-dimensional Western blots, suggesting that all detectable p16 is phosphorylated. The failure of p16 to resolve into a single band after prolonged PAP treatment may be a consequence of phosphorylation at sites on p16 that are not recognized efficiently by PAP, or alternatively, a fraction

[4] C. Sandhu, J. Donovan, N. Bhattacharya, M. Stampfer, P. Worland, and J. Slingerland. Loss of cdc25A contributes to cyclin E1/cdk2 inhibition at senescence in human mammary epithelial cells, submitted for publication.

of the cellular p16 may undergo other posttranslational modifications, such as glycosylation, that serve to alter its gel mobility.

PAP treatment and 2D IEF confirmed the existence of different p16 phosphorylation patterns in early passage and senescent HPECs. The dominant p16 band seen on immunoblots from both early passage and senescent cdk6 immune complexes was composed of two p16 isoforms. Two additional p16 isoforms of delayed mobility consistently appeared in senescent cells, suggesting that p16 undergoes senescence-specific posttranslational modifications. These senescent-specific isoforms (Fig. 6, *arrowheads 1* and *2*) of p16 focused at a slightly higher pH, and thus represent p16 isoforms with a lower of level of phosphorylation when compared with the two dominant isoforms of p16 (Fig. 6, *arrowhead 3*). After PAP treatment, all of the p16 isoforms focused at a higher pH. These results are consistent with the interpretation that all of the detected p16 is phosphorylated but that novel phosphoforms appear in senescent cells.

The increased expression of p16 translated into an increased association of p16 with cdk4 and cdk6 complexes in senescent HPECs. In senescent HPECs, as in other forms of G_1 arrest, the accumulation of this INK4 molecule in target kinases was associated with loss of cyclin D1 and KIP binding (55, 56). However, only the senescence-specific phosphoforms of p16 showed an increased binding to cdk complexes. The accumulation of these novel p16 phosphoforms in cdk4 and cdk6 complexes suggests a senescence-activated mechanism of posttranslational modification of p16 contributing to kinase inhibition and senescence arrest in HPECs.

Phosphorylation of p16 may represent an important mechanism of p16 regulation. p16 phosphorylation may regulate either the affinity for cdk4 and cdk6 and/or the localization of p16 within the cell. Phosphorylation of p27 functions to regulate the stability of the protein and its affinity for cdk complexes (57–59). It is tempting to postulate that phosphorylation of specific sites on p16 in senescent HPECs facilitates the binding of p16 to target cdk complexes and contributes thereby to G_1 arrest in senescence. The identification of these phosphorylation sites and the pathways that influence phosphorylation of p16 would aid in the understanding of the regulation of the INK family of inhibitors and elucidate further the pathways regulating p16 inhibitory activity.

REFERENCES

1. Hayflick, L. The limited *in vitro* lifetime of diploid cell strains. Exp. Cell Res., *37:* 614–636, 1965.
2. Hayflick, L., and Moorhead, P. S. The serial cultivation of human diploid cell strains. Exp. Cell Res., *25:* 585–621, 1961.
3. Martin, G. M., Sprague, C. A., and Epstein, C. J. Replicative life-span of cultivated human cells. Effects of donor's age, tissue, and genotype. Lab. Investig., *23:* 86–92, 1970.
4. Rohme, D. Evidence for a relationship between longevity of mammalian species and life spans of normal fibroblasts in vitro and erythrocytes *in vivo*. Proc. Natl. Acad. Sci. USA, *78:* 5009–5013, 1981.
5. Dimri, G. P., Lee, X., Basile, G., Acosta, M., Scott, G., Roskelley, C., Medrano, E. E., Linskens, M., Rubelj, I., and Pereira-Smith, O. A biomarker that identifies senescent human cells in culture and in aging skin *in vivo*. Proc. Natl. Acad. Sci. USA, *92:* 9363–9367, 1995.
6. Vojta, P. J., and Barrett, J. C. Genetic analysis of cellular senescence. Biochim. Biophys. Acta, *1242:* 29–41, 1995.
7. Sommerfeld, H. J., Meeker, A. K., Piatyszek, M. A., Bova, G. S., Shay, J. W., and Coffey, D. S. Telomerase activity: a prevalent marker of malignant human prostate tissue. Cancer Res., *56:* 218–222, 1996.
8. Zhang, W., Kapusta, L. R., Slingerland, J. M., and Klotz, L. H. Telomerase activity in prostate cancer, prostatic intraepithelial neoplasia, and benign prostatic epithelium. Cancer Res., *58:* 619–621, 1998.
9. Scates, D. K., Muir, G. H., Venitt, S., and Carmichael, P. L. Detection of telomerase activity in human prostate: a diagnostic marker for prostatic cancer? Br. J. Urol., *80:* 263–268, 1997.
10. Lin, Y., Uemura, H., Fujinami, K., Hosaka, M., Harada, M., and Kubota, Y. Telomerase activity in primary prostate cancer. J. Urol., *157:* 1161–1165, 1997.
11. van Steenbrugge, G. J., Groen, M., van Dongen, J. W., Bolt, J., van der Korput, H., Trapman, J., Hasenson, M., and Horoszewicz, J. The human prostatic carcinoma cell line LNCaP and its derivatives. An overview. Urol. Res., *17:* 71–77, 1989.
12. Kaighn, M. E., Narayan, K. S., Ohnuki, Y., Lechner, J. F., and Jones, L. W. Establishment and characterization of a human prostatic carcinoma cell line (PC-3). Investig. Urol., *17:* 16–23, 1979.
13. Webber, M. M., Bello, D., and Quader, S. Immortalized and tumorigenic adult human prostatic epithelial cell lines: characteristics and applications. Part 3. Oncogenes, suppressor genes, and applications. Prostate, *30:* 136–142, 1997.
14. Sherr, C. J. G_1 phase progression: cycling on cue. Cell, *79:* 551–555, 1994.
15. Morgan, D. O. Principles of Cdk regulation. Nature (Lond.), *374:* 131–134, 1995.
16. Solomon, M. J., and Kaldis, P. Regulation of CDKs by phosphorylation. Results Probl. Cell Differ., *22:* 79–109, 1998.
17. Dowdy, S. F., Hinds, P. W., Louie, K., Reed, S. I., Arnold, A., and Weinberg, R. A. Physical interaction of the retinoblastoma protein with human D cyclins. Cell, *73:* 499–511, 1993.
18. Ewen, M. E., Sluss, H. K., Whitehouse, L. L., and Livingston, D. M. TGF-β inhibition of cdk4 synthesis is linked to cell cycle arrest. Cell, *74:* 1009–1020, 1993.
19. Sherr, C. J., and Roberts, J. M. Inhibitors of mammalian G_1 cyclin-dependent kinases. Genes Dev., *9:* 1149–1163, 1995.
20. Sherr, C. J., and Roberts, J. M. CDK inhibitors: positive and negative regulators of G_1-phase progression. Genes Dev., *13:* 1501–1512, 1999.
21. Hengst, L., Gopfert, U., Lashuel, H. A., and Reed, S. I. Complete inhibition of Cdk/cyclin by one molecule of p21(Cip1). Genes Dev., *12:* 3882–3888, 1998.
22. Alcorta, D. A., Xiong, Y., Phelps, D., Hannon, G., Beach, D., and Barrett, J. C. Involvement of the cyclin-dependent kinase inhibitor p16 (INK4a) in replicative senescence of normal human fibroblasts. Proc. Natl. Acad. Sci. USA, *93:* 13742–13747, 1996.
23. Hara, E., Smith, R., Parry, D., Tahara, H., Stone, S., and Peters, G. Regulation of p16CDKN2 expression and its implications for cell immortalization and senescence. Mol. Cell. Biol., *16:* 859–867, 1996.
24. Palmero, I., McConnell, B., Parry, D., Brookes, S., Hara, E., Bates, S., Jat, P., and Peters, G. Accumulation of p16INK4a in mouse fibroblasts as a function of replicative senescence and not of retinoblastoma gene status. Oncogene, *15:* 495–503, 1997.
25. Zindy, F., Quelle, D. E., Roussel, M. F., and Sherr, C. J. Expression of the p16INK4a tumor suppressor versus other INK4 family members during mouse development and aging. Oncogene, *15:* 203–211, 1997.
26. Reznikoff, C. A., Yeager, T. R., Belair, C. D., Savelieva, E., Puthenveettil, J. A., and Stadler, W. M. Elevated p16 at senescence and loss of p16 at immortalization in human papillomavirus 16 E6, but not E7, transformed human uroepithelial cells. Cancer Res., *56:* 2886–2890, 1996.
27. Noda, A., Ning, Y., Venable, S. F., Pereira-Smith, O. M., and Smith, J. R. Cloning of senescent cell-derived inhibitors of DNA synthesis using an expression screen. Exp. Cell Res., *211:* 90–98, 1994.
28. Brown, J. P., Wei, W., and Sedivy, J. M. Bypass of senescence after disruption of p21$^{CIP1/WAF1}$ gene in normal diploid human fibroblasts. Science (Washington DC), *277:* 831–834, 1997.
29. Cairns, P., Polascik, T. J., Eby, Y., Tokino, K., Califano, J., Merlo, A., Mao, L., Herath, J., Jenkins, R., Westra, W., Rutter, J. L., Buckler, A., Gabrielson, E., Tockman, M., Cho, K. R., Hedrick, L., Bova, G. S., Isaacs, W., Koch, W., Schwab, D., and Sidransky, D. Frequency of homozygous deletion at p16/CDKN2 in primary human tumours. Nat. Genet., *11:* 210–212, 1995.
30. Tsihlias, J., Kapusta, L., and Slingerland, J. The prognostic significance of altered cyclin-dependent kinase inhibitors in human cancer. Annu. Rev. Med., *50:* 401–423, 1999.
31. Park, D. J., Wilczynski, S. P., Pham, E. Y., Miller, C. W., and Koeffler, H. P. Molecular analysis of the *INK4* family of genes in prostate carcinomas. J. Urol., *157:* 1995–1999, 1997.
32. Tamimi, Y., Bringuier, P. P., Smit, F., van Bokhoven, A., Debruyne, F. M., and Schalken, J. A. p16 mutations/deletions are not frequent events in prostate cancer. Br. J. Cancer, *74:* 120–122, 1996.
33. Jarrard, D. F., Bova, G. S., Ewing, C. M., Pin, S. S., Nguyen, S. H., Baylin, S. B., Cairns, P., Sidransky, D., Herman, J. G., and Isaacs, W. B. Deletional, mutational, and methylation analyses of CDKN2 (p16/MTS1) in primary and metastatic prostate cancer. Genes Chromosomes Cancer, *19:* 90–96, 1997.
34. Chi, S. G., deVere, W. R., Muenzer, J. T., and Gumerlock, P. H. Frequent alteration of CDKN2 [p16(INK4A)/MTS1] expression in human primary prostate carcinomas. Clin. Cancer Res., *3:* 1889–1897, 1997.
35. Peehl, D. M. Culture of human prostatic epithelial cells. *In:* R. I. Freshney (ed.), Culture of Epithelial Cells, pp. 159–180. New York: Wiley-Liss, 1992.
36. Schmid, H. P., and McNeal, J. E. An abbreviated standard procedure for accurate tumor volume estimation in prostate cancer. Am. J. Surg. Pathol., *16:* 184–191, 1992.
37. Lees, E., Faha, B., Dulic, V., Reed, S. I., and Harlow, E. Cyclin E/cdk2 and cyclin A/cdk2 kinases associate with p107 and E2F in a temporally distinct manner. Genes Dev., *6:* 1874–1885, 1992.
38. Lauper, N., Beck, A. R., Cariou, S., Richman, L., Hofmann, K., Reith, W., Slingerland, J. M., and Amati, B. Cyclin E2: a novel CDK2 partner in the late G_1 and S phases of the mammalian cell cycle. Oncogene, *17:* 2637–2643, 1998.
39. Yamashita, M., Fukada, S., Yoshikuni, M., Bulet, P., Hirai, T., Yamaguchi, A., Lou, Y. H., Zhao, Z., and Nagahama, Y. Purification and characterization of maturation-promoting factor in fish. Dev. Biol., *1:* 8–15, 1992.
40. Enders, G. H., Koh, J., Rustigi, A. K., Missero, C., and Harlow, E. p16 inhibition of transformed and primary squamous epithelial cells. Oncogene, *12:* 1239–1245, 1995.
41. Dulic, V., Lees, E., and Reed, S. I. Association of human cyclin E with a periodic G_1-S phase protein kinase. Science (Washington DC), *257:* 1958–1961, 1992.

42. LaBaer, J., Garrett, M., Stevenson, L., Slingerland, J., Sandhu, C., Chou, H., Fattaey, A., and Harlow, E. New functional activities for the p21 family of cdk inhibitors. Genes Dev., *11:* 847–862, 1997.
43. Slingerland, J. M., Hengst, L., Pan, C-H., Alexander, D., Stampfer, M. R., and Reed, S. I. A novel inhibitor of cyclin-Cdk activity detected in transforming growth factor β-arrested epithelial cells. Mol. Cell. Biol., *14:* 3683–3694, 1994.
44. Sherwood, S. W., Rush, D., Ellsworth, J. L., and Schimke, R. T. Defining cellular senescence in IMR-90 cells: a flow cytometric analysis. Proc. Natl. Acad. Sci. USA, *85:* 9086–9090, 1988.
45. Cristofalo, V. J., and Sharf, B. B. Cellular senescence and DNA synthesis. Thymidine incorporation as a measure of population age in human diploid cells. Exp. Cell Res., *76:* 419–427, 1973.
46. Allsopp, R. C., Vaziri, H., Patterson, C., Goldstein, S., Younglai, E. V., Futcher, A. B., Greider, C. W., and Harley, C. B. Telomere length predicts replicative capacity of human fibroblasts. Proc. Natl. Acad. Sci. USA, *89:* 10114–10118, 1992.
47. Stein, G. H., Drullinger, L. F., Robetorye, R. S., Pereira-Smith, O. M., and Smith, J. R. Senescent cells fail to express cdc2, cycA, and cycB in response to mitogen stimulation. Proc. Natl. Acad. Sci. USA, *88:* 11012–11016, 1991.
48. Dulic, V., Drullinger, L. F., Lees, E., Reed, S. I., and Stein, G. H. Altered regulation of G_1 cyclins in senescent human diploid fibroblasts: accumulation of inactive cyclin E/Cdk2 and cyclin D1/Cdk2 complexes. Proc. Natl. Acad. Sci. USA, *90:* 11034–11038, 1993.
49. Lucibello, F. C., Sewing, A., Brusselbach, S., Burger, C., and Muller, R. Deregulation of cyclins D1 and E and suppression of cdk2 and cdk4 in senescent human fibroblasts. J. Cell Sci., *105:* 123–133, 1993.
50. Afshari, C. A., Vojta, P. J., Annab, L. A., Futreal, P. A., Willard, T. B., and Barrett, J. C. Investigation of the role of G_1/S cell cycle mediators in cellular senescence. Exp. Cell Res., *209:* 231–237, 1993.
51. Robetorye, R. S., Nakanishi, M., Venable, S. F., Pereira-Smith, O. M., and Smith, J. R. Regulation of p21$^{Sdi1/Cip1/Waf1/Imda-6}$ and expression of other cyclin-dependent kinase inhibitors in senescent human cells. Mol. Cell. Differ., *4:* 113–126, 1996.
52. Sayama, K., Shirakata, Y., Midorikawa, K., Hanakawa, Y., and Hashimoto, K. Possible involvement of p21 but not of p16 or p53 in keratinocyte senescence. J. Cell. Physiol., *179:* 40–44, 1999.
53. Erickson, S., Sangfelt, O., Heyman, M., Castro, J., Einhorn, S., and Grander, D. Involvement of the Ink4 proteins p16 and p15 in T-lymphocyte senescence. Oncogene, *17:* 595–602, 1998.
54. Jarrard, D. F., Sarkar, S., Shi, Y., Yeager, T. R., Magrane, G., Kinoshita, H., Nassif, N., Meisner, L., Newton, M. A., Waldman, F. M., and Reznikoff, C. A. p16/pRb pathway alterations are required for bypassing senescence in human prostate epithelial cells. Cancer Res., *59:* 2957–2964, 1999.
55. Sandhu, C., Garbe, J., Daksis, J., Pan, C-H., Bhattacharya, N., Yaswen, P., Koh, J., Slingerland, J., and Stampfer, M. R. Transforming growth factor β stabilizes p15^{INK4B} protein, increases p15^{INK4B}-cdk4 complexes and inhibits cyclin D1/cdk4 association in human mammary epithelial cells. Mol. Cell. Biol., *17:* 2458–2467, 1997.
56. Parry, D., Bates, S., Mann, D. J., and Peters, G. Lack of cyclin D-Cdk complexes in Rb-negative cells correlates with high levels of p16INK4/MTS1 tumour suppressor gene product. EMBO J., *14:* 503–511, 1995.
57. Vlach, J., Hennecke, S., and Amati, B. Phosphorylation-dependent degradation of the cyclin-dependent kinase inhibitor p27^{Kip1}. EMBO J., *16:* 5334–5344, 1997.
58. Sheaff, R. J., Groudine, M., Gordon, M., Roberts, J. M., and Clurman, B. E. Cyclin E-CDK2 is a regulator of p27Kip1. Genes Dev., *11:* 1464–1478, 1997.
59. Kawada, M., Yamagoe, S., Murakami, Y., Suzuki, K., Mizuno, S., and Uehara, Y. Induction of p27Kip1 degradation and anchorage independence by Ras through the MAP kinase signaling pathway. Oncogene, *15:* 629–637, 1997.

0022-5347/00/1643-0836/0
THE JOURNAL OF UROLOGY®
Copyright © 2000 by AMERICAN UROLOGICAL ASSOCIATION, INC.®
Vol. 164, 836–841, September 2000
Printed in U.S.A.

BREFELDIN A INDUCES p53 -INDEPENDENT APOPTOSIS IN PRIMARY CULTURES OF HUMAN PROSTATIC CANCER CELLS

ERIC WALLEN, ROBERT G. SELLERS AND DONNA M. PEEHL*

From the Department of Urology, Stanford University Medical Center, Stanford, California

ABSTRACT

Purpose: The objective of this study was to investigate growth-inhibitory and apoptotic activity of the experimental antitumor drug, brefeldin A (BFA), on primary cultures of human epithelial cells derived from prostatic adenocarcinomas.

Materials and Methods: Clonal assays were performed to evaluate the effects of BFA on growth of prostatic cancer cell strains. Loss of cell viability in response to BFA was assessed by trypan blue exclusion. Induction of apoptosis by BFA was evaluated by morphologic criteria, electrophoretic assay of DNA fragmentation, and a cell death ELISA. Immunoblots were used to monitor p53 and pRB expression in response to BFA.

Results: BFA was growth-inhibitory at a half-maximal concentration of 5 ng./ml. (18 nM). Morphological manifestations of apoptosis were evident by 24 hours of treatment. Cell viability declined and the cell death ELISA indicated an 18-fold increase in apoptosis in BFA-treated versus untreated cells at 48 hours. DNA fragmentation was also seen at 48 hours. Levels of p53 were not altered by BFA, but pRB was maintained in a hypophosphorylated state by BFA treatment.

Conclusions: BFA is a potent inducer of apoptosis in prostatic cancer cells via a p53-independent mechanism. Cells derived from low-grade as well as high-grade cancers responded similarly to BFA. Since p53-mediated pathways of apoptosis may frequently be abrogated in prostatic cancer cells, agents such as BFA that induce p53-independent cell death may be promising candidates for chemotherapeutic agents.

KEY WORDS: prostate cancer, p53, apoptosis, chemotherapy, brefeldin A

In 1999, it was estimated that 179,300 men would be diagnosed with cancer of the prostate, and that 37,000 men would die from the disease.[1] For cancers not entirely confined to the prostate, there are few options for longterm control of the disease. Despite investigations of the roles of known oncogenes and tumor suppressor genes, no unifying explanation of the molecular events involved in prostate cancer initiation and progression has been found, and therefore a molecular target for therapy remains elusive.

Recent advances in the understanding of apoptotic (programmed cell death) pathways have led to investigations of molecular promoters and inhibitors of apoptosis in the prostate. Cell growth and death are likely mediated by the balance of promoters of apoptosis (such as fas, bax, bad, bcl-xs and others) and inhibitors of the process (bcl-2, bcl-xl, jun, abl, mdm-2).[2] These factors exert their cumulative effects in part by modulating the activity of regulators of the cell cycle, such as p53 and pRB.

The p53 tumor suppressor gene product possesses the ability to stop a cell from proceeding through the cell cycle to mitosis in response to DNA damage, until the damage is repaired.[3] If repair is ineffective, p53 may direct the cell to undergo apoptosis. We have found that these functions of p53 appear to be attenuated in normal prostatic epithelial cells or in cells derived from prostatic adenocarcinomas, despite the presence of the wild-type p53 gene.[4] In response to numerous DNA-damaging agents or events (chemicals, irradiation, or hypoxia), primary cultures of prostatic epithelial cells do not induce p53 or undergo cell-cycle arrest in G_1 or undergo apoptosis. Many standard chemotherapeutic drugs exert their effects by activating a p53-dependent pathway of apoptosis.[5,6] The apparent absence of this pathway in prostatic epithelial cells, even in those with wild-type p53, may explain why these therapies are ineffective for the treatment of prostate cancer. Prostate cancer cells with mutant p53, which occurs fairly frequently in advanced disease,[7] would also be unresponsive to agents that require p53 for activity.

For this reason, it would be desirable to identify agents which exploit p53-independent pathways of apoptosis in prostate cancer cells. A large in vitro drug screen conducted under the auspices of the National Cancer Institute (NCI) identified brefeldin A (BFA) as an agent which markedly inhibited growth of primary cultures of epithelial cells grown from prostatic adenocarcinomas.[8] BFA showed some specificity for prostate cancer cells, with the half-maximal inhibitory dose for prostate cells about 10- to 100-fold lower than for a panel of cell lines derived from eight other types of malignancies.

BFA, a fungal macrolytic lactone, acts to inhibit intracellular transport by disrupting the vesicular coating process, thereby preventing transport of proteins from the endoplasmic reticulum to the Golgi and causing disintegration of the Golgi complex.[9,10] Because of this property, BFA has been extensively used as a tool to study mechanisms of protein secretion. Effects of BFA, though, are seemingly not limited to those on the Golgi apparatus. BFA has been shown to cause apoptosis in diverse human cancer cell lines, including those derived from leukemia, colon and prostate cancer.[11–15] The mechanism by which BFA induces apoptosis has not yet been elucidated, but the process appears to be p53-independent.

The purpose of our study was to establish and elucidate possible growth-inhibitory mechanisms, including apoptosis, of BFA on primary cultures of prostatic cell strains derived

Accepted for publication March 24, 2000.
* Requests for reprints: Department of Urology, Stanford Medical Center, Stanford, CA 94305-5118.
Supported by Department of the Army Grant DAMD 17-99-1-9004.

from adenocarcinomas of the prostate. Our results show that BFA induced apoptosis by a p53-independent pathway and caused a shift in the phosphorylation state of pRB. Our results support the potential of BFA as a chemotherapeutic agent against prostate cancer.

MATERIALS AND METHODS

Cell culture. Tissue samples were dissected from radical prostatectomy specimens. None of the patients had received prior chemical, hormonal or radiation therapy. Histological assessment was performed by Dr. John McNeal as previously described.[16] Epithelial cells were cultured and characterized as described previously.[17] Four cell strains used in this study were derived from tumors of Gleason grade 3+4 (E-CA-2), 4+3 (E-CA-1, E-CA-4), and 5+5 (E-CA-3). An additional cell strain (E-PZ-5) was derived from histologically normal tissue with no evidence of cancer. Both p53 and pRB genes in these cell strains were wild-type.

Clonal growth assays. Secondary passaged cells were grown to about 50% confluency, then were harvested by trypsinization. Clonal growth assays were initiated by inoculating 200 or 500 cells into each 60-mm. collagen-coated dish[17] containing 5 ml. of medium. Growth medium was MCDB 105 (Sigma, St. Louis, MO) supplemented with 10 ng./ml. of cholera toxin, 10 ng./ml. of epidermal growth factor, 10 μg./ml. of bovine pituitary extract, 4 μg./ml. of insulin, 1 μg./ml. of hydrocortisone, 0.1 mM phosphoethanolamine, 30 nM selenium, 0.03 nM all-trans retinoic acid, 2.3 μM α-tocopherol and 100 μg./ml. gentamicin. The sources and preparation of these supplements were previously described.[17]

A stock solution of 1 mg./ml. (3.6 mM) of BFA (Sigma) was prepared in 100% ethanol and stored at −20C. Dilutions were made in media and the ethanol concentration was kept constant at 0.01% in control and experimental media. After incubation in a humidified atmosphere of 5% CO_2/95% air at 37C for 10 days without feeding, the cells were fixed in 10% formalin and stained with crystal violet.[17] An Artek image analyzer (Dynatech, Chantilly, VA) was used to measure the total area of each dish covered by cells, which is directly proportional to cell number.[18] Triplicate dishes were tested for each control and experimental variable, and each experiment was performed twice. The Student's *t* test was used to evaluate significance.

Cell viability. Loss of cell viability was assessed by the trypan blue exclusion method. Cells treated with or without BFA were harvested by trypsinization. After incubation in 0.04% trypan blue (Sigma) for 4 minutes, cells were counted under a hemocytometer. The number of cells which retained the dye (nonviable) and the total cell number were noted.

Detection of apoptosis. Induction of apoptosis by BFA was evaluated by two methods. In the first assay, DNA laddering was monitored. Cells were treated with or without BFA and DNA was extracted at 0, 8, 24 and 48 hours.[19] Briefly, 10^6 cells were collected at each time point and pelleted in an Eppendorf tube. The cell pellet was suspended in 1 ml. of 0.02% EDTA in buffered saline, then the cells were pelleted again. TE lysis buffer (0.25% NP-40 in TE buffer, pH 8.0) (35 μL) and Rnase A (10 μL of a 10 mg./ml. stock) were added to each tube and the cells were suspended by gentle vortexing. After incubation at 37C for 20 minutes, 5 μL of proteinase K (from a 20 mg./ml. stock solution) were added to each tube. Following incubation for 20 minutes at 37C, aliquots of 25 μL each were mixed with loading buffer and analyzed by electrophoresis on a 1.8% agarose gel run at 40 V for 4 hours. DNA was visualized by staining with ethidium bromide and photographed under UV light.

Apoptosis was also evaluated with a cell death ELISA kit (Boehringer Mannheim, Indianapolis, IN) which utilizes a monoclonal antibody against histone to detect DNA fragments in the cytosolic fraction of lysed cells. Cells treated with or without BFA were harvested and lysed according to the manufacturer's instructions. The samples were transferred into 96-well dishes coated with a mouse monoclonal antibody against histone. After incubation and washing, anti-DNA-peroxidase was added to the wells. The reaction was developed with substrate supplied by the manufacturer and the absorbance of the wells was read at 410 nm. The ratio of the absorbance of the treated cells to the untreated cells was calculated as an enrichment factor, which provides a qualitative assessment of apoptosis.

Immunoblot analysis. Cells were grown to approximately 50% confluency. At time 0, cells were fed media containing 0 or 25 ng./ml. of BFA. At times 0, 3, 6, 24, and 48 hours after treatment, cell lysates were prepared by collecting trypsinized cells and solubilizing in lysis buffer (0.1 M Tris-HCL, pH 6.8, 1% SDS, 5% glycerol, 0.005% bromophenol blue, 0.005% pyronine Y and 1% β-mercaptoethanol). Aliquots of 20 μL containing lysate derived from 50,000 cells were loaded into each lane of a polyacrylamide-sodium dodecyl sulfate (PAGE-SDS) gel with a 4.6% stacking gel and a 10% running gel.

After separation of proteins by electrophoresis, the samples were transferred out of the gel onto nitrocellulose membrane, using a Transblot apparatus run at 1.5 mA for 90 minutes. Membranes were blocked overnight with 10% horse serum, then incubated with primary antibodies against p53 (Pharmingen, San Diego, CA; clone DO-1, used at 1:100) or pRB (Pharmingen, clone G3-245, used at 1:1000). Bound antibodies were detected using biotinylated secondary antibody (Vector Laboratories, Burlingame, CA, at 1:4000) and the ABC reagent (Vector Laboratories). TMB membrane reagent (Amresco, Solon, OH) was used to develop the color reaction.

RESULTS

Effect of BFA on cell growth. Clonal assays were used to evaluate the effect of BFA on growth of prostatic cancer cells. BFA was first tested at concentrations ranging from 0.1 to 100 ng./ml. and total growth after 10 days was compared with growth in the absence of BFA. Figure 1 shows the marked decrease in growth which occurred at concentrations of BFA between 1 and 10 ng./ml. At 1 ng./ml., growth was almost 100% of control, whereas with 10 ng./ml., growth dramatically declined to 20% of control. This pattern of inhibition was seen with all four cancer cell strains that were tested, as well as with one cell strain derived from normal tissue.

To more precisely determine the concentration of BFA which half-maximally inhibited clonal growth, the cancer cell strain E-CA-4 was tested in a clonal assay with a narrow range of BFA concentrations. In this assay, half-maximal growth inhibition was observed at 5 ng./ml. (18 nM) of BFA (fig. 2).

Effect of BFA on cell viability. Cells treated with BFA were incubated with trypan blue to evaluate the proportion of nonviable cells in treated versus untreated populations. Viable cells quickly exclude trypan blue, whereas nonviable cells retain trypan blue in their cytoplasm. After 48 hours of treatment with 25 ng./ml. of BFA, cells were trypsinized and incubated with trypan blue. The fraction of cells which retained trypan blue was evaluated microscopically with a hemocytometer. Two cell strains were evaluated. Untreated E-CA-1 cells had an average of 11 ± 3% nonviable cells at 48 hours, while BFA-treated cells averaged 27 ± 0% nonviable cells. Similarly, nonviable cells averaged 41 ± 6% in BFA-treated E-CA-4 populations, versus 11 ± 1% in untreated cells.

Morphological appearance of cells after treatment with BFA. The morphological appearance of cells during treat-

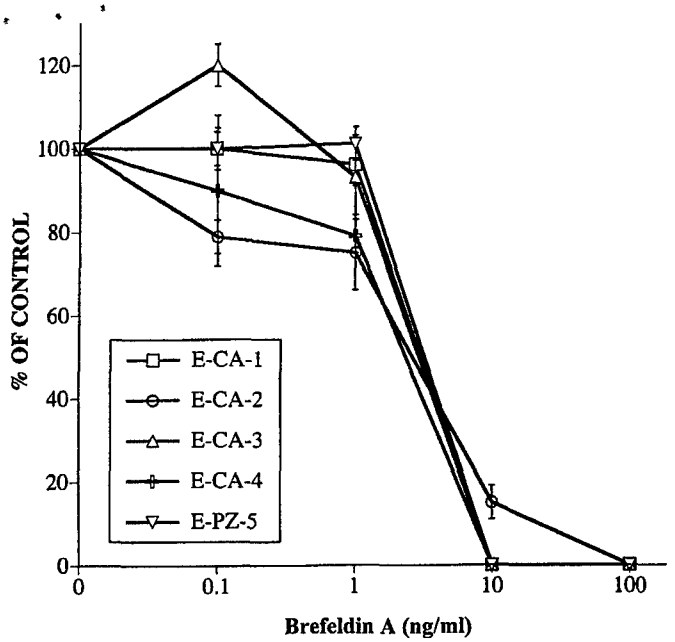

FIG. 1. Inhibition of clonal growth by BFA. On day 0, four cell strains derived from cancers (E-CA-1, E-CA-2, E-CA-3 or E-CA-4) and one cell strain from normal tissue (E-PZ-5) were inoculated at 200 or 500 cells per dish into growth medium with indicated concentrations of BFA. After 10 days of incubation, cells were fixed and stained and total growth was quantitated. For each cell strain, growth in absence of BFA was set at 100%. Each point represents average of duplicate experiments, with three dishes per point in each experiment, ± SEM.

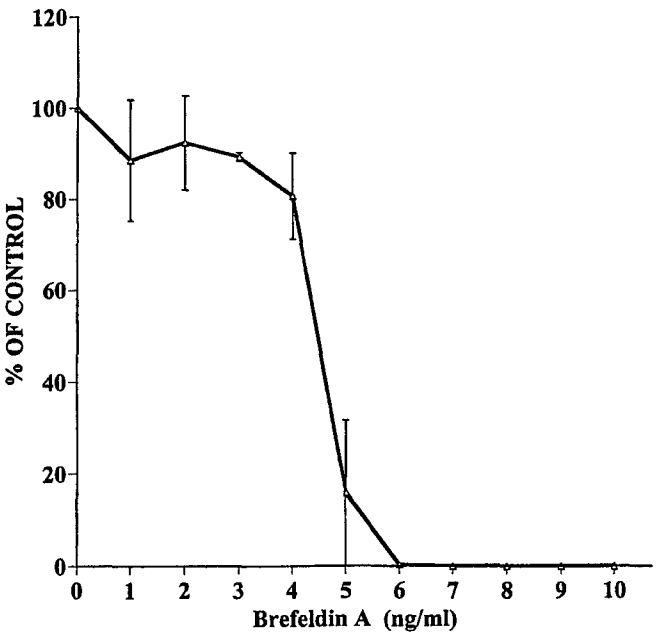

FIG. 2. Determination of half-maximal growth-inhibitory dose of BFA. On day 0, E-CA-4 cells were inoculated at 200 cells per dish into growth medium with indicated concentrations of BFA. After 10 days of incubation, cells were fixed and stained and total growth was quantitated. Growth in absence of BFA was set as 100%. Each point represents average of duplicate experiments, with three dishes per point in each experiment, ± SEM.

ment with BFA was observed microscopically. Morphological changes consistent with apoptosis were seen in treated cells as early as 24 hours after the initiation of treatment, and increased by 48 hours. These characteristic changes included cell shrinkage, nuclear condensation, membrane blebbing, and detachment from the substrate (fig. 3).

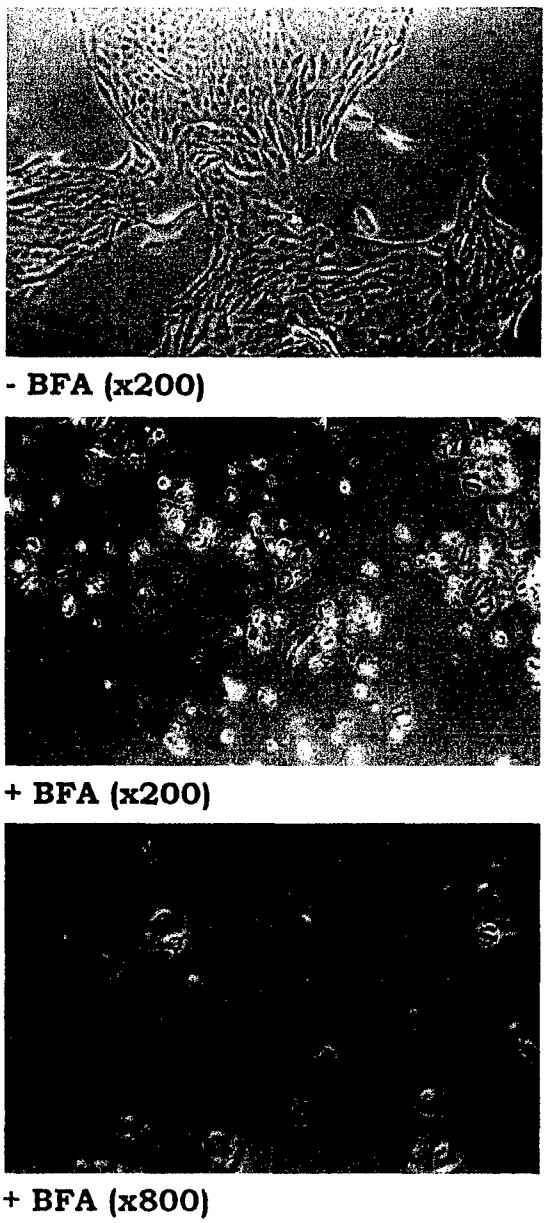

FIG. 3. Morphological characteristics of apoptosis. Semi-confluent populations of E-CA-4 cells were grown with or without 25 ng./ml. of BFA and photographed at 72 hours. Top panel: cells grown without BFA (x200); middle panel: cells grown with BFA (x200); bottom panel: cells grown with BFA (x800).

DNA laddering in response to BFA. Semi-confluent cultures of E-CA-4 cells were treated with or without 25 ng./ml of BFA. DNA was extracted at times 0, 8, 24 and 48 hours of treatment. Gel electrophoresis demonstrated a DNA laddering pattern of 180 bp subunits, characteristic of apoptosis, at 48 hours after treatment with BFA (fig. 4).

Measurement of relative levels of apoptosis. A cell death ELISA was used to measure relative apoptosis in untreated versus treated cultures. E-CA-4 cells were treated with or without 25 ng./ml. of BFA for 48 hours, then were harvested for the cell death ELISA, which detects DNA fragments in the cytosol with an antibody against histone. By this assay, apoptosis was 18-fold higher in BFA-treated cultures compared with untreated cultures.

Induction of p53 by BFA. Immunoblot analysis was used to examine levels of p53 protein during BFA treatment. Cells were treated with or without 10 ng./ml. of BFA. At times 0, 3, 6, 24, and 48 hours of treatment, cell lysates were prepared.

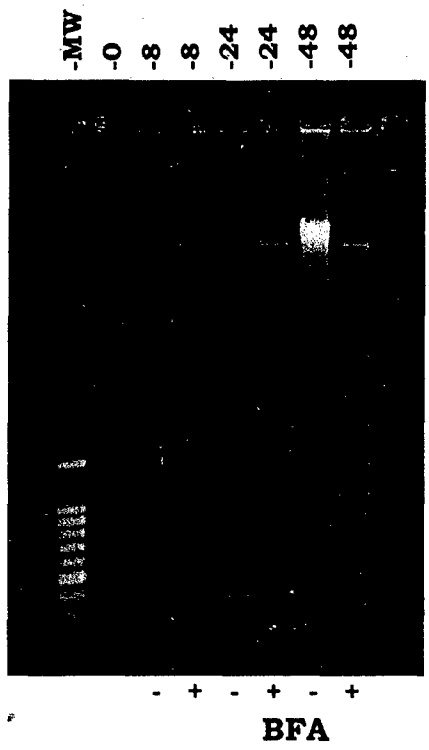

FIG. 4. DNA laddering in response to BFA. E-CA-4 cells were treated with or without 25 ng./ml. of BFA for 0, 8, 24 or 48 hours. DNA was extracted and electrophoresed on 1.8% agarose gel, followed by ethidium bromide staining. Molecular weight ladder (123 bp) was run as marker.

Proteins were separated by PAGE-SDS and transferred to filters. Monoclonal antibody specific for p53 was used to detect p53 protein expression. Protein levels of p53 in E-CA-2 cells remained low throughout the course of the experiment regardless of the presence or absence of BFA (fig. 5). As a control for the induction of p53 in these cells, we treated with an inhibitor of RNA transcription (DRB) for 24 hours. As expected, p53 protein levels increased, presumably due to inhibition of transcription of mdm-2, which targets p53 for degradation. This lack of induction of p53 protein by BFA was also seen in E-CA-1 and E-CA-3 cells.

Phosphorylation of pRB. Prostate cancer cells were grown to semi-confluency and fed 3 days before the start of the experiment. At time 0, cells were fed fresh media with or without 25 ng./ml. BFA. Cell lysates were prepared at times 0, 3, 6, 24 and 48 hours. Immunoblot analysis was performed to evaluate expression and phosphorylation of pRB (fig. 6). At times 0, 3 and 6 hours, untreated and treated cells had no immunoreactive pRB band of the size associated with the hyperphosphorylated state. However, at times 24 and 48 hours, untreated cells had bands typical of both hyperphosphorylated and hypophosphorylated pRB. This would be expected of cells entering the proliferative phase in response to feeding fresh medium at time 0. In contrast, lysates from BFA-treated cells exhibited only hypophosphorylated pRB, indicating blockage of cell progression into the proliferative cycle.

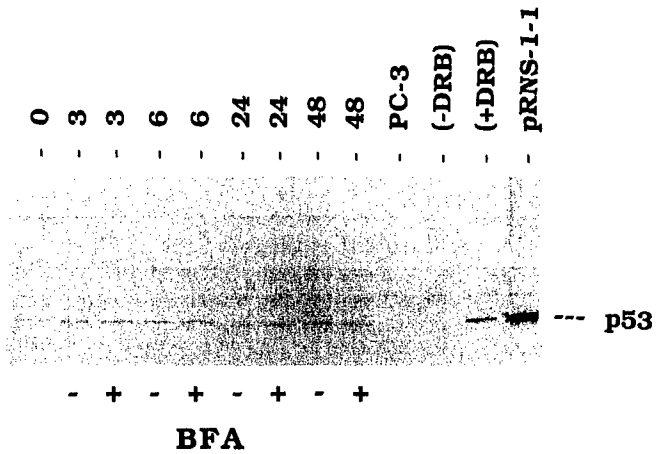

FIG. 5. Protein levels of p53 in response to BFA. E-CA-2 cells were treated with or without 10 ng./ml. of BFA and cell lysates were prepared at 0, 3, 6, 24 and 48 hours. Immunoblots were used to detect p53 protein. Control cells were SV40-transformed prostatic epithelial cells (pRNS-1-1), which have high levels of p53 protein, and E-CA-4 cells treated with DRB for 24 hours. PC-3 cells, which lack p53 expression, served as negative control. Equal loading of lysates in lanes is indicated by equivalent intensities of nonspecific bands.

DISCUSSION

Substantial evidence for unique growth-inhibitory and apoptotic activity of BFA is accumulating. Although first tested for anti-tumor activity more than 30 years ago, BFA did not demonstrate activity in murine models in use at the time and interest in BFA declined.[8] It is now known that murine cells are relatively resistant to BFA,[20] and promising activity of BFA in in vitro and in vivo models of human cancer has rekindled interest in this compound.[8]

Our interest in BFA was first aroused when we tested this compound in a drug screen for the NCI. In this screen, cells from four prostate cancer cell strains derived from tumors of Gleason grades 3, 4 or 5 were inoculated into 96-well microtiter dishes and exposed to experimental compounds for six days.[21] At the end of this assay, growth was evaluated by the sulforhodamine B assay, which measures total protein.[22] Using this assay, we discovered that BFA was a potent inhibitor of prostate cancer cell growth, with half-maximal growth inhibition at approximately 20 nM.[8] This value is almost exactly the concentration that we found for half-maximal inhibition of clonal growth in the current study.

Furthermore, when compared with a panel of cell lines from other types of human tumors that were evaluated at the NCI, prostate cancer cells were the most sensitive to growth inhibition by BFA. Melanoma cells, the most sensitive of the other types of cancers in the screen performed at the NCI, demonstrated half-maximal growth inhibition with approximately 29 nM of BFA.[8] The potent and differential activities of BFA on prostate cancer cell strains suggest that BFA might be a particularly effective chemotherapeutic agent for prostate cancer with minimal toxicity to other organs.

Analysis of patterns of growth inhibition in the NCI in vitro cancer agent screen suggests that agents with similar

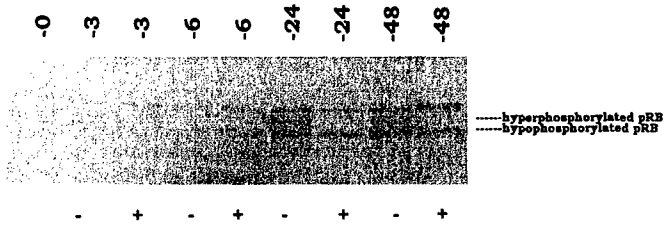

FIG. 6. Levels of pRB in response to BFA. E-CA-2 cells were treated with or without 10 ng./ml. of BFA and cell lysates were prepared at 0, 3, 6, 24 and 48 hours. Immunoblots were used to detect pRB protein. Bands corresponding to hyper- and hypophosphorylated pRB are indicated; nonspecific band at higher molecular weight serves as loading control and indicates equivalent loading of lysates from treated and untreated cells.

mechanisms of antiproliferative action yield similar patterns of growth inhibition.[23,24] Unique patterns of activity may therefore indicate potentially novel or unique mechanisms of action. It is intriguing that when this analysis was applied to BFA, a unique pattern of susceptibility that didn't resemble the pattern generated by known cytotoxic agents was noted. Therefore, identifying the mechanism of action of BFA on prostate cells becomes particularly relevant to further development of this or related agents as novel chemotherapeutic agents.

The NCI drug screen was not designed to investigate mechanisms of action of experimental compounds. Therefore, in our current studies, we developed additional assays to further define BFA's activity on prostate cancer cells.

One striking observation regarding BFA is the very steep concentration - effect relationship that has been found in diverse studies. In our assays, we found that 1 ng./ml. of BFA produced almost no effect on cell growth, whereas 10 ng./ml. of BFA completely inhibited growth. By testing a narrow range of concentrations, we demonstrated that half-maximal growth inhibition occurred at 5 ng./ml. (18 nM) of BFA. Similarly, inhibitory concentrations of BFA for the prostate cancer cell lines PC-3 and LNCaP were between 10 and 100 nM in the NCI screen[8] and between 10 and 30 ng./ml. (36 and 108 nM) in experiments performed with PC-3 and another cancer cell line, DU 145, by various other investigators.[14,15] This narrow range of effective concentrations of BFA is not peculiar to prostate cells but was also noted in studies with leukemia and colon carcinoma cell lines.[11]

During the course of the growth assays, it became apparent that BFA induced dramatic morphologic changes in the treated prostate cancer cell strains. These changes were reminiscent of those occurring during the process of apoptosis and included membrane blebbing, shrinkage of cytoplasm, and detachment from the substratum. To further assess the induction of apoptosis by BFA, we measured viability by trypan blue exclusion and found that the percentage of nonviable cells in the population increased significantly by 48 hours after exposure to BFA. The results of a cell death ELISA further indicated that nonviability was due to apoptosis, and that the number of apoptotic cells was enhanced 18-fold after 48 hours of BFA-treatment. Finally, the presence of DNA laddering, a classic manifestation of apoptosis, was demonstrated in treated cells.

The time course of induction of apoptosis in prostate cancer cell strains is reminiscent of that reported for the K562 human leukemia cell line and the HT-29 colon carcinoma cell line, but is much slower than that found for HL60 cells, in which DNA laddering was visible after only 15 hours of BFA-treatment.[11] Interestingly, although BFA induced apoptosis in DU 145 cells,[15] it did not do so in PC-3 cells.[14] BFA-treatment caused growth inhibition and detachment of a majority of PC-3 cells after 72 hours of treatment, but >85% of those cells were still viable and the effects were reversible upon removal of BFA. PC-3 cells were found to be blocked in the G_1 - phase of the cell cycle by BFA; in preliminary studies, we did not find this to be the case for prostatic cancer cell strains (data not shown).

Effective chemotherapy for cancer of the prostate is lacking. We hypothesize that the chemoresistance of prostate cancer may be due in part to an attenuated response of p53 in prostatic epithelial cells. While the exact role of p53 in regulating chemosensitivity is still under investigation,[25] in at least some types of cells, p53 enhances chemosensitivity by promoting apoptosis. Mutation of p53 in prostate cancer is seemingly less frequent than in some other cancers and is generally a late event,[26] so loss of p53 activity would not be predicted to play a large role in chemoresistance of prostate cancer. However, we observed that prostate cancer cells with wild-type p53 did not induce p53 or undergo cell arrest or apoptosis in response to DNA-damaging drugs or radiation.[4] This lack of activity of p53, despite the widespead maintainance of wild-type p53 in prostate cancer, may therefore explain lack of activity of chemotherapeutic agents, many of which induce apoptosis through p53-mediated pathways. These observations suggest that effective new therapies for prostate cancer will be based on agents that induce p53-independent pathways of cell arrest or apoptosis.

BFA appears to be one such agent that is capable of inducing p53-independent cell arrest or apoptosis. Treatment of several human leukemia or colon carcinoma cell lines with BFA induced apoptosis in a p53-independent manner.[11] Other investigators have shown that PC-3 cells, which have mutated p53, are growth-inhibited by BFA. We found that apoptosis of prostate cancer cell strains induced by BFA was also p53-independent. After 3 to 48 hours of exposure to BFA, levels of p53 protein remained low in treated and untreated cells.

On the other hand, Mordente et al showed that BFA-treatment of PC-3 cells modulated phosphorylation of pRB.[14] In their experiments, substantial levels of hyperphosphorylated and hypophosphorylated pRB were present at 24 hours in treated and untreated cells. Declining levels of hyperphosphorylated pRB were seen after 48 hours of BFA-treatment, and by 72 hours, hypophosphorylated pRB was the main form present in the treated cells. Our results were similar. At 48 hours, both hyperphosphorylated and hypophosphorylated pRB were present in untreated prostate cancer cell strains, whereas only hypophosphorylated pRB was present in BFA-treated cells. Although these results suggest that modulation of pRB is part of the mechanism of action of BFA on prostate cancer cells, DU 145 cells with defective pRB nevertheless underwent apoptosis in response to BFA with no change in the phosphorylation status of pRB.[14]

The potent growth-inhibitory and apoptosis-inducing properties of BFA against prostate cancer cells make this compound an interesting candidate for chemotherapeutic application against prostate cancer. Although activity of BFA in human xenograft models of prostate cancer has not yet been reported, in vivo antitumor activity of BFA has been shown against human melanoma xenografts.[8] Certainly, however, BFA has properties that diminish its appeal as a therapeutic drug. For one, it is poorly soluble in aqueous medium, making clinical application problematic. In addition, the very narrow range of toxic concentrations may make dosing difficult. The slow nature of its action and potential reversibility also are problematic.

Nevertheless, these problems may be overcome or modified as we learn more about the mechanism of action of BFA. In their investigations of the effects of BFA on leukemic and colon cancer cell lines, Shao et al found that BFA potentiated induction of apoptosis by protein kinase C inhibitors.[11] BFA was less enhancing with inhibitors of topoisomerase inhibitors, suggesting that BFA may act more selectively through the apoptosis pathway mediated by protein kinase C inhibitors than the pathway induced by DNA damage. Particularly exciting is the recent discovery that BFA specifically inhibits a Golgi - associated guanine nucleotide exchange activity for the small GTP-binding protein ADP-ribosylation factor 1 (ARF1).[27] It has been suggested that inhibition by BFA of ARF1 activation by trapping the exchange reaction in a dead-end complex may have profound implications on the development of drugs targeting other exchange factors for small G proteins.[28] The fact that different ARF exchange factors have different sensitivities to BFA may be the basis for the differential sensitivity of cells derived from different organs to BFA. Further studies such as these will identify the molecular mechanisms of BFA activity and contribute to the development of novel therapeutic agents.

REFERENCES

1. Landis, S. H., Murray, T., Bolden, S. and Wingo, P. A.: Cancer statistics, 1999 [see comments]. CA Cancer J Clin, **49:** 8, 1999
2. Tang, D. G. and Porter, A. T.: Target to apoptosis: a hopeful weapon for prostate cancer. Prostate, **32:** 284, 1997
3. Ko, L. J. and Prives, C.: p53: puzzle and paradigm. Genes Dev, **10:** 1054, 1996
4. Girinsky, T., Koumenis, C., Graeber, T. G., Peehl, D. M. and Giaccia, A. J.: Attenuated response of p53 and p21 in primary cultures of human prostatic epithelial cells exposed to DNA-damaging agents. Cancer Res, **55:** 3726, 1995
5. Lowe, S. W., Ruley, H. E., Jacks, T. and Housman, D. E.: p53-dependent apoptosis modulates the cytotoxicity of anticancer agents. Cell, **74:** 957, 1993
6. Hannun, Y. A.: Apoptosis and the dilemma of cancer chemotherapy. Blood, **89:** 1845, 1997
7. Navone, N. M., Troncoso, P., Pisters, L. L., Goodrow, T. L., Palmer, J. L., Nichols, W. W., von Eschenbach, A. C. and Conti, C. J.: p53 protein accumulation and gene mutation in the progression of human prostate carcinoma. J Natl Cancer Inst, **85:** 1657, 1993
8. Sausville, E. A., Duncan, K. L. K., Senderowicz, A., Plowman, J., Randazzo, P. A., Kahn, R., Malspeis, L. and Grever, M. R.: Antiproliferative effect in vitro and antitumor activity in vivo of brefeldin A. Cancer J Sci Am, **2:** 52, 1996
9. Fujiwara, T., Oda, K., Yokota, S., Takatsuki, A. and Ikehara, Y.: Brefeldin A causes disassembly of the Golgi complex and accumulation of secretory proteins in the endoplasmic reticulum. J Biol Chem, **263:** 18545, 1988
10. Pelham, H. R.: Multiple targets for brefeldin A. Cell, **67:** 449, 1991
11. Shao, R. G., Shimizu, T. and Pommier, Y.: Brefeldin A is a potent inducer of apoptosis in human cancer cells independently of p53. Exp Cell Res, **227:** 190, 1996
12. Guo, H., Tittle, T. V., Allen, H. and Maziarz, R. T.: Brefeldin A-mediated apoptosis requires the activation of caspases and is inhibited by Bcl-2. Exp Cell Res, **245:** 57, 1998
13. Konno, S., Mordente, J. A., Chen, Y., Wu, J. M., Tazaki, H. and Mallouh, C.: Effects of brefeldin A on androgen receptor-mediated cellular responses in human prostatic carcinoma LNCaPcells. Mol Urol, **2:** 7, 1998
14. Mordente, J. A., Konno, S., Chen, Y., Wu, J. M., Tazaki, H. and Mallouh, C.: The effects of brefeldin A (BFA) on cell cycle progression involving the modulation of the retinoblastoma protein (pRB) in PC-3 prostate cancer cells. J Urol, **159:** 275, 1998
15. Chapman, J. R.: Brefeldin A-induced apoptosis in prostatic cancer DU-145 cells: a possible p53-independent death pathway. Br J Urol Int, **83:** 703, 1999
16. Schmid, H. P. and McNeal, J. E.: An abbreviated standard procedure for accurate tumor volume estimation in prostate cancer. Am J Surg Pathol, **16:** 184, 1992
17. Peehl, D. M., in: Culture of Epithelial Cells. Edited by R. I. Freshney. Wiley-Liss, Inc.: New York, p 159, 1992
18. Tsao, M. C., Walthall, B. J. and Ham, R. G.: Clonal growth of normal human epidermal keratinocytes in a defined medium. J Cell Physiol, **110:** 219, 1982
19. Park, D. J. and Patek, P. Q.: Detergent and enzyme treatment of apoptotic cells for the observation of DNA fragmentation. Biotechniques, **24:** 558, 1998
20. Ishii, S., Nagasawa, M., Kariya, Y. and Yamamoto, H.: Selective cytotoxic activity of brefeldin A against human tumor cell lines. J Antibiot (Tokyo), **42:** 1877, 1989
21. Peehl, D. M., Erickson, E., Malspeis, L., Mayo, J., Camalier, R. F., Monks, A., Cronise, P., Paull, K. and Grever, M. R., in Fundamental Approaches to the Diagnosis and Treatment of Prostate Cancer and BPH. Edited by K. Imai, J. Shimazaki, and J. P. Karr. Academic Press: New York, p 57, 1994
22. Skehan, P., Storeng, R., Scudiero, D., Monks, A., McMahon, J., Vistica, D., Warren, J. T., Bokesch, H., Kenney, S. and Boyd, M. R.: New colorimetric cytotoxicity assay for anticancer-drug screening. J Natl Cancer Inst, **82:** 1107, 1990
23. Paull, K. D., Shoemaker, R. H., Hodes, L., Monks, A., Scudiero, D. A., Rubinstein, L., Plowman, J. and Boyd, M. R.: Display and analysis of patterns of differential activity of drugs against human tumor cell lines: development of mean graph and COMPARE algorithm. J Natl Cancer Inst, **81:** 1088, 1989
24. Weinstein, J. N., Myers, T. G., PM, O. C., Friend, S. H., Fornace, A. J., Jr., Kohn, K. W., Fojo, T., Bates, S. E., Rubinstein, L. V., Anderson, N. L., Buolamwini, J. K. and van Osdol, W. W.: An information-intensive approach to the molecular pharmacology of cancer. Science, **275:** 343, 1997
25. Weller, M.: Predicting response to cancer chemotherapy: the role of p53. Cell Tissue Res, **292:** 435, 1998
26. Heidenberg, H. B., Bauer, J. J., McLeod, D. G., Moul, J. W. and Srivastava, S.: The role of the p53 tumor suppressor gene in prostate cancer: a possible biomarker? Urology, **48:** 971, 1996
27. Peyroche, A., Antonny, B., Robineau, S., Acker, J., Cherfils, J. and Jackson, C. L.: Brefeldin A acts to stabilize an abortive ARF-GDP-Sec7 domain protein complex: involvement of specific residues of the Sec7 domain. Mol Cell, **3:** 275, 1999
28. Chardin, P. and McCormick, F.: Brefeldin A: the advantage of being uncompetitive. Cell, **97:** 153, 1999

Cell Death Diff., in press

Role of glutathione depletion and reactive oxygen species generation in apoptotic signaling in a human B lymphoma cell line.

Jeffrey S. Armstrong[1], Kirsten K. Steinauer[2], **Brita Hornung[3]**, **Jonathan M. Irish[4]**, **Philip Lecane[5]**, Geoff Birrell[6], Donna M. Peehl[7] and Susan J. Knox[8]

Departments of Radiation Oncology[1,2,3,6,8], Urology[5,7], and **Molecular Pharmacology[4]**, Stanford University, Stanford, California CA 94305-5105, USA

[1,2] These authors contributed equally to this work.

Running title: reactive oxygen species and apoptosis

Correspondence and reprint requests:
Susan J. Knox M.D. Ph.D.[5]
Department of Radiation Oncology
Stanford University Medical Center
300 Pasteur Drive
Stanford, CA 943053
Tel. (650) 725-2720
Fax. (650) 498-4093
email: knox@.stanford.edu

[1] This work was supported by grant number PHS NRSA 5T32 CA09302, the [2]Kurt and Senta Herrmann-Foundation and the Swiss Cancer League (Zuerich), [3]Department of the Army DAMD 17-99-1-9004 (DMP and PL), **and [4]The James H. Clark Stanford Graduate Fellowship.**

ABSTRACT

The primary objective of this study was to determine the sequence of biochemical signaling events that occur after modulation of the cellular redox state in the B cell lymphoma line, PW, with emphasis on the role of mitochondrial signaling. L- Buthionine sulphoximine (BSO), which inhibits gamma glutamyl cysteine synthetase (γGCS), was used to modulate the cellular redox status. The sequence and role of mitochondrial events and downstream apoptotic signals and mediators was studied. After BSO treatment, there was an early decline in cellular glutathione (GSH), followed by an increase in reactive oxygen species (ROS) production, which induced a variety of apoptotic signals (detectable at different time points) in the absence of any external apoptotic stimuli. The sequence of biochemical events accompanying apoptosis included a 95% decrease in total GSH and a partial (25%) preservation of mitochondrial GSH, without a significant increase in ROS production at 24 hours.

Early activation and nuclear translocation of the nuclear factor kappa B subunit Rel A was observed at approximately 3 hours after BSO treatment. Cytochrome c release into the cytosol was also seen after 24 h of BSO treatment. p53 protein expression was unchanged after redox modulation **for** up to **72 h**, and p21 ^{wafl} independent loss of cellular proliferation was observed. Surprisingly, a truncated form of p53 was expressed in a time dependent manner, beginning at 24 h after BSO incubation. Irreversible commitment to apoptosis occurred between **48 and 72h** after BSO treatment when mitochondrial GSH was depleted, and there was an increase in ROS production. Procaspase 3 protein levels showed a time dependent reduction following incubation with BSO, notably after 48 h, that corresponded with increasing ROS levels. At 96 h, caspase 3 cleavage products were detectable. The pan-caspase inhibitor zVADfmk, partially blocked the induction of apoptosis at 48 h, and was ineffective after 72 h.

PW cells could be rescued from apoptosis by removing them from BSO after up to 48, but not 72 h incubation with BSO. Mitochondrial transmembrane potential ($\Delta\Psi_m$) remained intact in most of the cells during the 72 h observation period, indicating that $\Delta\Psi_m$ dissipation is not an early signal for the induction of redox dependent apoptosis in PW cells. These data suggest that a decrease in GSH alone can act as a potent early activator of apoptotic signaling. Increased ROS production following mitochondrial GSH depletion, represents a crucial event, which irreversibly commits PW cells to apoptosis.

KEY WORDS

apoptosis
reactive oxygen species
GSH
mitochondria
redox

INTRODUCTION

Therapeutic strategies designed to increase the susceptibility of tumor cells to apoptosis have the potential to significantly augment the efficacy of a variety of cancer treatments. We have previously shown that enhancement of the apoptotic potential of tumor cells increases tumor responses to radiotherapy (1). Many chemotherapeutic agents have profound effects on the cellular redox status (2-4), and alteration of redox status may play an important role in the induction of apoptosis (5-8). We have recently reported that changes in the redox status of cells can modulate the sensitivity of tumor cells to apoptosis induced by uncoupling mitochondrial electron transport with the protonophore carbonyl cyanide *m*-chlorophenylhydrazone (8).

Cellular redox potential is largely determined by glutathione (GSH), which accounts for more than 90% of cellular non-protein thiols (9). The majority of GSH is found in the cytosol (10), however a small, but significant, percentage of total cellular GSH (10%-15%) is located in the mitochondria. Mitochondrial GSH is of paramount importance in protecting the organelle from reactive oxygen species (ROS) produced during coupled mitochondrial electron transport and oxidative phosphorylation (10).

Many agents that induce apoptosis are either oxidants or stimulate oxidative metabolism, while many inhibitors of apoptosis are antioxidants or mediators of cellular antioxidant defenses (11). Depletion of cellular antioxidant defenses allows for the generation of significant quantities of ROS, which have been suggested to act as a signal for the induction of apoptosis (12). However, other investigators have suggested that depletion of antioxidants (e.g. GSH), rather than production of ROS, is an important mediator of apoptosis (13).

GSH is important for many cellular biochemical functions including the regulation of gene transcription, as well as the modulation of apoptosis (7, 14). The binding of many transcription factors to their cognate DNA sequences is sensitive to the redox environment (14,15). One redox sensitive transcription factor involved in cell proliferation is nuclear factor kappa B (NFκB) (14-16). NFκB translocation to the nucleus can induce the transcription of a variety of genes, including cytokines, cell cycle regulatory proteins and anti-apoptotic proteins (17). **Although it has been suggested that NFκB activation is critical for the regulation of the expression of genes mediating cell survival, and may have an anti-apoptotic role (18-20), others have found that activation of this transcription factor is pro-apoptotic (21-23).**

While, NFκB activation may play a role in either cell survival or cell death, expression of the tumor suppressor gene p53 is known to induce either stable growth arrest or apoptosis (24, 25). In human colorectal cancers, the growth arrest is dependent on the transcriptional induction of the protein $p21^{wafl}$, but the precise mechanisms involved in p53-dependent apoptosis are unclear. However, recently it has been reported that **many** important genes transactivated by p53 **prior to** the onset of apoptosis encode proteins that are involved in oxidative stress (26). **These findings as reported by** Polyak and coworkers (1997) suggest that p53 expression results in apoptosis **via** a three-step process, including the transcriptional induction of redox-related genes, the formation of reactive oxygen species, and the oxidative degradation of mitochondrial components resulting in cell death (26).

Recently, mitochondria and potential signaling molecules such as cytochrome c released from mitochondria have been reported to be key regulators of apoptosis (27-32). Cytochrome c can combine with Apaf-1, and procaspase-9 to form the apoptosome (33), which activates caspase-9, and can then activate caspase 3. Nevertheless, the importance of cytochrome c

release as an apoptotic signal has recently been challenged. For example, cytochrome c release from mitochondria has been reported to be the result of cellular redox imbalance rather than a signal committing the cell to death (34), and Budd et al. **(2000)** showed that cytochrome c release was not sufficient for caspase activation or apoptosis in neuronal cells (35). Activation of caspases may be redox dependent, but the optimal cellular redox environment for activation of caspases is unclear (36, 37). Reports in the literature suggest that **mitochondrial permeability transition (MPT)** induction and mitochondrial transmembrane potential ($\Delta\Psi_m$) depolarization are apoptotic signals (29-32), but we and other investigators have recently reported that $\Delta\Psi_m$ depolarization and MTP are fully reversible events and do not irreversibly commit cells to die (8, 38, 39). Therefore, the role of potential mitochondrial signals in the induction of apoptosis remains controversial.

The primary objective of this study was to characterize the sequence of biochemical events occurring in B cell lymphoma PW cells after modulation of the cellular redox state, with emphasis on the role of mitochondria. The early decline in cellular GSH, in response to BSO treatment, coincided with the induction of mediators of apoptotic signaling including NFκB, p53, and cytochrome c release from mitochondria. ROS generation increased significantly following depletion of mitochondrial GSH, after which procaspase 3 was activated. $\Delta\Psi_m$ was intact in a large proportion of the cell population at a time when cells were committed to die.

RESULTS

Apoptosis following BSO treatment. PW cells were incubated for various times with BSO (1mM), which depletes GSH from cellular compartments in a time dependent manner, by inhibition of cytosolic γGCS. **Apoptosis was then assessed by staining cells with P.I. and using flow cytomestry analysis to determine the proportion of hypodiploid (sub-G1) apoptotic cells.** Figure 1A shows a time dependent increase in the apoptotic fraction of PW cells following BSO incubation (control {no BSO}:1.5 ± 0.3%, 24 h: 2.5 ± 1.2%, 48 h: 5.0 ± 3% and 72 h: 16.4 ± 3%).

Commitment to cell cycle arrest is irreversible after BSO treatment for 72 hours. Cells were treated with BSO (1mM) for **0, 12, 24, 36, 48, 60, and 72 hours. Cells were then rescued by washing cells and plating them in fresh RPMI for 24, 48 and 72 hr. After treatment with BSO (1 mM) for 12-36 hours, there was no marked difference in the viability of BSO treated cells compared with untreated control cells, whereas after 48 and 60 hours under the same conditions, there was a significant increase in cell death compared to control cells. After incubation with BSO (1mM) for 72 h, cells could not be rescued by removing BSO from the media and viability dropped dramatically (Figure 1B and 1C), with the most cell death occuring in the first 24 hours following washout of BSO from the media (data not shown for 48 and 72 hours following washout of BSO).**

Cytosolic and mitochondrial GSH levels following BSO treatment. Figure 2A shows that PW cells rapidly lost GSH in a time dependent manner after BSO (1mM) treatment. At 12 h, total GSH levels were almost 95% depleted, and GSH was undetectable at 24 h (Figure 2A). The level of GSH in the enriched mitochondrial fraction of cells treated with BSO (1mM) for 24

hours was 593 ± 119 pmol/10^6 cells compared to 2460 ± 203 pmol/10^6 cells in control cells (Figure 2B), and was below the limit of detection after incubation with BSO (1mM) for 48 h (Figure 2B).

DTT can rescue cells from BSO-induced apoptosis. PW cells were incubated with BSO with or without DTT for 0-72 hours prior to assessment of apoptosis. Incubation with BSO alone resulted in a time-dependent induction of apoptosis, whereas the concomittant incubation of DTT with BSO prevented the induction of apoptosis, demontrating that PW cells could be "rescued" from BSO-induced apoptosis by incubating them with DTT to preclude depletion of GSH (Figure 3).

ROS production following BSO treatment. DCFH-DA was used to indirectly measure cellular generation of hydrogen peroxide (H_2O_2) before it reacted to form stable organic peroxides. As a positive control, PW cells were incubated with H_2O_2 (100 μM) for 30 m prior to the analysis. Cell samples were incubated with BSO (1 mM) for 0, 24, 36, 48, 54, 60, 72 and 96 h prior to collection, and analyzed by flow cytometry for DCF fluorescence on the FITC/FL-1 channel as an indicator of ROS production. Cells with a higher level of DCF fluorescence than untreated controls shifted right on the x axis into the ROS^{high} compartment (arbitrary units). Figures 4A and 4B show that incubation of the control cell population with BSO (1 mM) shifts cells into the ROS^{high} compartment as a function of time. In addition, Figures 4A and 4B demonstrate that adding DTT to the media during BSO incubation abolishes this shift into the ROS^{high} compartment. Figure 4C is a positive control showing cells treated with H_2O_2 (100 μM). By comparing Figure 4A and 4C it is clear that the ROS^{high} compartment indicates the presence of increased levels of peroxide. After 48 h of incubation with BSO (1 mM) a significant cell population (14.0 ± 1.1%) has

begun to appear in the ROS^{high} compartment at the same DCF fluorescence level as the population of cells treated with H_20_2 (Figures 4A and 4B). This observation is consistent with the generation of similar levels of peroxides in the two ROS^{high} cell populations. At 72 h there is a significant increase in the non-viable cell population (seen as a new population appearing at the leftmost edge of the x axis). Non-viable cells do not fluoresce since they have lost their ability to entrap the DCFH-DA dye and convert it to the membrane impermeable form DCF (a function of their intracellular esterase activity). Cells without functional esterases are considered non-viable, and the cell population with non-functional eserases is comprised of those cells to the far left on the x axis in the 60 h and 72 h timepoints in Figure 4A. All experiments were repeated in triplicate. 10,000 events were recorded in each experiment, and data for each cell population (non-viable, viable and hyperfluorescent) is shown as the mean percentage (% of total population) ± SEM.

Rel A translocation. Figure 5A shows the Rel A band at 65 k-Da following 1, 3 and 5 h of incubation with BSO (1mM). The earliest time point at which increased nuclear Rel A expression was observed compared to the controls was at 3 h.

p53 expression after BSO treatment of PW cells. p53 expression was determined following modulation of the redox state in PW cells by incubation with BSO (1 mM). p53 protein was detectable at 53 k-Da in both control and BSO (1mM) treated PW cells without change in the level of expression during the 72 h incubation period (**Figure 5B**). **A truncated form of p53 protein band was also detected at approximately 50 k-Da using the α p53 monoclonal antibody DO-1**. Truncated p53 was increasingly expressed as a function of time following incubation with BSO (1mM). Incubation of PW cells with BSO (1 mM) failed to induce the expression of $p21^{wafl}$ (data not shown).

Release of mitochondrial cytochrome c after BSO incubation. Cytochrome c release was measured in the cytosolic extracts from PW cells after incubation with BSO (1mM) for 24 to 96 h by immunoblot analysis. A time dependent increase in cytosolic cytochrome c was observed, with cytochrome c first being detected at 24 hours after incubation with BSO (1mM) (**Figure 6**).

Activation of procaspase 3 by BSO incubation, and inhibition of apoptosis with zVADfmk. Procaspase 3 **activation** was assessed following incubation of cells with BSO (1mM) for 24 to 96 h in PW extracts by immunoblot analysis. There was a time dependent decrease in the **procaspase 3** protein band, at 32 k-Da, following incubation with BSO (1mM). At 72 hours, caspase 3 cleavage products were observed (**Figure 7A**). Furthermore, the pan caspase inhibitor zVADfmk, which partially blocked apoptosis induction after 48 hours of BSO treatment, was ineffective after 72 hours (**Figure 7B**) when caspase **3** cleavage products were evident (**Figure 7A**).

$\Psi\Delta_m$ in PW cells after incubation with BSO. PW cells incubated with and without BSO (1mM) for 24 and 72 h, were stained with TMRM and imaged by fluorescence microscopy. The average fluorescent signal was not significantly different in cells treated with or without 1mM BSO (24 or 72 h) (**Figure 8A and 8B**). To further confirm that the $\Psi\Delta_m$ was intact after incubation with BSO (1mM), cells were treated with 50 μM of the uncoupler CCCP, and the fluorescence of at least 20 cells in the microscope field was continuously monitored **(Figure 8B).** **Figure 8A** shows representative images of relative fluorescence at time point zero and 10 minutes after CCCP treatment. The dissipation of fluorescence was both rapid and similar in control and BSO treated cells (1mM), demonstrating the presence of an intact $\Psi\Delta_m$ in both

control (untreated) and BSO treated cells prior to CCCP treatment, with similar kinetics of depolarization following exposure to CCCP.

DISCUSSION

Cellular redox status is an important regulator of apoptotic potential. The effect of modulating the redox status on apoptotic potential was studied using BSO to inhibit GSH synthesis, **and** create a progressively oxidizing environment. Prolonged exposure to BSO led to apoptotic cell death within a time frame that **allowed us to characterize** the sequence of biochemical events involved in BSO-induced apoptosis.

It is known that GSH is an important regulator of the cellular redox state. However, the relative importance of cytosolic and mitochondrial GSH levels as mediators of apoptotic signaling **has not been clearly** defined. Mitochondria do not possess the enzymes required for *de novo* GSH synthesis (40), but utilize cytosolic GSH derived from a multi-component, ATP dependent, mitochondrial transporter that translocates GSH from the cytosol into the mitochondrial matrix (41, 42). **The transporter has a high affinity component which functions at low cytosolic GSH levels, to maintain mitochondrial GSH levels during periods of cytosolic GSH depletion (41). Evidence for this transporter function in PW cells is provided by the observation t**hat after cytosolic GSH depletion, the enriched mitochondrial GSH fraction still **contains** approximately 25% of the pretreatment GSH content compared with untreated control samples. After 48 hours of treatment with BSO, GSH was undetectable in mitochondrial fractions. This finding suggests that during cytosolic GSH depletion that the mitochondrial GSH pool also loses GSH, but at a slower rate. Since it is known that the mitochondrial electron transport chain is **a major** source of cellular ROS, retention of GSH by mitochondria may be an important mechanism for protection against ROS (43, 44). **ROS production following 48 hours of BSO treatment was followed by an increased apoptotic fraction (flow cytometry analysis of PI stained cells), and an increased proportion of non-**

viable cells (detected by flow cytomery analysis, showing an increased proportion of non-fluorescent DCF stained cells and an increase in sub-G1 P1 stained cells), which was prevented by coincubation of cells with BSO and DTT. These observations are consistent with the hypothesis that mitochondrial ROS may be important effector molecules for the induction of apoptosis (43, 44), and that the level of ROS generated may be a determinant of the apoptotic potential of cells (44, 45). **Elegant work by Tan et al. (1998) (46) is in agreement with our data and also suggests that mitochondrial generation of ROS plays a role in the induction of apoptosis. They found that while GSH depletion was necessary for an initial increase in ROS production, that GSH depletion alone was not sufficient to generate the late exponential increase in mitochondrial ROS observed in a murine hippocampal cell line (HT22) after treatment with glutamate. A high rate of ROS production occurred only after GSH levels dropped below ~20 % of baseline in the HT22 cells. The results reported here with PW cells demonstrate minimal ROS generation after cytosolic GSH depletion, but a large increase in ROS production after mitochondria are depleted of GSH. It is probable that in both HT22 and PW cells, the large increase in ROS generation following GSH depletion is primarily related to the induction of apoptosis, rather than being a direct and simple response to the GSH depletion alone.**

The transcription factor NFκB plays an important role in inducing genes involved in inflammation, protective responses (17), and apoptosis (18-23). Activation of NFκB is redox sensitive (14-16), and oxidants have been shown to increase NFκB-mediated expression of c-fos, c-jun and AP1 (47-48). Here we report that **the** Rel A **component of NFκB** translocates to the nucleus early after GSH depletion, before increased ROS levels are detectable. Interestingly,

Hoare et al. **(1999)** reported cytokine-induced NFκB activation was also independent of ROS production (49).

The p53 protein is a tumor suppressor gene product. Increased levels of p53 have been found to block cell proliferation by inducing the transcription of other regulatory genes such as $p21^{wafl}$ (25, 26). Since p53 is induced after genotoxic stress, we performed experiments to determine whether or not the stress imposed by GSH depletion induced p53 expression. We found that p53 was constitutively expressed at high levels in PW cells, and GSH depletion did not induce $p21^{wafl}$ expression **(data not shown).** Therefore, we **suggest** that PW cell growth arrest following GSH depletion **was $p21^{wafl}$ independent. It is possible that p21 expression is not increased along with truncated p53 because $p21^{wafl}$ induction by oxidative stress is independent of the induction of p53. It is also possible that unlike wild type p53, truncated p53 may not act as a transcriptional activator for $p21^{wafl}$. Interestingly, Esposito et al. (2000) recently showed that modulation of intracellular redox status with diethylmaleate, also a glutathione-depleting agent, induced a p53-independent growth arrest that was mediated by the accumulation of $p21^{wafl}$ (50).**

Despite the known role of p53 **as a** mediator of growth arrest, the precise mechanism(s) involved in p53-dependent apoptosis **have not been fully elucidated** (24, 25). **Interestingly, we found trace levels of truncated p53 after 24 hours of incubation with BSO, which increased in a time dependent manner, with the highest levels observed when apoptosis was irreversibly induced**. **Truncated** p53 lacks the N terminus binding region for mdm2, and may be unable to negatively induce the p53 target gene mdm2 (24). Since mdm-2 can block both p53-mediated cell cycle arrest and apoptosis (24, 25), **truncated** p53 may function as a positive inducer of apoptosis (24) in PW cells.

Since cytochrome c has been shown to activate apoptosis (51, 52), experiments were performed to determine whether induction of apoptosis in the PW cell line involved cytochrome c or the downstream caspase 3 pathway. Cytochrome c release in response to incubation with BSO increased in a time dependent manner. When the labile cytosolic GSH pool was depleted, **after approximately 24 h of BSO treatment, mitochondria** released only trace amounts of cytochrome c. However, after incubation with BSO for 72 hours, **relatively** large quantities of cytosolic cytochrome c were detected by immunoblot. Therefore, mitochondria **of PW cells** release cytochrome c after GSH depletion, but before increased levels of ROS are detectable. These results are in agreement with **those** of Ghibelli et al. (1999) (36), however, they reported the release of large quantities of cytochrome c from HepG2 and U937 **mitochondria** as early as 3 hours after incubation with BSO, which did not commit these cells to apoptosis. It is not clear **from our findings** whether cytochrome c is released from cells as a consequence of apoptosis, or if it is an early signal for the induction of redox-dependent apoptosis. However, the observation that we were able to rescue many cells **from subsequent cell death** by withdrawal of BSO after $\leq$ 48 hours incubation, despite the release of **detectable amounts of cytochrome c release, suggests that cytochrome c release from mitochondria may not irreversibly commit cells to death.**

Procaspase 3 protein levels decreased as a function of time **of** incubation with BSO, and after 96 h, caspase 3 cleavage products were observed (Figure 6A). These data are supported by a recent study by Chen et al. (2000) who reported that procaspase 3 cleavage could be induced **with H_2O_2** (53). **Furthermore, Yoshimura et al. (1999) showed that hypoxia-induced pro-caspase 3 activation is blocked by GSH (54).** Since, the activation of caspase proenzymes occurs by cleavage at specific aspartate cleavage sites (36), oxidative modification of cysteine

sulfhydryls in the caspase 3 protein **may** be involved in cleavage of the protein (36). **The oxidizing conditions created by BSO treatment may play a role in these cleavage reactions and result in procaspase 3 activation.** The results reported here with the zVADfmk **pan-**caspase inhibitor further confirm the involvement of procaspase activation in BSO-mediated apoptosis, and demonstrate that following incubation with BSO for 48 h, when mitochondrial GSH is depleted, that **increased ROS generation precedes procaspase 3 activation.**

The role of $\Psi\Delta_m$ depolarization as an apoptotic signal is controversial (8, 32, 38, 39). Here we report that neither early GSH depletion, nor later increased ROS caused dissipation of the $\Psi\Delta_m$, with similar TMRM fluorescence in control and BSO (72 h) treated samples. This result is surprising because it has previously been reported that loss of $\Psi\Delta_m$ is an early and irreversible signal for apoptosis (32). The preservation of $\Psi\Delta_m$ after GSH depletion and ROS production indicates that $\Psi\Delta_m$ depolarization **may** not play a causal role in redox dependent apoptosis in the PW cell line. These observations have been recently substantiated in a study where it was shown that caspases were activated independently of dissipation of the $\Psi\Delta_m$ during apoptosis (55). The integrity of the MPT **pore** is also dependent upon the redox environment of the cell (56-57). Petronilli et al. (1994) found that the MPT **pore** complex contains a critical thiol residue that is in redox equilibrium with GSH (58). Therefore, modulation of the cellular redox state could increase the gating potential of the MPT **pore** and promote the dissipation of $\Psi\Delta_m$. Since the release of cytochrome c was evident at 24 hours after GSH depletion, it is possible that cytochrome c release is regulated by determinants other than the $\Psi\Delta_m$ (59).

In conclusion, the loss of mitochondrial GSH appears to be a key regulator of apoptotic potential in PW cells, since the subsequent increase in ROS production precedes

the induction of apoptosis. GSH depletion in PW cells is sequentially associated with a decline in total cellular GSH, along with NFkB activation, the release of cytochrome c from mitochondria, and the expression of a truncated form of p53. ROS production is then increased, at which time pro-caspase 3 is cleaved and apoptosis is irreversibly induced. Future experiments will be designed to further elucidate the role of Δp53, wild type p53, and NFκB in this process and to test the hypothesis that Δp53 and NFκB are direct mediators of survival/apoptotic signals in this system. Since ionizing radiation and chemotherapy alter redox status, elucidation of the role of redox modulation on apoptotic signaling pathways may have broad clinical relevance and ultimately allow for the development of novel therapeutic strategies to improve the efficacy cytotoxic therapies.

MATERIALS AND METHODS

Cell culture and treatments. PW cells **(a kind gift from Dr. Amato Giaccia, Stanford University)** were cultured in RPMI medium supplemented with 10% (v/v) fetal bovine serum (FBS), 300 μg/L L-Glutamine, 100 μg/ml streptomycin, and 100 U/ml penicillin. They were incubated in a controlled atmosphere (5% CO_2) incubator at 37° C, and were split every two days to maintain them in log-phase. Cultures were maintained at a concentration of between 5 x 10^5/ ml and 1 x 10^6/ ml to prevent apoptosis induced by overgrowth, and all experiments were performed at a cell density of 5 **x** 10^5 cells/ml. GSH was depleted with BSO (1 mM) which inhibits the cytosolic gamma glutamyl cysteine synthetase (γGCS). **Experiments were also performed with dithiotreitol (DTT) at 500 μM (Sigma, St. Louis, MO) and BSO to determine if DTT could protect cells from the effects of BSO on ROS generation and the induction of apoptosis.** The protonophore carbonyl cyanide *m*-chlorophenylhydrazone (CCCP) 50 μM was used to induce $\Delta\Psi_m$ depolarization.

Cell viability and apoptosis assays. Cell viability was assessed by **flow cytometry using propidium iodide (PI) to differentiate between cells with and without intact plasma membranes.** Since the nuclei in apoptotic cells contain hypodiploid amounts of DNA, **flow cytometry** analysis **of** PI stained **permeabilized** cells was used to quantitate the percentage of apoptotic **(sub-G1)** cells as described in reference 8.

Rescue of PW cells after BSO incubation. PW cells were incubated (under standard conditions in RPMI 1640 containing 10% FBS, and supplements) with BSO (1 mM) for 0, **12,** 24, **36,** 48, **60** and 72 h. Cells were then washed in fresh RPMI 1640 to remove the BSO, and seeded at a

density of 5 x 10^5/ml in fresh RPMI 1640 for an additional 72 h. At 24, 48 and 72 h after removal of the BSO cell proliferation was assessed by **cell cytometry of PI stained cells.**

Measurement of glutathione. GSH was measured as previously described (8). Briefly, PW cell samples (4 x 10^6) were rinsed in phosphate buffered saline and sonicated for 10 s on ice. Proteins were precipitated on ice for 15 min with sulfosalicylic acid (6.5%) and centrifuged at 2000g for 15 min at 4°C. Supernatants were stored at –70°C until the time of analysis. GSH in enriched mitochondrial fractions was determined on samples that had been previously permeabilized with digitonin to release the cytosol. Post cytosolic cell fractions were washed three times in ice-cold PBS and centrifuged. Cell pellets were processed in an identical manner to whole cells. GSH was determined by the GSH-reductase recycling assay (60), in microtitre plates.

ROS determination. Dichorofluorescein diacetate (DCFH-DA) was used to assess levels of net intracellular generation of ROS (61). DCFH-DA is a peroxide-sensitive fluorescent probe that is nonpolar and diffuses into the cell. Intracellular esterases cleave the diacetate ester group and entrap the polar, nonfluorescent DCFH within the cell. ROS can oxidize this substance to the fluorescent compound DCF. Cells were treated with BSO (1 mM) for the indicated times, and washed in Hanks Buffered Saline Solution (HBSS) (Gibco, Gaithersburg, MD). 1 x 10^6/ml cells were incubated in HBSS containing 50 μM DCFH-DA for **30** min prior to ROS measurement. Samples incubated with hydrogen peroxide (100 μM) were used as a positive control. The fluorescence of the cell population is proportional to the levels of intracellular ROS generated (61), and was measured with a FACScan (Becton Dickinson, Mountain View, CA) at 588nm emission.

Immunoblotting. For immunoblotting post cytosolic (nuclear) fractions and cytosolic fractions were obtained from digitonin permeabilized PW cells as previously described (8). Nuclear fractions were used to determine Rel A protein levels. Briefly, 3-5 x 10^6 cells were harvested and resuspended in 100 μL of mitochondrial isolation buffer (250 mM mannitol, 17 mM MOPS (pH 7.4), 2.5 mM EDTA and 0.2 mg/ml digitonin). The suspension was centrifuged at 3000 rpm for 5 minutes at 4°C and the cell pellet was washed x 2 in ice cold PBS. After re-suspension in 200 μL sodium dodecyl sulfate (SDS) buffer, the extract was boiled for 10 minutes to denature the proteins. The cell extract was aspirated through a 27 gauge needle and transferred to a new tube. The protein concentration was measured using a protein assay kit (DC protein assay reagent, Bio-Rad, Hercules, CA). Fifty micrograms of denatured protein were resolved on 10% SDS-PAGE gels and electro-blotted onto nitrocellulose membrane. Rel A was detected using a rabbit polyclonal antibody to Rel A (1: 250) for 1 hour (Santa Cruz, San Diego, CA). Membranes were incubated in anti-species-HRP conjugated secondary antibody for **1 hour** at (1:1000) (Dako, Carpinteria, CA). Detection was carried out by incubating membranes for 5 min with the enhanced chemiluminescence reagent (ECL kit; Amersham Pharmacia Biotech), followed by exposure to ECL X-ray film (Amersham).

For cytochrome c, cytosolic fractions recovered from digitonin permeabilized cells were mixed (1:1) with SDS sample buffer and boiled to denature the proteins. Thirty micrograms of cytosolic protein extracts were resolved on 15% SDS-PAGE gels, and electro-blotted onto a nitrocellulose membrane (Bio-Rad). Anti-cytochrome c mouse monoclonal antibody (PharMingen, San Diego, CA) was used as the primary antibody. Membranes were incubated in anti-species-HRP conjugated secondary antibody for 2 hours at (1:1000) (Dako). Detection was

carried out by incubating membranes for 5 min with the ECL reagent (Amersham) as described for Rel A.

For p53, cells were initially washed in ice cold PBS and were pelleted and resuspended in UTB buffer (9 M urea, 75 mM Tris-HCl, pH 7.5, 0.15 M 2-mercaptoethanol) and sonicated briefly. The protein concentration was determined as described above (Bio Rad). Fifty micrograms of protein were separated on SDS-PAGE gels and electro-blotted on to nitrocellulose membranes (Osmonics, Westborough, MA). Proteins were detected with the following antibodies: mouse mAb against the N- (DO-1, Santa Cruz, Ca) and C-(pAb 421) termini of p53, **and** mouse mAb against p21WAF1/CIP1 (Chemicon International Inc., Temecula, CA). Membranes were incubated in anti species-HRP conjugated secondary antibody for **1 hour** at (1:1000) (Dako). Detection was carried out by incubating membranes with the enhanced chemiluminescence reagent (ECL kit; Amersham) Pharmacia Biotech), followed by exposure to ECL X-ray film (Amersham) as described for Rel A.

For caspase 3, twenty micrograms of denatured protein were resolved on 12% SDS-PAGE gels and electro-blotted onto nitrocellulose membranes. The membrane was incubated with mouse anti-human CPP32 monoclonal antibody (Calbiochem, La Jolla, CA) as the primary antibody (1:500) for 1 hour. Membranes were incubated in anti species-HRP conjugated secondary antibody for 2 hours at (1:1000) (Dako). Detection was carried out by incubating membranes for 5 min with the (ECL kit; Amersham) as described for Rel A.

Apoptosis following BSO incubation and addition of the caspase inhibitor zVADfmk. PW cells were incubated with RPMI containing BSO (1mM) for 48 and 72 h after which time the broad spectrum caspase inhibitor benzyloxycarbonyl-val-glu-asp fluoromethylketone

(zVADfmk) (50 μM) or vehicle control (DMSO) was added, and cultures were incubated for an additional 24 hours. Apoptosis was assessed by flow cytometry analysis of PI stained cells. Data are expressed as mean ± S.E.M (n = 3).

Analysis of the mitochondrial membrane potential. Mitochondrial membrane potential was determined by measuring the fluorescence of cells stained with the dye tetra-methyl rhodamine methyl ester (TMRM) before and after exposure to BSO (1 mM) and/ or CCCP (50 μM) in at least 20 individual cells. Cells (2 _ 10^6/ ml) loaded with TMRM (150 nM) were seeded onto glass cover slips (previously coated with polylysine) in 1 ml of RPMI 1640 with 10% FBS and left to attach for 30 minutes at 37°C. Cells were transferred to a temperature-controlled perfusion chamber (Bioptechs, Butler, PA). During the experiment, cells were maintained at 37°C in culture media containing 50 nM TMRM. Fluorescence images were obtained with a cooled CCD camera (Photometrics Quantix, Tucson, AZ) connected to an epifluorescence inverted microscope (Nikon TE 300) equipped with a 40X oil immersion objective. Excitation light from a 75 W zenon arc lamp was coupled to the microscope by a liquid light guide (Sutter Instrument Co., Navato, CA) and directed onto a filter cube (535 ± 25 nm exitation, 575 nm dichroic mirror, 590 nm long pass emission filter). Exitation light was reduced by > 90% with neutral density filters and a computer controlled shutter to minimize photobleaching and phototoxicity. Images were collected for 250 milliseconds every 10 s and analyzed using Metafluor imaging software (Universal Imaging, West Chester, PA). To further determine that the mitochondrial membrane potential was intact, CCCP (50 μM) was injected into the perfusate and the fluorescence of ≥ 20 representative cells was monitored at 10 s intervals for a total of 500 measurements per cell. The intensity of the fluorescence was monitored kinetically, and averaged for ≥ 20 cells over the total time period.

Statistical analysis. Statistical analyses were performed using Student's t test for unpaired data, and p values <0.05 were considered significant. Data are presented as mean ± SEM.

REFERENCES

1. Rupnow BA, Murtha AD, Alarcon RM, Giaccia AJ and Knox SJ (1998) Direct evidence that apoptosis enhances tumor responses to fractionated radiotherapy. Cancer Res. 58: 1779-1784.
2. Alemany M and Levin J (2000) The effects of arsenic trioxide (As2O3) on human megakaryocytic leukemia cell lines. With a comparison of its effects on other cell lineages. Leuk. Lymphoma 38: 153-163.
3. Mallery SR, Clark YM, Ness GM, Minshawi OM, Pei P and Hohl CM (1999) Thiol redox modulation of doxorubicin mediated cytotoxicity in cultured AIDS-related Kaposi's sarcoma cells. J. Cell. Biochem. 73: 259-277.
4. Dolan ME, Frydman B, Thompson CB, Diamond AM, Garbiras BJ, Safa AR, Beck WT and Marton LJ (1998) Effects of 1,2-naphthoquinones on human tumor cell growth and lack of cross-resistance with other anticancer agents. Anticancer Drugs 9: 437-448.
5. Green DR and Reed JC (1998) Mitochondria and apoptosis. Science 281: 1309-1312.
6. Marchetti P, Decaudin D, Macho A, Zamzami N, Hirsch T, Susin SA and Kroemer G (1997) Redox regulation of apoptosis: impact of thiol oxidation status on mitochondrial function. Eur. J. Immunol. 27: 289-296.
7. Coffey RN, Watson RW, Hegarty NJ, O'Neill A, Gibbons N, Brady HR and Fitzpatrick (2000) Thiol-mediated apoptosis in prostate carcinoma cells. J. M. Cancer 88: 2092-2104
8. Armstrong JS, Steinauer KK, Killoran P, Walleczek Y and Knox S (2001) Bcl-2 inhibits apoptosis after mitochondrial "uncoupling" but does not prevent mitochondrial transmembrane depolarization. Exp. Cell. Research 262: 170-179.

9. Deneke SM and Fanburg BL (1989) Regulation of cellular glutathione. Am. J. Physiol. 257: L163-173.

10. Fernandez-Checa JC, Kaplowitz N, Garcia-Ruiz C, Colell A, Miranda M, Mari M, Ardite E and Morales A (1997) GSH transport in mitochondria: defense against TNF-induced oxidative stress and alcohol-induced defect. Am. J. Physiol. 273: G7-17.

11. Buttke TM and Sandstrom PA (1994) Oxidative stress as a mediator of apoptosis. Immunol. Today 15: 7-10.

12. Langer C, Jurgensmeier JM and Bauer G (1996) Reactive oxygen species act at both TGF-beta-dependent and -independent steps during induction of apoptosis of transformed cells by normal cells. Exp. Cell. Res. 222: 117-124.

13. Hug H, Enari M and Nagata S (1994) No requirement of reactive oxygen intermediates in Fas-mediated apoptosis. FEBS Lett. 12;351: 311-313.

14. Arrigo AP (1999) Gene expression and the thiol redox state. Free. Radic. Biol. Med. 27: 936-944.

15. Sen CK (2000) Cellular thiols and redox-regulated signal transduction. Curr. Top Cell Regul. 36: 1-30.

16. Hutter D and Greene JJ Influence of the cellular redox state on NF-kappaB- (2000) regulated gene expression. J. Cell Physiol. 183: 45-52.

17. Palayoor ST, Youmell MY, Calderwood SK, Coleman CN and Price BD (1999) Constitutive activation of IkappaB kinase alpha and NF-kappaB in prostate cancer cells is inhibited by ibuprofen. Oncogene 18: 7389-7394.

18. Baeuerle PA and Baltimore D (1996) NF-kappa B: ten years after. Cell 87: 13-20.

19. Wang CY, Mayo MW, Korneluk RG, Goeddel DV and Baldwin ASJr (1998) NF-kappaB antiapoptosis: induction of TRAF1 and TRAF2 and c-IAP1 and c-IAP2 to suppress caspase-8 activation. Science 281: 1680-1683.

20. Wu MX, Ao Z, Prasad KV, Wu R and Schlossman SF (1998) IEX-1L, an apoptosis inhibitor involved in NF-kappaB-mediated cell survival. Science 281: 998-1001.

21. Hettmann T, DiDonato J, Karin M, Leiden JM. An essential role for nuclear factor kappaB in promoting double positive thymocyte apoptosis. J Exp Med 1999 Jan 4;189(1):145-58.

22. Post A, Crochemore C, Uhr M, Holsboer F, Behl C. Differential induction of NF-kappaB activity and neural cell death by antidepressants in vitro. Eur J Neurosci 2000 Dec;12(12):4331-7.

23. Panet H, Barzilai A, Daily D, Melamed E, Offen D. Activation of nuclear transcription factor kappa B (NF-kappaB) is essential for dopamine-induced apoptosis in PC12 cells. Neurochem 2001 Apr;77(2):391-8.

24. Okorokov AL, Ponchel F and Milner J (1997) Induced N- and C-terminal cleavage of p53: a core fragment of p53, generated by interaction with damaged DNA, promotes cleavage of the N-terminus of full-length p53, whereas ssDNA induces C-terminal cleavage of p53. EMBO J. 16: 6008-6017.

25. Chen J, Wu X, Lin J and Levine AJ (1996) mdm-2 inhibits the G1 arrest and apoptosis functions of the p53 tumor suppressor protein. Mol. Cell. Biol. 16: 2445-2452.

26. Polyak K, Xia Y, Zweier JL, Kinzler KW and Vogelstein B (1997) A model for p53-induced apoptosis. Nature 389: 300-305.

27. Kroemer G, Zamzami N and Susin SA (1997) Mitochondrial control of apoptosis. Immunol. Today 18: 44-51.

28. Kroemer G (1996) Mitochondrial control of nuclear apoptosis. J. Exp. Med. 183: 1533-1544.

29. Hirsch T, Marzo I and Kroemer G (1997) Role of the mitochondrial permeability transition pore in apoptosis. Biosci. Rep. 17: 67-76.

30. Marchetti P, Castedo M, Susin SA, Zamzami N, Hirsch T, Macho A, Haeffner A, Hirsch F, Geuskens M and Kroemer G (1996) Mitochondrial permeability transition is a central coordinating event of apoptosis. J. Exp. Med. 184: 1155-1160.

31. Crompton M (1999) The mitochondrial permeability transition pore and its role in cell death. Biochem. J. 341: 233-249.

32. Zamzami N, Marchetti P, Castedo M, Zanin C, Vayssiere JL, Petit PX and Kroemer G (1995) Reduction in mitochondrial potential constitutes an early irreversible step of programmed lymphocyte death in vivo. J. Exp. Med. 181: 1661-1672.

33. Li P, Nijhawan D, Budihardjo I, Srinivasula SM, Ahmad M, Alnemri ES and Wang X (1997) Cytochrome c and dATP-dependent formation of Apaf-1/caspase-9 complex initiates an apoptotic protease cascade. Cell 91: 479-489.

34. Ghibelli L, Coppola S, Fanelli C, Rotilio G, Civitareale P, Scovassi AI, Ciriolo MR (1999) Glutathione depletion causes cytochrome c release even in the absence of cell commitment to apoptosis. FASEB J. 13: 2031-2036.

35. Budd SL Tenneti L, Lishnak T and Lipton SA (2000) Mitochondrial and extramitochondrial apoptotic signaling pathways in cerebrocortical neurons. Proc. Natl. Acad. Sci. USA 97: 6161-6166.

36. Hampton MB, Fadeel B and Orrenius S (1998) Redox regulation of the caspases during apoptosis. N.Y. Acad. Sci. 854: 328-35.

37. Baker A, Santos BD and Powis G (2000) Redox control of caspase-3 activity by thioredoxin and other reduced proteins. Biochem. Biophys. Res. Commun. 268: 78-81.

38. Minamikawa T, Williams DA, Bowser DN and Nagley P (1999) Mitochondrial permeability transition and swelling can occur reversibly without inducing cell death in intact human cells. Exp. Cell. Res. 246: 26-37.

39. Finucane DM, Waterhouse NJ, Amarante-Mendes GP, Cotter TG and Green DR (1999) Collapse of the inner mitochondrial transmembrane potential is not required for apoptosis of HL60 cells. Exp. Cell. Res. 251: 166-174.

40. Griffith OW and Meister A (1985) Origin and turnover of mitochondrial glutathione. Proc. Natl. Acad. Sci. USA 82: 4668-4672.

41. Martensson J, Lai JC and Meister A (1990) High-affinity transport of glutathione is part of a multicomponent system essential for mitochondrial function. Proc. Natl. Acad. Sci. USA 87: 7185-7189.

42. Garcia-Ruiz C, Morales A, Colell A, Rodes J, Yi JR Kaplowitz N and Fernandez-Checa JC (1995) Evidence that the rat hepatic mitochondrial carrier is distinct from the sinusoidal and canalicular transporters for reduced glutathione. Expression studies in Xenopus laevis oocytes. J. Biol. Chem. 270: 15946-15949.

43. Suzuki S, Higuchi M, Proske RJ, Oridate N, Hong WK and Lotan R (1999) Implication of mitochondria-derived reactive oxygen species, cytochrome C and caspase-3 in N-(4-hydroxyphenyl)retinamide-induced apoptosis in cervical carcinoma cells. Oncogene 18: 6380-6387.

44. Sanchez A, Alvarez AM, Benito M and Fabregat I (1996) Apoptosis induced by transforming growth factor-beta in fetal hepatocyte primary cultures: involvement of reactive oxygen intermediates. J. Biol. Chem. 271: 7416-7422.

45. Li P-F, Dietz R and von Harsdorf R (1999) p53 regulates mitochondrial membrane potential through reactive oxygen species and induces cytochrome c-independent apoptosis blocked by Bcl-2. The EMBO Journal 18: 6027-603.

46. Tan S, Sagara Y, Liu Y, Maher P, Schubert D. The regulation of reactive oxygen species production during programmed cell death. Cell Biol 1998 Jun 15;141(6):1423-32.

47. Cerutti P, Shah G, Peskin A and Amstad P (1992) Oxidant carcinogenesis and antioxidant defense. Ann. N.Y. Acad. Sci. 663: 158-166.

48. Rahman I and MacNee W (2000) Regulation of redox glutathione levels and gene transcription in lung inflammation: therapeutic approaches. Free Radic. Biol. Med. 28: 1405-1420.

49. Hoare GS, Marczin N, Chester AH and Yacoub MH (1999) Role of oxidant stress in cytokine-induced activation of NF-kappaB in human aortic smooth muscle cells. Am. J. Physiol. 277: H1975-1984.

50. Esposito F, Russo L, Russo T and Cimino F (2000) Retinoblastoma protein dephosphorylation is an early event of cellular response to prooxidant conditions. FEBS Lett. 470: 211-215.

51. Zou H, Li Y, Liu X and Wang X (1999) An APAF-1.cytochrome c multimeric complex is a functional apoptosome that activates procaspase-9. J. Biol. Chem. 274: 11549-11556.

52. **Yang J, Liu X, Bhalla K, Kim CN, Ibrado AM, Cai J, Peng TI, Jones DP, Wang X (1997) Prevention of apoptosis by Bcl-2: release of cytochrome c from mitochondria blocked. Science 275:1129-1132.**

53. Chen QM, Liu J and Merrett JB (2000) Apoptosis or senescence-like growth arrest: influence of cell-cycle position, p53, p21 and bax in H2O2 response of normal human fibroblasts. Biochem. J. 347: 543-551.

54. Yoshimura S, Banno Y, Nakashima S, Hayashi K, Yamakawa H, Sawada M, Sakai N, and Nozawa Y. (1999) Inhibition of neutral sphingomyelinase activation and ceramide formation by glutathione in hypoxic PC12 cell death. J. Neurochem. 73: 675-683.

55. Li X, Du L and Darzynkiewicz Z (2000) During apoptosis of HL-60 and U-937 cells caspases are activated independently of dissipation of mitochondrial electrochemical potential. Exp. Cell Res. 257: 290-297.

56. Costantini P, Chernyak BV, Petronilli V and Bernardi P (1995) Selective inhibition of the mitochondrial permeability transition pore at the oxidation-reduction sensitive dithiol by monobromobimane. FEBS Lett. 362: 239-242.

57. Costantini P, Chernyak BV, Petronilli V and Bernardi P (1996) Modulation of the mitochondrial permeability transition pore by pyridine nucleotides and dithiol oxidation at two separate sites. J. Biol. Chem. 271: 6746-67451.

58. Petronilli V, Costantini P, Scorrano L, Colonna R, Passamonti S and Bernardi P (1994) The voltage sensor of the mitochondrial permeability transition pore is tuned by the oxidation-reduction state of vicinal thiols. Increase of the gating potential by oxidants and its reversal by reducing agents. J. Biol. Chem. 269: 16638-16642.

59. Vander Heiden MG, Chandel NS, Li XX, Schumacker PT, Colombini M and Thompson CB (2000) Outer mitochondrial membrane permeability can regulate coupled respiration and cell survival. Proc. Natl. Acad. Sci. USA. 97: 4666-4671.

60. Tietze, F. (1969) Enzymic method for quantitative determination of nanogram amounts of total and oxidized glutathione: applications to mammalian blood and other tissues. Anal. Biochem. 27: 502-22.

61. Bass DA, Parce JW, Dechatelet LR, Szejda P, Seeds MC and Thomas M (1983) J Flow cytometric studies of oxidative product formation by neutrophils: a graded response to membrane stimulation. Immunol. 130: 1910-1917.

Figure Legends

Figure 1.

Apoptosis and cell proliferation after incubation with BSO

A. Apoptosis following incubation with BSO. PW cells were incubated with RPMI containing BSO (1mM) for 0, 24, 48 and 72 h (as described in the materials and methods section). The apoptotic fraction was determined by **flow cytometry** analysis **of** PI stained cells (as described in the materials and methods section). Data are expressed as mean ± S.E.M (n = 3).

B. Representative plots of flow cytometry data showing rescue of PW cells following incubation with BSO.

C. Graph showing rescue of PW cells following incubation with BSO. PW cells were incubated with RPMI 1640 containing BSO (1 mM) for **0, 12, 24, 36, 48, 60 and 72 hours.** After the incubation period cells were washed in fresh RPMI, seeded at an approximate density of 5 x 10^5/ml, and incubated for an additional 72 h. At 24 h after removal of the BSO, cell viability was determined by counting **viable PI stained cells with flow cytometry.** Data are expressed as mean ± S.E.M (n = 3).

Figure 2.

GSH levels in PW cells.

A. Effect of BSO on total GSH levels. PW cell aliquots (4 x 10^6/ ml) were incubated with RPMI containing BSO (1 mM) for up to 24 hours. GSH levels were determined at various times on these samples by the GSH reductase recycling assay described in the materials and methods section. The GSH concentration was plotted as a function of time and expressed as nmol/mg protein.

B, Effect of BSO on mitochondrial GSH levels. PW cells were treated with BSO for 24, 48 and 72 h. Mitochondrial fractions from these cells were isolated as described in the materials and methods section. GSH levels were determined using the GSH reductase recycling assay. The GSH concentration was expressed in pmol/10^6 cells. Data are expressed as mean ± S.E.M (n = 3).

Figure 3.

Apoptosis in cells treated with BSO with or without DTT.

PW cells were incubated with BSO (1mM) in the presence or absence of DTT (500 μM) for 0-72 hours prior to assessment of apoptosis by flow cytometry of permeabilized, PI/RNAase stained BSO treated cells, or unpermeabilized, PI stained cells treated with BSO + DTT.

A. Representative plots of flow cytometry data at key time points showing increasing apoptosis of PW cells as a function of the incubation time with BSO. Apoptosis was determined as the percentage of sub-G1 cells in an ungated population of 10,000 events. In BSO + DTT treated samples, cell viability was verified by PI exclusion.

B. Graph of BSO induced apoptosis over time contrasted with very low cell death observed in samples incubated with BSO + DTT. Data in (B) are shown as the mean ± S.E.M. (n = 3) for apoptosis shown as the percentage of control at time 0 hr.

Figure 4.

ROS levels following Incubation with BSO.

A. Representative plots of flow cytometry data showing ROS levels in PW cells after GSH depletion. PW cells were incubated with BSO (lmM) for 0, 24, 36, 48, 54, 60, 72 and 96 h as

described in the materials and methods section. 1.0 x 1 0^6ml cells were loaded with 50 μM DCFH-DA and incubated at 37^0 C for 30 minutes. Determination of intracellular ROS generation was performed by flow cytometry analysis of 10,000 cells using the FL1 channel in logarithmic mode (as described in the materials and methods section). Three cell populations differing significantly in their relative mean fluorescence were observed by flow cytometry analysis: 1) a cell population with medium fluorescence corresponding to viable and untreated control cells, 2) a hyperfluorescent cell population labeled ROS^{high} corresponding to cells that had generated significant quantities of ROS compared to the positive control sample treated with H_2O_2 (100 μM), and 3) a non-viable cell population with low fluorescence corresponding to cells that had failed to cleave and entrap DCFH-DA (labeled in the 60 h timepoint where it first appears). Cell numbers in the ROS^{high} compartment are expressed as percent cells of whole population. Results are representative of four experiments. As a control, PW cells were incubated with BSO (1 mM) ± DDT (500 μM) for 0-72 h prior to measurement of ROS and representative plots were included in Figure 4A.

B. Graph of the induction of ROS as a function of time in PW cells treated with BSO in the presence or absence of DTT. Percentages of cells in the ROS high compartment from Figure 4A were graphed as mean ± S.D. (n = 3). The dark line represents BSO treated PW cells and the light line demonstrates the contrasting lack of ROS in the cells incubated with both BSO and DTT.

C. Representative plot of the induction of ROS in H_2O_2 treated control PW cells. Control PW cells were incubated with BSO + H_2O_2 for 30 minutes prior to staining (as in the 0 h

timepoints in 4A). The shift of > 95% of the cell population into the ROS^{high} compartment demonstrates the presence of increased levels of peroxide.

Figure 5.

Effect of BSO incubation on NFkB activation and p53 induction.

A. Effect of BSO incubation on NFkB activation. PW cells were incubated with RPMI containing BSO (1mM) for 1, 3 and 5 hours. Post cytosolic nuclear fractions were prepared from digitonin permeabilized cells as described in the materials and methods section. Rel A translocation was determined by immunoblot analysis performed on nuclear fractions, and shows the Rel A protein band at 65-kDa. Equal amounts of protein (50 μg) were loaded in each lane (determined by the Biorad assay).

B. Effect of BSO incubation on p53 induction. PW cells were incubated with RPMI containing BSO (1 mM) for 24, 48, 72 and 96 h. The expression of p53, p21wafl and truncated p53 was determined by immunoblot analysis described in the materials and methods section. Equal amounts of protein (50 μg) were loaded in each lane (determined by the BioRad assay).

Figure 6.

Cytochrome c release after incubation with BSO.

Cytochrome c release after incubation with BSO. PW Cells were incubated with BSO (1mM) for 0, 24, 48, 72 and 96 h. The cytosolic fraction was recovered by digitonin permeabilization as described in the materials and methods section. Cytochrome c (15 k-Da) was determined by immunoblot analysis. Bovine cytochrome c was used as a positive control. Equal amounts of protein (25 μg) were loaded in each lane (determined by the BioRad assay).

Figure 7.

A. Caspase 3 activation after incubation with BSO. PW cells were incubated with BSO (1mM) for 0, 24, 48, 72 and 96 h. Caspase 3 (32 k-Da) activation was determined by immunoblot analysis and shows the protein band at 32-kDa. Caspase cleavage products were observed at 72 hours after BSO treatment. Equal amounts of protein (20 μg) were loaded in each lane (determined by the Biorad assay).

B. Inhibition of apoptosis by zVADfmk. PW cells were incubated with RPMI containing BSO (1mM) for 48 and 72 h. zVADfmk was then added to cultures, and cultures were incubated for an additional 24 hours as described in the materials and methods section. Apoptosis was assessed by FACS analysis of PI stained cells. Data are expressed as mean ± S.E.M (n = 3).

Figure 8.

Mitochondrial membrane potential ($\Psi\Delta_m$) after incubation with BSO.

A. $\Psi\Delta_m$ after incubation with BSO. PW cells were incubated with BSO (1mM) for 0, 24, and 72 hours. Cells were loaded with the dye TMRM, and $\Psi\Delta_m$ was determined in these cells by monitoring the intensity in fluorescence of the dye. After establishment of baseline fluorescence (≥ 20 minutes), the uncoupler CCCP (50 μM) was perfused into the system and the fluorescence of ≥ 20 representative cells was monitored at 10 second intervals for 200 additional measurements.

B. $\Psi\Delta_m$ after incubation with BSO. Graphical representation of the mean TMRM fluorescence of PW cells A) control B) incubation with BSO (1mM) for 24 h and C) incubation

with BSO (1mM) for 72 h. The TMRM fluorescence of 20 randomly picked cells was monitored before and after perfusion with CCCP (50 μM) for a total time of 25 minutes. This fluorescence was averaged and plotted as a function of time after the background fluorescence had been subtracted.

Acknowledgments:

The authors thank Chuck DiBari for his assistance with the preparation of this manuscript and Dr. Jeff Carson for his assistance with the figures. We also thank Dr Garry Nolan for his support of the flow cytometry work represented in this manuscript.

Submitted to Eur. J. Cancer

ANTIPROLIFERATIVE AND PROAPOPTOTIC ACTIVITY OF TRIPTOLIDE ON HUMAN PROSTATIC EPITHELIAL CELLS

Taija M. KIVIHARJU, Philip S. LECANE, Robert G. SELLERS, and Donna M. PEEHL *

Department of Urology, Stanford University School of Medicine, Stanford, California 94305

Running title: triptolide inhibits prostate growth

Key words: *triptolide; prostatic epithelial cells; prostate cancer; chemoprevention; chemotherapy; p53*

Grant sponsor: Department of Army Grant DAMD 17-99-1-9004.

*Correspondence to: Dr. Donna Peehl, Department of Urology, Stanford Medical Center, Stanford, CA 94305-5118. Phone: 1 (650) 725-5531; Fax: 1 (650) 723-0765; E-mail: dpeehl@stanford.edu.

[a] The abbreviations used are: ECL, enhanced chemiluminescence; h, hour; hdm-2, human homologue of the murine double minute-2; HEPES, 4-(2-hydroxyethyl)-1-piperazineethanesulfonic acid; HRP, horseradish peroxidase; mAb, monoclonal antibody; mdm-2, murine double minute-2; p21, $p21^{WAF1/CIP1}$; pAb, polyclonal antibody; PBS, phosphate-buffered saline; PVDF, polyvinylidene fluoride; SA-β-gal, senescence-associated β-galactosidase; SDS-PAGE, sodium dodecyl sulfate-polyacrylamide gel electrophoresis; UTB, urea-TRIS buffer.

ABSTRACT

Interest in exploiting traditional medicines for prevention or treatment of cancer is increasing. Triptolide is a purified compound from a plant that has been used in China for centuries to treat immune-related disorders. Recently it has been reported that triptolide possesses anti-tumor properties in addition to its anti-inflammatory activity. In particular, triptolide induces apoptosis by p53-independent mechanisms in a variety of malignant cell lines. We previously found that primary cultures of human prostatic epithelial cells derived from normal tissues and adenocarcinomas are in general extremely resistant to apoptosis. Furthermore, the function of p53 is impaired in these cells, so that drugs that require p53 activity to induce cell death are ineffective in these cells. Therefore, the properties of triptolide suggested that it was a promising candidate to test for anti-tumor activity against prostate cells. Experiments presented here demonstrate that treatment of prostatic epithelial cells with triptolide had dose-dependent effects. Low concentrations of triptolide inhibited cell proliferation and induced a senescence-like phenotype. Higher concentrations of triptolide induced apoptosis that was unexpectedly associated with nuclear accumulation of p53. Paradoxically, levels of the p53 target genes, p21 and hdm-2, were reduced, as was bcl-2. Our results suggest that triptolide might be an effective preventive as well as therapeutic agent against prostate cancer, and that triptolide may activate a functional p53 pathway in prostatic epithelial cells.

INTRODUCTION

Extracts of the Chinese herb, Tripterygium Wilfordii hook, have been used extensively for centuries in traditional Chinese medicine to treat a variety of autoimmune and inflammatory diseases including rheumatoid arthritis.[1] One of the purified compounds from Tripterygium extracts with immunosuppressive activity is the diterpene triepoxide, triptolide.[2] Recent explorations of the mechanisms of action of triptolide revealed many properties relevant not only to anti-inflammatory activity but to anti-cancer activity as well. Antiproliferative and proapoptotic activity of triptolide has been shown with a number of different types of cancer cells in vitro and in vivo.[3,4]

We became interested in triptolide because it was reported to direct cancer cells to undergo apoptosis independent of p53 activity.[4] The tumor suppressor protein p53 responds to different forms of cellular stress such as DNA damage by ionizing radiation or chemotherapeutic drugs by targeting the checkpoint genes that inhibit cell cycle progression[5] and/or trigger apoptosis (review in[6,7]). Previous studies conducted in this laboratory showed that activation of p53 in response to γ-irradiation, or other stresses such as hypoxia or DNA-damaging drugs, is attenuated in primary cultures of normal and malignant prostatic epithelial cells, despite the presence of the wild-type p53 gene.[8] Since many chemotherapeutic drugs use p53-mediated pathways to induce growth arrest or apoptosis, we have suggested that dysfunction of 53 may partially explain the resistance of prostate cancer to drug treatment. The prevalence of mutated p53 in advanced prostate cancer[9] may also impact response to chemotherapy. We therefore hypothesize that drugs using p53-independent pathways would be most efficacious against prostate cancer.

Signaling pathways involved in the induction of growth inhibition or apoptosis by triptolide are not yet clear. An attempt to discern these pathways was approached by cDNA microarray analysis of triptolide-treated normal and transformed bronchial epithelial cells. Triptolide reduced expression of cell cycle regulators and survival genes such as cyclins D1, B1 and A1, cdc-25, bcl-x and c-jun.[10] Anti-inflammatory, antiproliferative and proapoptotic properties of triptolide have also been associated with inhibition of NF-κB.[10-12]

In our study, we found dose-dependent effects of triptolide on prostatic epithelial cells. Low concentrations of triptolide inhibited growth and induced senescence, an irreversible growth-arrested state of cells that is postulated to be important in tumor suppression. Higher concentrations of triptolide triggered apoptosis. Interestingly, apoptosis was accompanied by nuclear accumulation of p53. Our pre-clinical findings support further investigation of chemopreventive and chemotherapeutic activity of triptolide against prostate cancer.

MATERIALS AND METHODS

Cell Culture and Reagents. Tissue samples were dissected from radical prostatectomy specimens. None of the patients had received prior chemical, hormonal or radiation therapy. Histological assessment was performed as previously described.[13] Epithelial cells were cultured and characterized as described previously.[14] Culture medium was MCDB 105 (Sigma-Aldrich, St. Louis, MO) supplemented with 10 ng/ml of cholera toxin, 10 ng/ml of epidermal growth factor, 10 μg/ml of bovine pituitary extract, 4 μg/ml of insulin, 1 μg/ml of hydrocortisone, 0.1 mM phosphoethanolamine, 30 nM selenium, 0.03 nM all-trans retinoic acid, 2.3 μM α-tocopherol and 100 μg/ml gentamycin ("Complete MCDB 105"). The sources and preparation of these supplements were previously described.[14] Four cells strains used in this study were derived from prostatic adenocarcinomas of Gleason grade 3/3 (E-CA-11), 30% intraductal carcinoma/ 70% Gleason grade 4 (E-CA-12), and Gleason grade 3/4 (E-CA-13 and E-CA-14). An additional cell strain (E-PZ-10) was derived from histologically normal tissue of the peripheral zone. Triptolide (PG490) was provided by Pharmagenesis (Palo Alto, CA).

Clonal Growth Assay. Cells at ~30% confluency were trypsinized, suspended in medium, and centrifuged. The cell pellet was suspended in HEPES[a] at a concentration of 2×10^3 cells/ml. One hundred microliters, containing 500 cells, were inoculated into each collagen-coated, 60-mm dish containing 5 ml of Complete MCDB 105 with experimental factors. Cells were incubated for 10 days without feeding, and then were fixed with 10% formalin and stained with crystal violet.[14] Growth was quantitated with an Artek image analyzer (Dynatech, Chantilly, VA), which measures the total area of the dish covered by cells. This relative value has been shown to be directly proportional to cell number.[15]

High Density Growth Assay. Cells were inoculated at 10^5 cells/dish into collagen-coated, 60-mm dishes containing Complete MCDB 105. One day later (day 0), various concentrations (1 - 100 ng/ml) of triptolide were added. Cells treated with diluent (0.001% DMSO) were included as controls. After 3 days, fresh media containing diluent or triptolide were replaced. Cells in replicate dishes were counted by hemocytometer following trypsinization on days 0, 3 and 6.

Cell Viability. Loss of cell viability was assessed by the trypan blue exclusion method. Cells treated with or without triptolide were harvested by trypsinization. After incubation in 0.04% trypan blue (Sigma-Aldrich) for 4 minutes, cells were counted under a hemocytometer. The number of cells which retained the dye (nonviable) and the total cell number were noted.

Apoptosis. Cells were inoculated at 10^5 cells/dish into collagen-coated, 60-mm dishes containing Complete MCDB 105. One day later, the medium was replaced and cells were treated with various concentrations (1 - 100 ng/ml) of triptolide. Cells treated with diluent (0.001% DMSO) were included as controls. After 24, 48 and 72 h[a], Hoechst 33342 and propidium iodide (Sigma-Aldrich) were added to medium at 10 μg/ml and 20 μg/ml, respectively. After incubation for 15 min at 37 C°, 400 cells from each dish were counted (from ten randomly selected fields) under fluorescence to determine the proportion of viable and apoptotic cells.

Cell Cycle Analyses. Semi-confluent cells were fed fresh medium containing triptolide (1 or 50 ng/ml). Cells treated with diluent (0.001% DMSO) were included as controls. At 24 and 48 h, cells were harvested by trypsinization, washed with cold PBS[a] and fixed by dropwise addition of ice-cold 70% ethanol. After 1 hour of fixation at 4°C, cells were pelleted, then incubated with RNase A (50 μg/ml) (Sigma-Aldrich) and stained with propidium iodide (20 μg/ml). Analyses

of DNA content were carried out on a FACScan flow cytometer and cell-cycle phase distribution was quantified using Cellfit software.

Staining for SA-β-gal[a]. Forty thousand cells were inoculated into each collagen-coated, 60-mm dish containing 5 ml of Complete MCDB 105. The next day, cells were treated with or without 1 ng/ml of triptolide. SA-β-gal- positive cells were detected by the method of Dimri et al[16] after 3, 5 and 10 days of treatment with triptolide. Cells were fed with fresh media and diluent or triptolide on day 5. The presence of positive staining was observed microscopically and photographed.

Immunoblot Analyses. Cells were trypsinized and centrifuged. The cell pellet was washed in ice-cold PBS, resuspended in UTB[a] buffer (9 M urea, 75 mM Tris-HCl, pH 7.5, 0.15 M 2-mercaptoethanol) and sonicated briefly. The protein concentration was determined by a BioRad assay (Bio Rad, Hercules, CA). Typically, 50 or 80 μg of protein were separated by SDS-PAGE[a], transferred to PDVF[a] membranes (Osmonics, Westborough, MA) and blocked in PBS with 5% non-fat milk. Proteins were detected with the following antibodies: mouse anti-p53 mAb[a] (DO-1), mouse anti-p21[a] mAb, rabbit anti-$p16^{INK4a}$ pAb[a], rabbit anti-$p27^{Kip1}$ pAb, mouse anti-bax mAb, mouse anti-hdm-2[a] mAb (SMP14) (Santa Cruz Biotechnology, Santa Cruz, CA); mouse anti-bcl-2 mAb (Chemicon, Temecula, CA); and mouse anti-hdm-2 mAb (2A10) [a gift from Dr. Arnold Levine, Princeton University, NJ.].[17] Anti-species HRP[3]- conjugated secondary antibodies were obtained from Dako (Carpenteria, CA) and visual detection was performed using the ECL[a] method (Amersham, Piscataway, NJ).

Immunocytochemistry. Cells (inoculated at 10^4/chamber) were grown in 8-chamber slides (Nalge Nunc International, Naperville, IL), fixed with 2% paraformaldehyde, and permeabilized with ethanol. Non-specific binding was blocked with 10% horse serum, and then cells were

incubated with following primary antibodies: mouse mAb against p53 (DO-1) and mouse mAb against p21. After rinsing and incubating with biotinylated secondary antibody (Vector Laboratories, Burlingame, CA), labeling was detected with the ABC reagent (Vector Laboratories) and the chromagen diaminobenzidine. After counterstaining with hematoxylin, the slides were coverslipped and examined microscopically.

RESULTS

Triptolide inhibited the growth of prostatic epithelial cells. Clonal assays were used to test the effect of triptolide on the growth of primary cultures of prostatic epithelial cells derived from normal and malignant tissues. Cells were inoculated at 500 cells per dish into medium with or without triptolide (0.01 - 1 ng/ml) and clonal growth was evaluated after 10 days of incubation. Altogether five cell strains, one derived from normal peripheral zone tissue and four derived from adenocarcinomas, were assayed. Figure 1 shows that triptolide was growth inhibitory. Complete growth inhibition of all cell strains occurred with 1 ng/ml of triptolide, with half-maximal growth inhibition at ~ 0.1 ng/ml of triptolide.

We then tested the effect of triptolide on growth of higher density cell cultures. Cells (10^5 per dish) were inoculated into culture medium and one day later treated with or without triptolide (1 - 100 ng/ml). Cell numbers were determined on days 3 and 6. Two cell strains, one derived from normal tissue (E-PZ-10) and one derived from cancer (E-CA-12), were assayed. As shown in Figure 2*a,* treatment with triptolide inhibited cell proliferation in a concentration-dependent manner. Triptolide at 1 ng/ml, which completely inhibited clonal growth, was less inhibitory in high density cultures, with only slight (6%) inhibition on day 3. However, after 6 days of treatment with 1 ng/ml of triptolide, growth inhibition was more apparent (38% reduction of growth compared to control). Slightly higher doses of triptolide (5 – 15 ng/ml) inhibited growth by ~30% at day 3 and ~90% at day 6. The highest concentrations of triptolide (50 and 100 ng/ml) caused loss of cells over time. The response of E-CA-12 cells in high density assays to triptolide was comparable to E-PZ-10 cells. On day 6, growth was inhibited by 1 ng/ml of triptolide to 58% of control. With 50 ng/ml of triptolide, cell number on day 6 declined by 66% from day 0.

E-PZ-10 cells in this assay were also incubated with trypan blue to evaluate the proportion of nonviable cells in treated versus untreated populations. Concentrations of triptolide $\geq$ 50 ng/ml created > 90% nonviable cells by day 3 (Fig. 2*b*). By day 6, > 90% of the cells treated with triptolide concentrations $\geq$ 5 ng/ml were nonviable. Cell viability declined by 47% after 6 days of treatment with 1 ng/ml of triptolide. Comparable results were seen with E-CA-12 cells (data not shown).

Induction of Apoptosis by Triptolide. After observing the decline in cell viability caused by triptolide, particularly at the higher concentrations, we evaluated the induction of apoptosis by triptolide (Fig. 3). For that purpose, E-CA-12 cells (inoculated at 10^5/dish) were stained with Hoechst 33342 and propidium iodide after 24, 48 and 72 h of culture with or without triptolide. The number of live and apoptotic cells was determined on the basis of differential fluorescence and nuclear morphology. The Hoechst 33342 dye is membrane permeable and stains the DNA of viable cells blue. Propidium iodide does not cross intact cell membranes and therefore incorporates into DNA only in apoptotic cells. Triptolide at 1 ng/ml did not cause apoptosis during the 3-day period of exposure. After 24 h of exposure to higher concentrations of triptolide ($\geq$ 50 ng/ml), a modest increase in the apoptotic rate was detected (at maximum, 19% apoptosis with 100 ng/ml of triptolide compared to 7.5% in control populations). However, at 48-72 h, the number of apoptotic cells in the treated populations increased substantially, especially with 50 and 100 ng/ml of triptolide. Triptolide had similar effects on the apoptotic rate of E-PZ-10 cells (data not shown).

Cell Cycle Distribution with Low and High Concentrations of Triptolide. Progression of cells through the cell cycle was evaluated by flow cytometric determination of cellular DNA content. Cell cycle analyses were performed on E-PZ-10 and E-CA-12 cells that had been treated with 1

or 50 ng/ml of triptolide for 24 - 72 h (Table I). The lower concentration of triptolide (1 ng/ml) slightly increased the accumulation of the cells in S-phase after 24 h. However, this effect was transient and not present at 72 h. Triptolide at 50 ng/ml for 24 h increased the proportion of E-PZ-10 cells in S-phase from 20.3% in untreated cells to 32.3% in treated cells, and in E-CA-12 from 22.8% to 30.5%. While the percentage of cells in the S-phase in untreated populations declined with time, the percentage of cells in the S-phase in treated populations remained elevated.

Senescence of Cells Treated with Low Concentrations of Triptolide. We found that 1 ng/ml of triptolide completely inhibited clonal growth of normal and cancer-derived prostatic epithelial cells (Fig. 1). However, inhibition was cell density-dependent, and higher concentrations of triptolide were required to completely inhibit the growth of higher density cultures. We also observed that 1 ng/ml of triptolide did not induce apoptosis in high density cultures (see previous sections and Fig. 3). We considered the possibility that senescence might be involved in growth inhibition of prostatic epithelial cells by low doses of triptolide. SA-β-gal assays were conducted to address this possibility. Semi-confluent cultures of normal and cancer-derived cells (E-PZ-10 and E-CA-13) were treated with or without 1 ng/ml of triptolide for up to 10 days. SA-β-gal activity was found to be minimal in untreated cells throughout the course of the experiment. In contrast, significant SA-β-gal activity, as evidenced by blue cytoplasmic staining, was noted in normal cells after 5 days of triptolide treatment (Fig. 4). SA-β-gal activity became somewhat more pronounced after 10 days (data not shown). Cancer-derived cells exhibited relatively faint levels of SA-β-gal after 5 days of treatment with triptolide compared to normal cells. Blue staining was more evident after 10 days of treatment of cancer-derived cells (data not shown).

Modulation of Signaling Pathways by Low Concentration of Triptolide. Triptolide at 1 ng/ml inhibited clonal growth as well as high-density cell proliferation after 6 days of incubation. This concentration of triptolide also induced SA-β-gal, a marker of senescence. We wanted to further investigate the possible molecular pathways associated with the observed inhibition of cell proliferation and induction of senescence by low concentrations of triptolide. Expression of p53 protein and cell cycle regulators $p16^{INK4a}$, p21 and $p27^{Kip1}$ were investigated in E-CA-12 and E-PZ-10 cells after 3, 5 and 10 days of exposure to 1 ng/ml of triptolide. These time points corresponded to those at which expression of SA-β-gal became apparent. None of these proteins were altered in E-CA-12 (Fig. 5) or E-PZ-10 (data not shown) cells by 1 ng/ml of triptolide. Protein levels of p53 were also analyzed at earlier time points (6 and 24 h after exposure to triptolide) in E-PZ-10 and E-CA-11 cells. No changes in p53 protein levels were observed at these time points (data not shown).

Modulation of Signaling Pathways by High Concentration of Triptolide. Higher concentrations of triptolide were shown to induce apoptotic cell death. Since p53 may trigger apoptosis, we investigated the expression of p53 in E-CA-12 and E-PZ-10 cells after 6, 24, 48 and 72 h of treatment with 50 ng/ml of triptolide. Triptolide increased p53 levels in E-CA-12 cells at 6 h, reaching a maximum after 24 and 48 h (Fig. 6*a*). Levels of p53 declined towards basal level after 72 h of exposure to triptolide. Similar patterns of p53 expression were observed in E-PZ-10 cells (Fig. 6*b*, 72 h time point not shown).

The expression levels of p53 target gene products (hdm-2, p21, bax and bcl-2) and other p53-independent cell cycle regulators ($p16^{INK4a}$ and $p27^{Kip1}$) were also analyzed in immunoblots. Triptolide decreased levels of the intact, 90 kDa hdm-2 protein in E-CA-12 and E-PZ-10 (data not shown) cell strains significantly after 24 h as detected by the hmd2-specific 2A10 (Fig. 6*a*)

and SMP14 monoclonal antibodies (data not shown). Cleaved forms of Hdm-2 (60 kDa) detected by the same hdm-2-specific antibodies increased steadily after 24 h of treatment with triptolide in E-CA-12 (Fig. 6*a*, results with mAb 2A10 against 60 kDa hdm-2 not shown) and E-PZ-10 cells (data not shown).

Triptolide (50 ng/ml) reduced p21 levels in E-PZ-10 cells below the basal expression level of this protein at 24 h (Fig. 6*b*). The non-p53-regulated cell cycle inhibitor $p27^{Kip1}$ declined in triptolide-treated cells in a similar manner to p21 (Fig. 6*b*). No changes in the non-p53-regulated cell cycle inhibitor $p16^{INK4a}$ were found after triptolide treatment (Fig. 6*b*). Triptolide reduced levels of the anti-apoptotic protein, bcl-2, after 48 – 72 h (72 h not shown). The decline in bcl-2 levels corresponded with 43% and 79% of cells undergoing apoptotic cell death at 48 and 72 h, respectively, in response to 50 ng/ml of triptolide (Fig. 3 and 6*b*). No change in expression of the p53 target and proapoptotic protein bax was found after triptolide treatment (Fig. 6*b*). Effects on signaling pathways (p21, $p27^{Kip1}$, $p16^{INK4a}$ and bax) by triptolide in E-CA-12 cells were similar to E-PZ-10 cells (data not shown). The decline in bcl-2 levels was not so obvious in E-CA-12 cells compared to E-PZ-10 cells, because the basal level of expression of bcl-2 in E-CA-12 cells was relatively low compared to E-PZ-10 cells.

Immunocytochemical Analyses of p53 and p21. We wanted to further explore the dose-dependent responses of p53 and p21 to triptolide after observing the changes in the levels of these proteins after treatment with 50 but not 1 ng/ml of triptolide. E-PZ-10 cells were treated with triptolide (1 – 100 ng/ml) and the levels and intracellular localization of p53 and p21 were analyzed after 24 h by immunocytochemistry. A dose-dependent accumulation of p53 was seen in nuclei of E-PZ-10 cells (Fig. 7, *a* - *d*). The nuclear accumulation of p53 became evident with concentrations of triptolide ≥ 10 ng/ml. Levels of the p53 target protein p21 were seen to decline

at 24 h. Decreased expression of p21 was most evident with ≥ 50 ng/ml of triptolide (Fig. 7, *e* - *h*). A similar dose response was evaluated with E-PZ-10 cells and protein levels of p53 and p21 were analyzed by immunoblot. Total protein data showed that 15 ng/ml of triptolide was sufficient to induce p53 accumulation at 24 h (data not shown). Comparable to results from immunocytochemistry, only higher concentrations of triptolide (50 and 100 ng/ml) reduced p21 levels when protein levels were analyzed on immunoblots (data not shown).

DISCUSSION

Chemotherapy for prostate cancer is still of limited efficacy although development of several promising new modalities is under way.[18] Our previous studies on the role of p53 in mediating growth inhibition or apoptosis of prostate cancer cells by DNA damage- inducing drugs and γ-irradiation led us to suggest that drugs that work through p53-independent mechanisms might be most useful for treating prostate cancer, even those cancers that retain wild-type p53. Previous studies reported that triptolide inhibited growth and induced apoptosis of HL-60 cancer cells in a p53-independent manner.[4] However, a more recent study by Chang et al.[19] showed that triptolide-mediated enhancement of chemotherapy-induced apoptosis was accompanied by enhanced translation and accumulation of wild-type p53 protein in HT1080 cells. Altogether these results suggest that triptolide may use multiple signaling pathways, some perhaps involving p53, when causing cell death. We decided to test the effects of triptolide on primary cultures of prostatic epithelial cells to see if this type of reagent would show anti-tumor activity.

Our results demonstrate that triptolide indeed exhibits many anti-tumor activities against prostate cells in a dose-dependent manner. Low concentrations of triptolide (1 ng/ml) inhibited growth completely in clonal assays and partially in high cell density assays. Growth inhibition with 1 ng/ml of triptolide was accompanied by the induction of SA-β-gal activity, a widely used marker of senescence. In addition to expression of SA-β-gal, cells adopted several morphological changes that have been associated with a senescent-like phenotype.[20, 21] These changes included an enlarged and flattened shape and the development of vacuoles.

We did not observe any regulation of p53, p21, $p27^{Kip1}$ or $p16^{INK4a}$ in prostatic epithelial cells in response to 1 ng/ml of triptolide, despite the induction of a senescent-like phenotype. Replicative senescence of prostatic epithelial cells, in contrast to fibroblasts, does not seem to

involve p53 or p21.[22, 23] However, increased expression of $p16^{INK4a}$ was found in association with replicative senescence of prostatic epithelial cells,[22] which was not the case for the senescent-like phenotype induced by triptolide. A number of factors have been reported to induce a senescent-like state in cells, but it is not known if this phenotype is exactly equivalent to replicative senescence.[20, 24]

Higher concentrations of triptolide (15 - 100 ng/ml) effectively inhibited high density cell growth, and 50 - 100 ng/ml of triptolide induced apoptosis in the majority of cells after 3 days of treatment. High doses of triptolide caused a number of molecular changes in prostatic epithelial cells in conjunction with the induction of apoptosis. Interestingly, protein levels of p53 were significantly increased and predominantly accumulated in the nuclei of prostatic epithelial cells. However, we did not find induction of p53 downstream target genes (such as hdm-2, p21 or bax), as has been described to accompany p53-mediated apoptosis in response to cellular stresses such as DNA damage.[25, 26] On the contrary, protein levels of many p53 target genes were reduced after triptolide treatment. For example, our results showed reduction of hmd-2 (the intact 90 kDa form) after triptolide treatment. Given that hdm-2 targets p53 for degradation,[27] the reduction in hdm-2 protein could partially provide an explanation for the observed sustained elevation of p53. Reduction of 90 kDa hdm-2 was detected by two antibodies, 2A10 and SMP14. The former antibody does not bind hdm-2 protein that is phosphorylated in the middle portion of the molecule.[28] However, the fact that lower levels of hdm-2 were also detected by SMP14, whose reactivity with hdm-2 is not altered by phosphorylation, suggests that total protein was decreased.

As the intact, 90 kDa form of hdm-2 protein decreased in response to triptolide, a 60 kDa form of hdm-2 accumulated. It has been reported that mdm-2, the mouse homologue of hdm-2,

is a substrate for proteases involved in apoptosis that share specificity with CPP32 (caspase-3). These proteases cleave mdm-2 at residue 361, generating a 60 kDa fragment.[29, 30] More recently, work from the same investigators showed that a distinct caspase activity for hdm-2 was induced by p53 prior to the onset of apoptosis in H1299 cells expressing a temperature-sensitive human p53.[31] The p53 binding and inhibitory functions of hdm-2 have not been reported to be affected by the cleavage. However, cleaved hdm-2 has been reported to be unable to promote p53 degradation and may function in a dominant-negative fashion to stabilize p53.[29, 31] The relationship of cleaved hdm-2 to accumulation of p53 and apoptosis in prostatic epithelial cells in response to triptolide is under investigation.

Another interesting feature associated with the induction of p53 by triptolide in prostate cells and in other cells[19] was decreased p21 expression. Reduction in p21 protein levels by triptolide was reported to be due to transcriptional inhibition of p21, and triptolide did not affect p21 expression in the p53-mutant HT29 colon cancer cell line.[19] However, caspase-mediated cleavage of p21 has also been reported,[32, 33] so we cannot rule out the possibility that reduced levels of p21 protein may be a consequence of apoptosis and not directly mediated by p53 in prostatic cells. It has been reported that the p21 protein can antagonize p53-mediated apoptosis, as the induction of endogenous p21 or overexpression of a p21 transgene prevents apoptosis.[34, 35] Chang et al. showed that triptolide blocked doxorubicin-mediated induction of p21 and accumulation of cells in G2/M.[19] Together, doxorubicin and triptolide showed cooperative proapoptotic effects. The investigators proposed that triptolide, by blocking p21-mediated growth arrest, caused conflicting cell cycle checkpoints that enhanced apoptosis. These results stimulate further investigation of triptolide not only as a single agent but also in combination with other cytotoxic drugs for cancer treatment.

Apoptosis was also associated with reduction of the p53 target gene product and anti-apoptotic bcl-2 protein. Protein levels of the pro-apoptotic protein bax remained unchanged. The increased ratio of bax/bcl-2 may have a role in the induction of apoptosis by triptolide.

Triptolide also reduced expression of $p27^{Kip1}$, which is not a direct target of p53. Reduction in $p27^{Kip1}$ protein can be due to S-phase block and activity of ubiquitin protein ligase $p45^{SKP2}$ that is known to promote $p27^{Kip1}$ degradation and induction of S-phase.[36, 37] Therefore, the reduced levels of $p27^{Kip1}$ that we observed may be a consequence of the S-phase arrest induced in prostatic cells by triptolide. Alternatively, reduction of $p27^{Kip1}$ protein levels could reflect caspase activity in conjunction with apoptosis.[38]

Further investigations are underway to determine if upregulation of p53 is coincidental to or required for the induction of apoptosis by triptolide in prostatic cells. Nevertheless, it is noteworthy that triptolide is one of the few agents that we have found to induce p53 in primary cultures of prostatic epithelial cells. DNA-damaging drugs and γ-irradiation do not induce p53 in these cells, and the signaling pathway used by these agents to activate p53 appears nonfunctional in prostatic cells. It is known that p53 can trigger apoptosis through both transactivation-dependent[39] and transactivation-independent mechanisms.[40] For instance, Koumenis et al.[41] reported that hypoxia-induced p53-dependent apoptosis failed to induce endogenous downstream p53 effector mRNAs and proteins. Disparate mechanisms of p53-mediated apoptosis exist and it is believed that different types of stresses use different signaling pathways to activate p53.[42] Identification of agents such as triptolide that activate p53 and/or apoptosis in prostate cancer cells may be very relevant to developing novel therapeutic drugs.

The dose-dependent effects of triptolide are reminiscent of those of certain other compounds that have been studied for anti-tumor activity. The microtubule inhibitor paclitaxel is an

example of a compound that at low concentrations was reported to induce mitotic arrest in several types of cancer cells, but at high concentrations triggered rapid apoptosis.[43] Another example is the induction of senescence in normal human fibroblasts by low concentrations of hydrogen peroxide and apoptosis in response to high concentrations of hydrogen peroxide.[44] The effects of different doses of triptolide on prostatic epithelial cells might be exploited for different applications. The moderate growth-inhibitory activity and induction of senescence by low doses of triptolide might be appropriate for chemopreventive strategies against prostate cancer. The fact that normal as well as cancer-derived cells responded to triptolide is supportive of this possibility. The proapoptotic activity of higher doses of triptolide might be more suitable for chemotherapeutic applications. It is noteworthy that primary cultures of prostatic cancer cells, in contrast to established cell lines, are very resistant to apoptosis. We have identified few agents capable of causing apoptosis in these cells, so if this resistance to cell death is reflective of cancer in vivo, then any compound capable of inducing apoptosis of primary cultures may be particularly worthy of further investigation.

ACKNOWLEDGEMENTS

We thank Dr. Glenn Rosen for helpful discussions and critical reading of the manuscript.

REFERENCES

1. Ramgolam V, Ang SG, Lai YH, Loh CS, Yap HK. Traditional Chinese medicines as immunosuppressive agents. Ann Acad Med Singapore 2000;29:11-16.
2. Kupchan SM, Court WA, Dailey RG, Jr., Gilmore CJ, Bryan RF. Triptolide and tripdiolide, novel antileukemic diterpenoid triepoxides from Tripterygium wilfordii. J Am Chem Soc 1972;94:7194-95.
3. Shamon LA, Pezzuto JM, Graves JM, Mehta RR, Wangcharoentrakul S, Sangsuwan R, et al. Evaluation of the mutagenic, cytotoxic, and antitumor potential of triptolide, a highly oxygenated diterpene isolated from Tripterygium wilfordii. Cancer Lett 1997;112:113-17.
4. Wei YS, Adachi I. Inhibitory effect of triptolide on colony formation of breast and stomach cancer cell lines. Zhongguo Yao Li Xue Bao 1991;12:406-10.
5. el-Deiry WS, Tokino T, Velculescu VE, Levy DB, Parsons R, Trent JM, et al. WAF1, a potential mediator of p53 tumor suppression. Cell 1993;75:817-25.
6. Amundson SA, Myers TG, Fornace AJ, Jr. Roles for p53 in growth arrest and apoptosis: putting on the brakes after genotoxic stress. Oncogene 1998;17:3287-99.
7. Jimenez GS, Khan SH, Stommel JM, Wahl GM. p53 regulation by post-translational modification and nuclear retention in response to diverse stresses. Oncogene 1999;18:7656-65.
8. Girinsky T, Koumenis C, Graeber TG, Peehl DM, Giaccia AJ. Attenuated response of p53 and p21 in primary cultures of human prostatic epithelial cells exposed to DNA-damaging agents. Cancer Res 1995;55:3726-31.

9. Navone NM, Troncoso P, Pisters LL, Goodrow TL, Palmer JL, Nichols WW, et al. p53 protein accumulation and gene mutation in the progression of human prostate carcinoma. J Natl Cancer Inst 1993;85:1657-69.

10. Zhao G, Vaszar LT, Qiu D, Shi L, Kao PN. Anti-inflammatory effects of triptolide in human bronchial epithelial cells. Am J Physiol Lung Cell Mol Physiol 2000;279:L958-66.

11. Lee KY, Chang W, Qiu D, Kao PN, Rosen GD. PG490 (triptolide) cooperates with tumor necrosis factor-alpha to induce apoptosis in tumor cells. J Biol Chem 1999;274:13451-55.

12. Qiu D, Zhao G, Aoki Y, Shi L, Uyei A, Nazarian S, et al. Immunosuppressant PG490 triptolide) inhibits T-cell interleukin-2 expression at the level of purine-box/nuclear factor of activated T- cells and NF-kappaB transcriptional activation. J Biol Chem 1999;274:13443-50.

13. Schmid HP, McNeal JE. An abbreviated standard procedure for accurate tumor volume estimation in prostate cancer. Am J Surg Pathol 1992;16:184-91.

14. Peehl DM. Culture of human prostatic epithelial cells. In: Freshney RI, ed. Culture of Epithelial Cells. New York, NY: Wiley- Liss, Inc., 1992:159-80.

15. Tsao MC, Walthall BJ, Ham RG. Clonal growth of normal human epidermal keratinocytes in a defined medium. J Cell Physiol 1982;110:219-29.

16. Dimri GP, Lee X, Basile G, Acosta M, Scott G, Roskelley C, et al. A biomarker that identifies senescent human cells in culture and in aging skin in vivo. Proc Natl Acad Sci U S A 1995;92:9363-67.

17. Chen J, Marechal V, Levine AJ. Mapping of the p53 and mdm-2 interaction domains. Mol Cell Biol 1993;13:4107-14.

18. Wang J, Waxman J. Chemotherapy for prostate cancer. Urol Oncol 2000;5:93-96.

19. Chang WT, Kang JJ, Lee KY, Wei K, Anderson E, Gotmare S, et al. Triptolide and chemotherapy cooperate in tumor cell apoptosis. A role for the p53 pathway. J Biol Chem 2001;276:2221-27.

20. Young J, Smith JR. Epigenetic aspects of cellular senescence. Exp Gerontol 2000;35:23-32.

21. Chang BD, Broude EV, Dokmanovic M, Zhu H, Ruth A, Xuan Y, et al. A senescence-like phenotype distinguishes tumor cells that undergo terminal proliferation arrest after exposure to anticancer agents. Cancer Res 1999;59:3761-67.

22. Sandhu C, Peehl DM, Slingerland J. p16INK4A mediates cyclin dependent kinase 4 and 6 inhibition in senescent prostatic epithelial cells. Cancer Res 2000;60:2616-22.

23. Jarrard DF, Sarkar S, Shi Y, Yeager TR, Magrane G, Kinoshita H, et al. p16/pRb pathway alterations are required for bypassing senescence in human prostate epithelial cells. Cancer Res 1999;59:2957-64.

24. Collado M, Medema RH, Garcia-Cao I, Dubuisson ML, Barradas M, Glassford J, et al. Inhibition of the phosphoinositide 3-kinase pathway induces a senescence-like arrest mediated by p27Kip1. J Biol Chem 2000;275:21960-68.

25. Ljungman M. Dial 9-1-1 for p53: mechanisms of p53 activation by cellular stress. Neoplasia 2000;2:208-25.

26. el-Deiry WS. Regulation of p53 downstream genes. Semin Cancer Biol 1998;8:345-57.

27. Haupt Y, Maya R, Kazaz A, Oren M. Mdm2 promotes the rapid degradation of p53. Nature 1997;387:296-99.

28. Khosravi R, Maya R, Gottlieb T, Oren M, Shiloh Y, Shkedy D. Rapid ATM-dependent phosphorylation of MDM2 precedes p53 accumulation in response to DNA damage. Proc Natl Acad Sci U S A 1999;96:14973-77.

29. Chen L, Marechal V, Moreau J, Levine AJ, Chen J. Proteolytic cleavage of the mdm2 oncoprotein during apoptosis. J Biol Chem 1997;272:22966-73.

30. Erhardt P, Tomaselli KJ, Cooper GM. Identification of the MDM2 oncoprotein as a substrate for CPP32-like apoptotic proteases. J Biol Chem 1997;272:15049-52.

31. Pochampally R, Fodera B, Chen L, Lu W, Chen J. Activation of an MDM2-specific caspase by p53 in the absence of apoptosis. J Biol Chem 1999;274:15271-77.

32. Zhang Y, Fujita N, Tsuruo T. Caspase-mediated cleavage of p21Waf1/Cip1 converts cancer cells from growth arrest to undergoing apoptosis. Oncogene 1999;18:1131-38.

33. Park JA, Kim KW, Kim SI, Lee SK. Caspase 3 specifically cleaves p21WAF1/CIP1 in the earlier stage of apoptosis in SK-HEP-1 human hepatoma cells. European Journal of Biochemistry 1998;257:242-48.

34. Bissonnette N, Hunting DJ. p21-induced cycle arrest in G1 protects cells from apoptosis induced by UV-irradiation or RNA polymerase II blockage. Oncogene 1998;16:3461-69.

35. Gorospe M, Cirielli C, Wang X, Seth P, Capogrossi MC, Holbrook NJ. p21(Waf1/Cip1) protects against p53-mediated apoptosis of human melanoma cells. Oncogene 1997;14:929-35.

36. Sutterluty H, Chatelain E, Marti A, Wirbelauer C, Senften M, Muller U, et al. p45SKP2 promotes p27Kip1 degradation and induces S phase in quiescent cells. Nat Cell Biol 1999;1:207-14.

37. Carrano AC, Eytan E, Hershko A, Pagano M. SKP2 is required for ubiquitin-mediated degradation of the CDK inhibitor p27. Nat Cell Biol 1999;1:193-99.

38. Levkau B, Koyama H, Raines EW, Clurman BE, Herren B, Orth K, et al. Cleavage of p21Cip1/Waf1 and p27Kip1 mediates apoptosis in endothelial cells through activation of Cdk2: role of a caspase cascade. Mol Cell 1998;1:553-63.

39. Yonish-Rouach E, Deguin V, Zaitchouk T, Breugnot C, Mishal Z, Jenkins JR, et al. Transcriptional activation plays a role in the induction of apoptosis by transiently transfected wild-type p53. Oncogene 1995;11:2197-205.

40. Caelles C, Helmberg A, Karin M. p53-dependent apoptosis in the absence of transcriptional activation of p53-target genes. Nature 1994;370:220-23.

41. Koumenis C, Alarcon R, Hammond E, Sutphin P, Hoffman W, Murphy M, et al. Regulation of p53 by hypoxia: dissociation of transcriptional repression and apoptosis from p53-dependent transactivation. Mol Cell Biol 2001;21:1297-310.

42. Giaccia AJ, Kastan MB. The complexity of p53 modulation: emerging patterns from divergent signals. Genes Dev 1998;12:2973-83.

43. Wang TH, Wang HS, Soong YK. Paclitaxel-induced cell death: where the cell cycle and apoptosis come together. Cancer 2000;88:2619-28.

44. Chen QM, Liu J, Merrett JB. Apoptosis or senescence-like growth arrest: influence of cell-cycle position, p53, p21 and bax in H2O2 response of normal human fibroblasts. Biochem J 2000;347:543-51.

TABLE I. EFFECTS OF TRIPTOLIDE ON CELL CYCLE DISTRIBUTION[1]

		24 h			72 h		
		Triptolide (ng/ml)			Triptolide (ng/ml)		
	Cell Phase	0	1	50	0	1	50
E-PZ-10	**G1**	67.8 [2]	57.5	55.5	74.3	73.4	46.5
	S	20.3	26.4	32.3	15.4	12.8	40.4
	G2-M	11.7	16.3	12.2	10.3	13.8	13.1
E-CA-12	**G1**	59.5	55.8	59.2	70.5	75.0	52.6
	S	22.8	28.7	30.5	14.1	9.4	35.7
	G2-M	17.7	15.5	10.3	15.5	15.6	11.7

[1] Sub-confluent cultures of E-PZ-10 and E-CA-12 cells were treated with indicated concentrations of triptolide and harvested for cell cycle after 24h and 72 h of treatment with or without triptolide.

[2] Each entry indicates the proportion of cells (%) in the respective cell cycle compartments, as determined by flow cytometric analysis after propidium iodide staining.

FIGURE LEGENDS

FIGURE 1. Clonal growth response to triptolide. Five prostatic epithelial cell strains, four derived from cancer and one from normal tissue, were inoculated at 500 cells/dish and grown in the presence of varying concentrations of triptolide for 10 days. Growth of each cell strain without triptolide was set as 100%. Each point represents the average value from two separate experiments, with triplicate dishes in each experiment, ± SEM.

FIGURE 2. Growth response to triptolide in high cell density cultures. *(a)*, E-PZ-10 cells were inoculated at 10^5/dish. The next day (day 0), cell number was determined in triplicate dishes and replicate dishes were treated with varying concentrations of triptolide. Fresh medium with or without triptolide was replaced on day 3. The number of attached cells per dish was determined at the indicated times. Each point represents the average value from two to three replicate dishes ± SEM. *(b)*, loss of viability of E-PZ-10 cells in the assay described in panel *A* as determined by trypan blue exclusion. Each bar represents the average value from two to three replicate dishes ± SEM.

FIGURE 3. Induction of apoptosis by triptolide. E-CA-12 cells were treated with various concentrations of triptolide (1 - 100 ng/ml) for 24-72 h. The amount of apoptosis was quantified by Hoechst 33342/propidium iodide staining of nuclear DNA in conjunction with nuclear morphology. Four hundred cells were randomly selected and the number of cells with normal and abnormal nuclei was noted for each treatment. Data represents the mean (± SEM) of two separate experiments.

FIGURE 4. SA-β-gal expression in triptolide-treated cells. E-PZ-10 cells were treated with or without 1 ng/ml of triptolide for 5 days, then were stained for SA β-gal activity. Staining was minimal in untreated cultures, but substantial in treated populations (dark cells).

FIGURE 5. Western blot analysis of p53 and cell cycle regulators after incubation of E-CA-12 cells for 3, 5 and 10 days with 1 ng/ml of triptolide. Cells were fed fresh media with triptolide (+) or with diluent (-) on days 0, 2, 4, 7 and 9. Cell extracts were prepared and the equivalent of 50 or 80 μg ($p21^{WAF1/CIP1}$ panel) of protein per lane was subjected to SDS-PAGE. Blots were prepared and labeled with antibodies against p53, p21, $p27^{Kip1}$, and $p16^{INK4a}$.

FIGURE 6. Molecular changes with high concentration of triptolide. *(a)*, p53 and hdm-2 in E-CA-12 cells in response to 50 ng/ml of triptolide (+) or diluent (-) were evaluated at 6 – 72 h by Western blot. Anti-hmd-2 2A10 mAb was used to detect the intact, 90 kDa hdm-2 protein, and anti-hdm-2 SMP14 mAb was used to detect the 60 kDa hdm-2. Cell extracts were prepared and the equivalent of 50 μg of protein per lane was subjected to SDS-PAGE. *(b)*, p53, $p21^{WAF1/CIP1}$, $p27^{Kip1}$,$p16^{INK4a}$, bcl-2 and bax were evaluated by Western blot after incubation of E-PZ-10 cells for 6 - 48 h with 50 ng/ml of triptolide (+) or diluent (-). Cell extracts were prepared and the equivalent of 50 μg of protein per lane was subjected to SDS-PAGE. The cell extract from diluent -treated E-PZ-10 cells was included as a control at each indicated time point.

FIGURE 7. Immunocytochemical localization of p53 and p21 in prostatic epithelial cells after triptolide treatment. E-PZ-10 cells (10^4) were inoculated onto 8-well chamber slides and allowed to attach overnight. Diluent [*a*) and *e*)] or triptolide [1 ng/ml, *b*) and *f*), 10 ng/ml, *c*) and

g), or 50 ng/ml, *d*) and *h*)] was then added for 24 h before cells were fixed, stained and mounted. In *a*) – *d*), p53 expression was detected by anti-p53 mAb DO-1. In *e*) – *h*), p21 expression was detected by anti-p21$^{WAF1/CIP1}$ mAb.

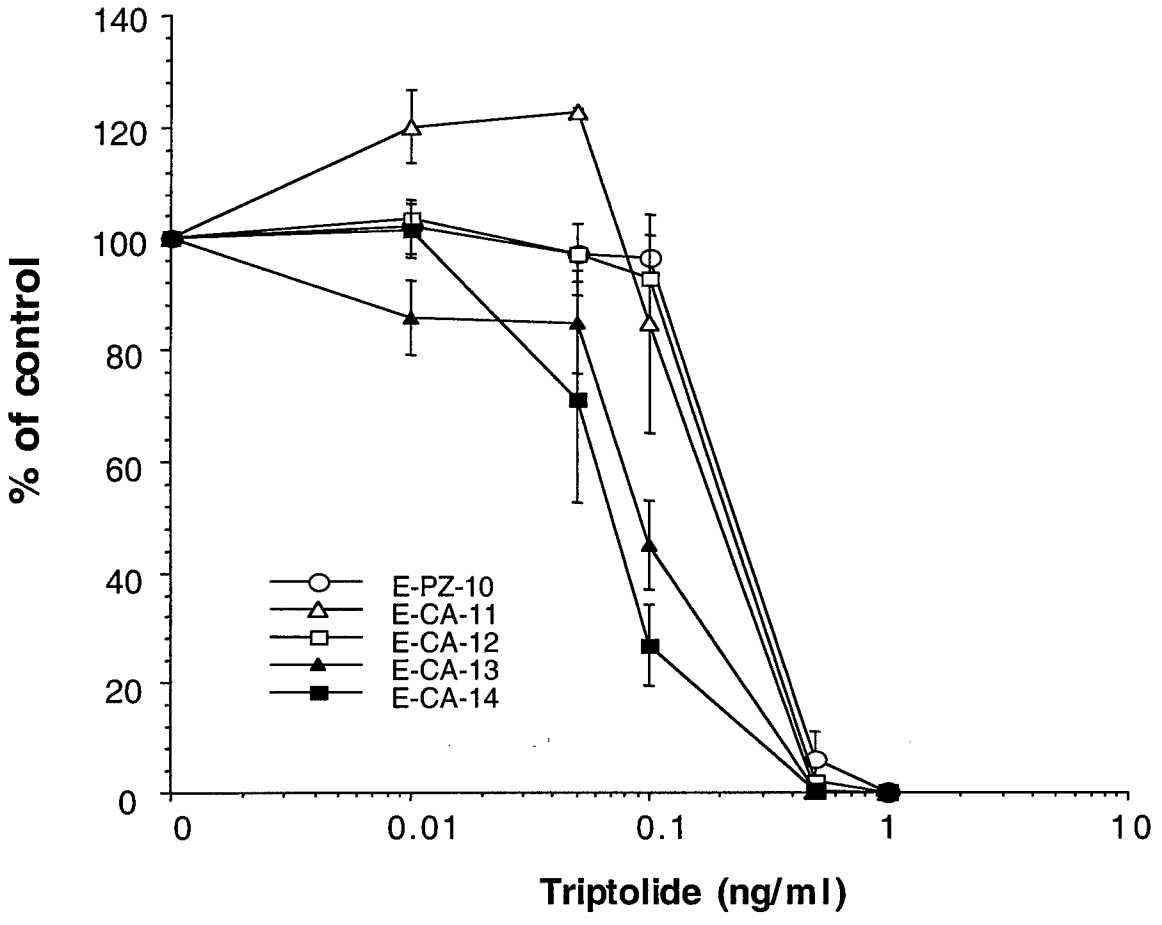
140
120
100
80
60
40
20
0
% of control
0
0.01
0.1
1
10
Triptolide (ng/ml)
E-PZ-10
E-CA-11
E-CA-12
E-CA-13
E-CA-14

A

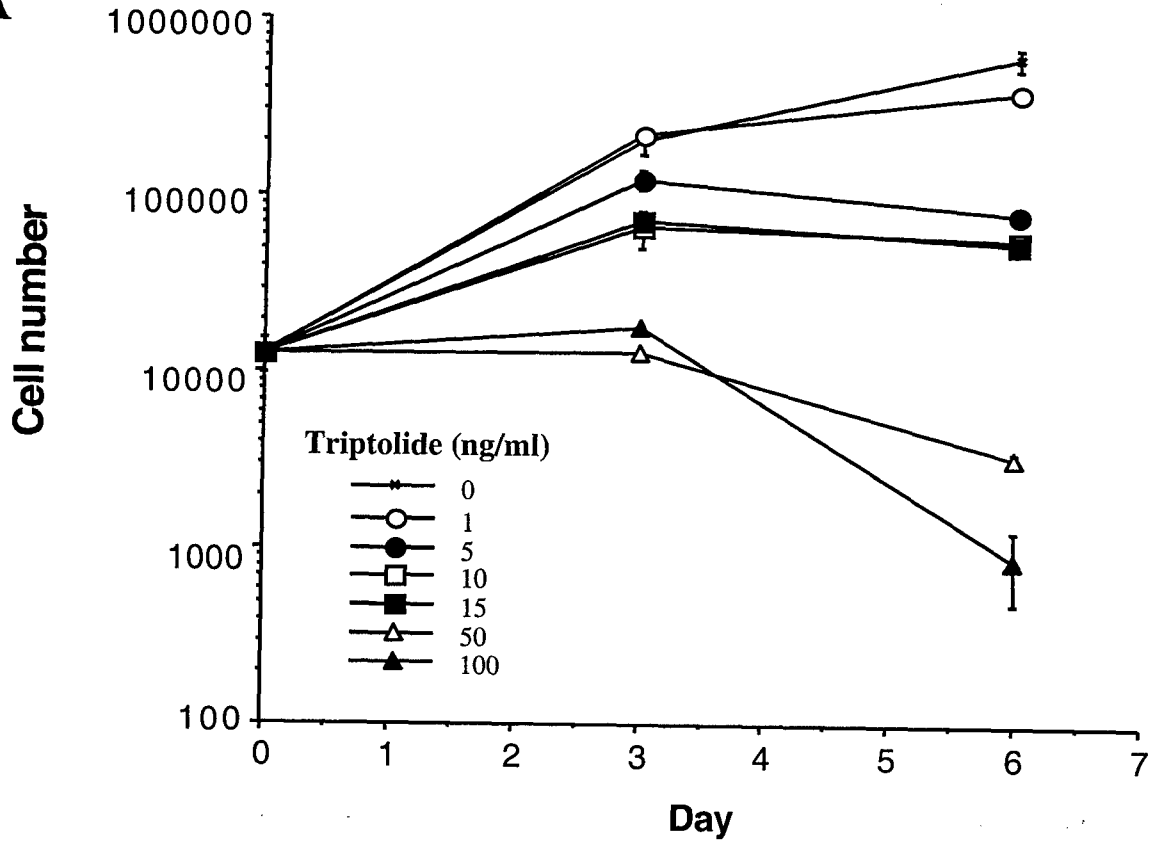
1000000
100000
10000
1000
100
Cell number
0
1
2
3
4
5
6
7
Day
Triptolide (ng/ml)
0
1
5
10
15
50
100

B

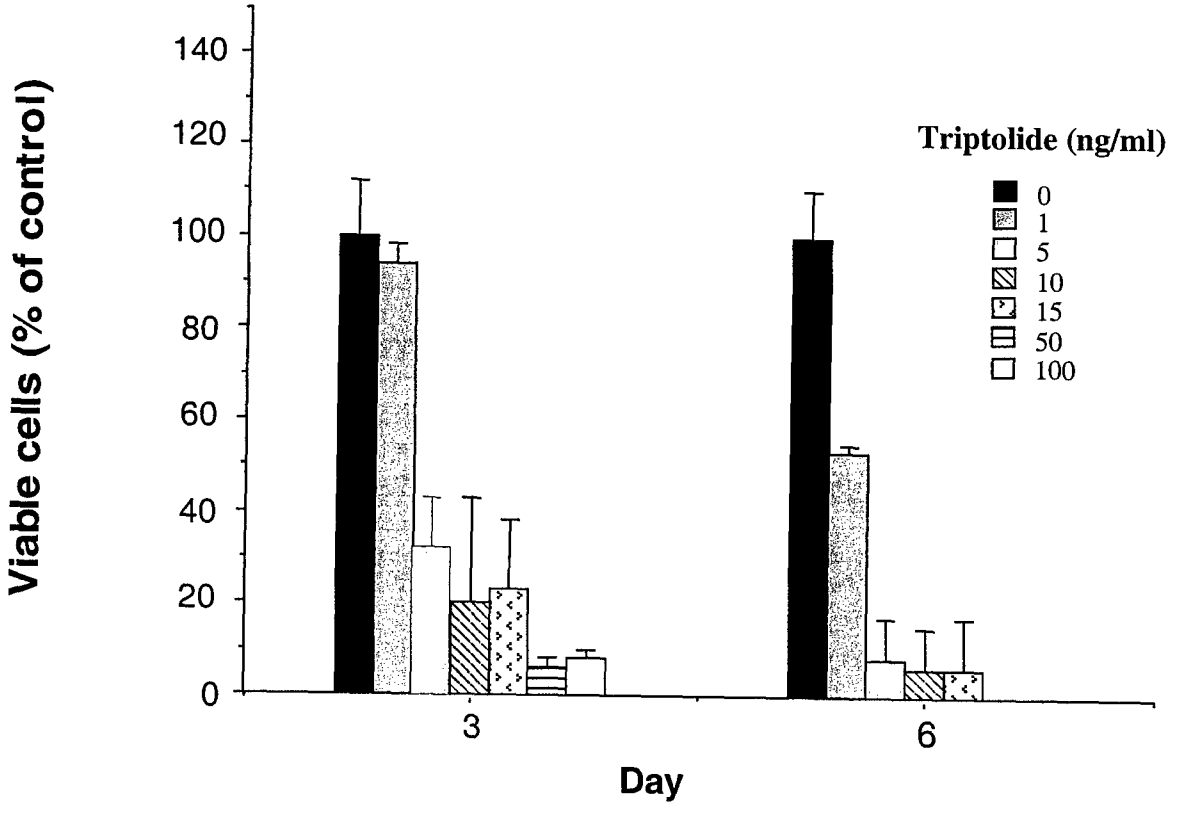
140
120
100
80
60
40
20
0
Viable cells (% of control)
3
6
Day
Triptolide (ng/ml)
0
1
5
10
15
50
100

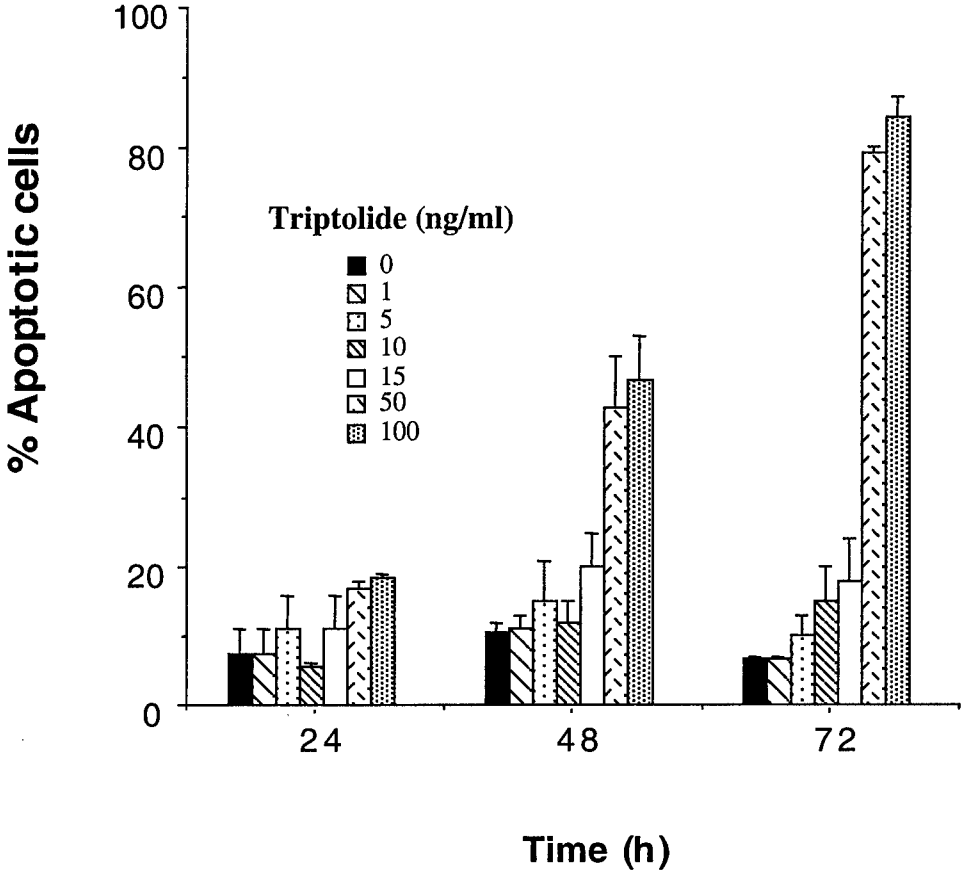
% Apoptotic cells
100
80
60
40
20
0
Triptolide (ng/ml)
0
1
5
10
15
50
100
24
48
72
Time (h)

Triptolide

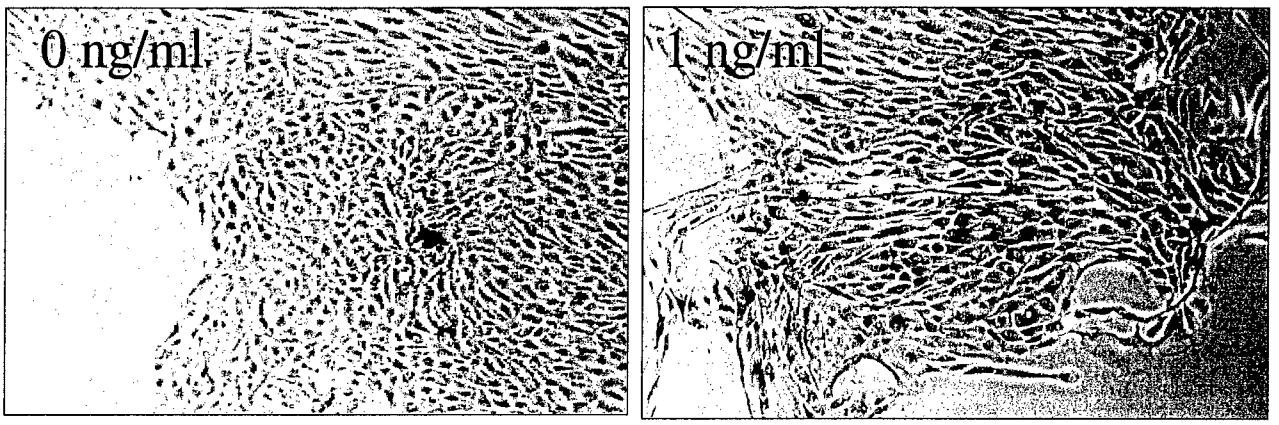

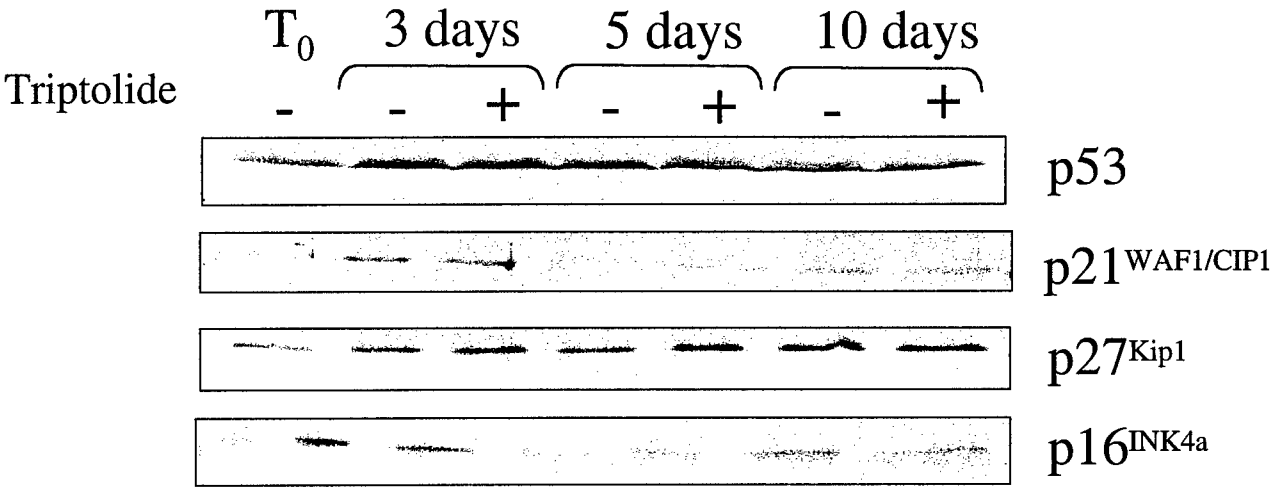
T0
3 days
5 days
10 days
Triptolide
- - + - + - +
p53
p21WAF1/CIP1
p27Kip1
p16INK4a

A

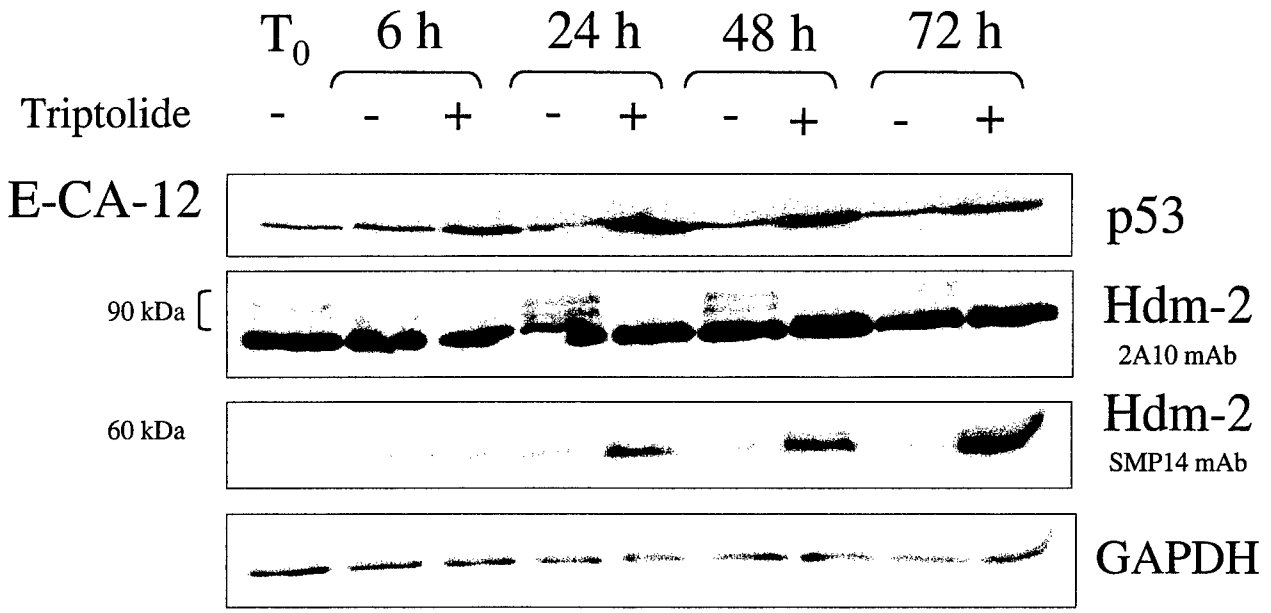
T0
6 h
24 h
48 h
72 h
Triptolide
- - + - + - + - +
E-CA-12
p53
90 kDa
Hdm-2
2A10 mAb
60 kDa
Hdm-2
SMP14 mAb
GAPDH

B

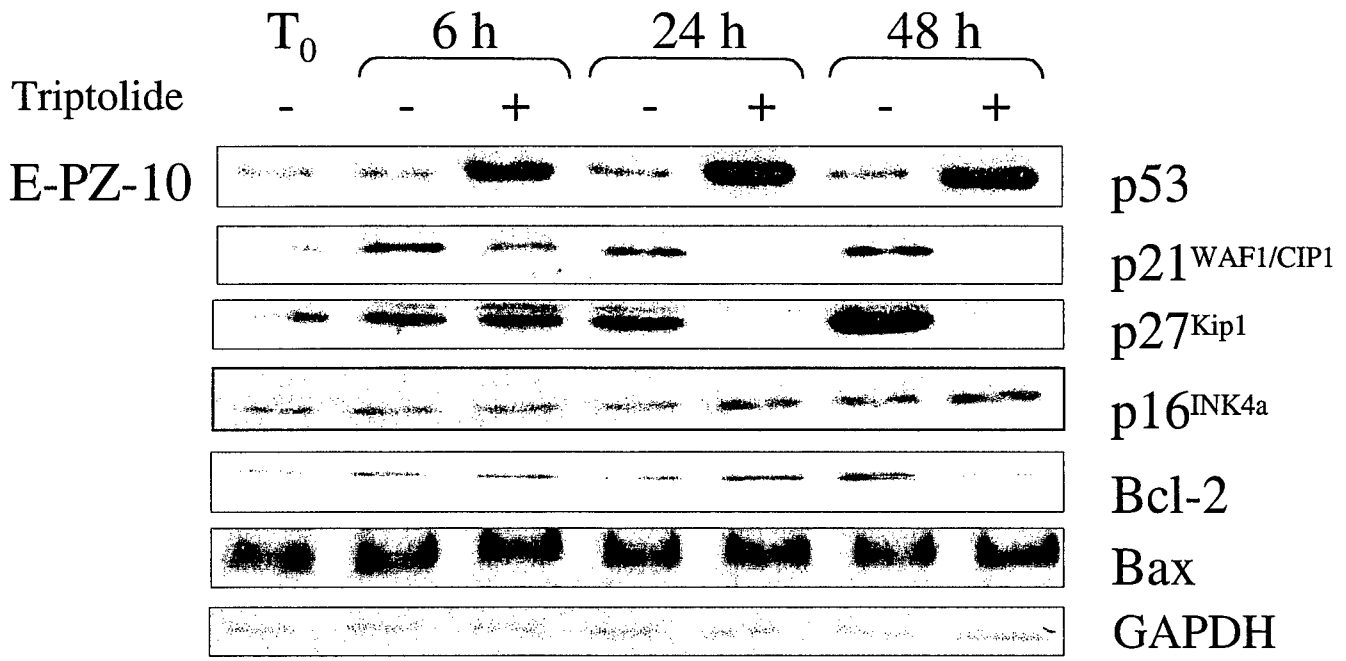
T0
6 h
24 h
48 h
Triptolide
- - + - + - +
E-PZ-10
p53
p21WAF1/CIP1
p27Kip1
p16INK4a
Bcl-2
Bax
GAPDH

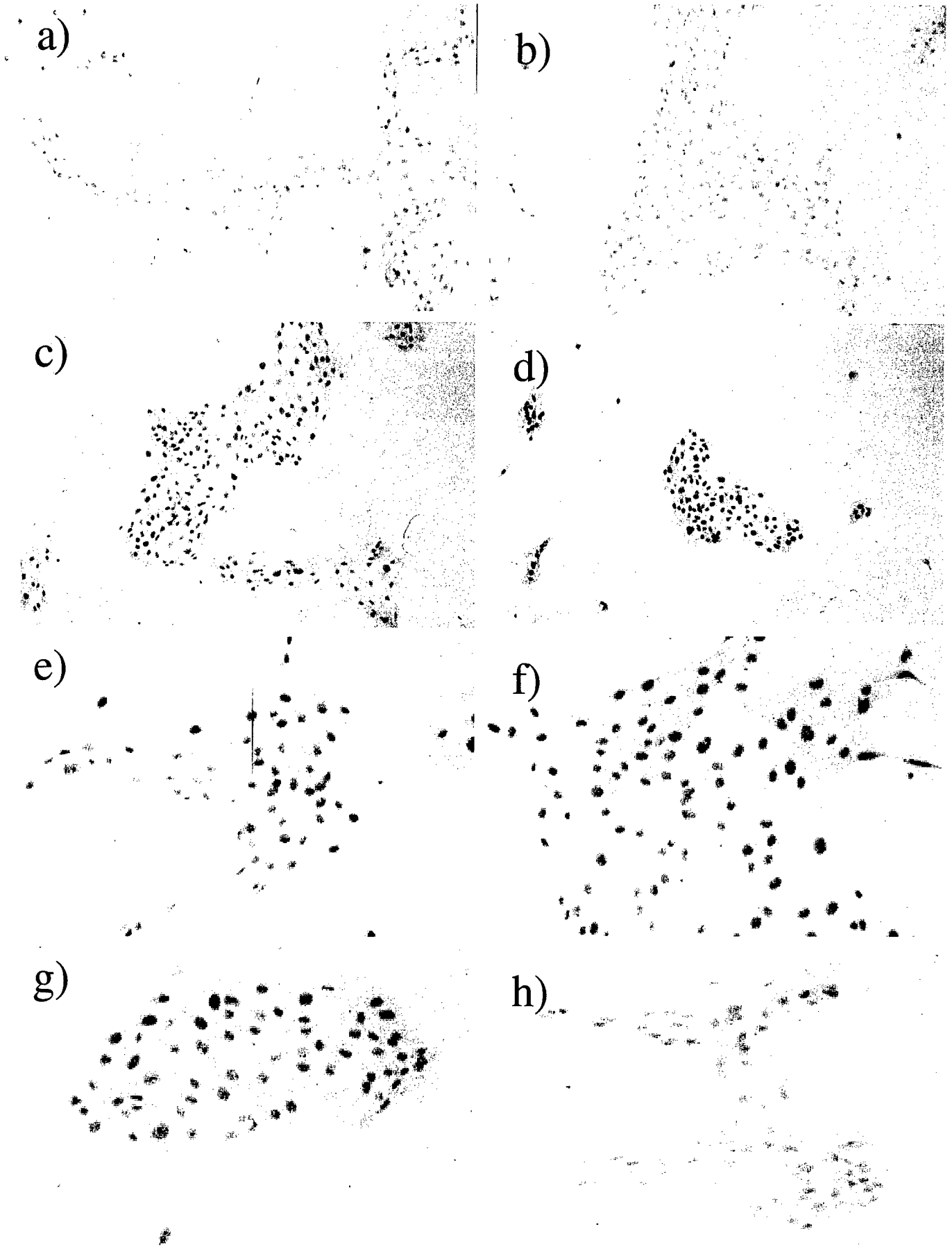
a)
b)
c)
d)
e)
f)
g)
h)

 In preparation

Leptomycin B Stabilizes and Activates p53 in Primary Prostatic Epithelial Cells and induces Apoptosis in the LNCaP Cell line[1]

Philip S. Lecane, Ester M. Hammond, Taija M. Kiviharju, Robert G. Sellers, Amato J. Giaccia and Donna M. Peehl[2]

Departments of Urology (P.S.L., T.M.K., R.G.S. and D.M.P.) and Radiation Oncology (E.M.H. and A.J.G.), Stanford University School of Medicine, Stanford, CA 94305-5118

Running Title: Activation of p53 in Prostatic Epithelial Cells

Key words: p53, Leptomycin B, prostatic epithelial cells, prostate cancer

[1] This work was supported by Department of Army Grant DAMD 17-99-1-9004.

[2] To whom requests for reprints should be addressed, at Department of Urology, Room S275, Stanford University School of Medicine, Stanford, CA 94305-5118, Tel: (650) 725-5531; FAX: (650) 723-0765; e-mail: dpeehl@stanford.edu

[3] Abbreviations used in this paper: LMB, Leptomycin B; HDM2, human homolog of the murine double minute 2 protein; NES, nuclear export signal; MAPK, mitogen activated protein kinase; mAb, monoclonal antibody; EtOH, ethanol; E-PZ-1 and –2, Primary epithelial cells from peripheral zone of prostrate; Gy, Gray; Act D, actinomycin D; hr, hour; GADD45, growth arrest and DNA damage inducible protein 45; ECL, enhanced chemiluminescence.

ABSTRACT

In both transformed and untransformed cells, oncogenic signals and stress-inducing stimuli such as DNA damage result in the stabilization and activation of the tumor suppressor protein p53. Previous studies have suggested that human prostatic epithelial cells derived from normal tissues and adenocarcinomas are defective in their ability to upregulate wild-type p53 after DNA damage induced by ionizing radiation or chemicals. This dysfunctional regulation of p53 may explain both the high frequency of prostate cancer and its resistance to conventional chemotherapeutic intervention. Leptomycin B (LMB) has recently been found to increase both the protein level and transcriptional activity of p53 by interfering with HDM2-dependent nucleocytoplasmic export and subsequent degradation by the proteasome. Experiments presented here demonstrate that treatment of prostatic epithelial cells with LMB leads to post-translational stabilization of p53, activation of downstream target genes and induction of cell cycle arrest. LMB-treatment of LNCaP cells, an established prostatic cancer cell line with wild-type p53, caused apoptosis. Therefore, the ability of LMB to stabilize p53 and induce expression of p53-responsive growth inhibitory genes may be a useful lead in the development of therapeutic small molecules that can modulate p53 function in prostate cancer.

INTRODUCTION

Prostate cancer occurs at an extremely high frequency, with an estimated 180,000 men diagnosed in the US in 1999 alone (1). Cancers predominantly arise in the peripheral zone of the prostate (2), display short-term responsiveness to androgen ablation therapy and are characteristically resistant to chemotherapy (3). Once metastasis has occurred, very few treatment options are available and are of limited efficacy. Despite investigation of the roles of known oncogenes and tumor suppressor genes, only a rudimentary understanding of the molecular events that initiate and drive the progression of this disease exists. As for cancer in general, the long-term goal for the treatment of prostate cancer remains the targeting of tumors via specific therapeutic manipulation of molecules or pathways that could impinge on tumor cell growth or activate cell death.

Previous studies have indicated that normal prostatic epithelial cells and the majority of prostatic adenocarcinomas contain a wild-type form of the tumor suppressor p53 (4). P53 normally responds to different forms of cellular stress by targeting the activation of checkpoint genes that inhibit cell cycle progression [such as cyclin-dependent kinase inhibitor $p21^{WAF1/CIP1}$ (5)], and/or trigger apoptotic cell death [reviewed in (6); (7)]. Stimuli that activate p53 include ionizing and non-ionizing radiation, ribonucleotide depletion, microtubule disruption, hypoxia, oncogenes and chemotherapeutic drugs. Modulation of the p53 molecule is in part achieved by post-translational modifications such as phosphorylation and acetylation which promote the formation of specific interactions with other proteins and target gene regulatory elements [reviewed in (8)]. Loss of p53 activity via mutation, deletion or inactivation by endogenous or viral oncogenes leads to the propagation of DNA damage, resulting in genetic instability.

Levels of p53 are tightly regulated in normal unstressed cells by the human homolog of the murine double minute 2 gene product, HDM2[3]. The *hdm2* gene itself is activated by p53, creating an autoregulatory feedback loop that controls the level of both proteins [reviewed in (9)]. The *hdm2* gene has been found to be overexpressed in several human tumors (10) and contributes to the oncogenic progression of cells, partially through binding the N-terminus of p53 (11). The HDM2 oncoprotein acts as a ubiquitin E3 ligase for p53 (11), triggers the rapid removal of p53 from the nucleus and stimulates the degradation of p53 (12, 13).

Work recently conducted in this laboratory has demonstrated that primary cultures of prostatic epithelial cells do not upregulate p53 protein in response to γ-irradiation or other stresses such as hypoxia and DNA-damaging drugs (14). In the absence of p53 stabilization and activation, transcriptional targets of p53 such as the $p21^{WAF1/CIP1}$ gene were not induced, and prostatic cells did not undergo G_1 cell cycle arrest or apoptosis. Since stabilization of p53 in response to stress stimuli and activation of target genes involved in growth arrest/apoptosis are considered to be central to its role as a tumor suppressor protein, it is plausible that the apparent lack of p53 activation might be the basis for the high incidence of cancer in the prostate (14). Furthermore, since many standard chemotherapeutic agents induce growth arrest or death via p53-mediated pathways, lack of functional p53 could contribute to resistance of prostate cancer to such drugs.

Recently the antifungal antibiotic Leptomycin B (LMB) has been shown to inhibit protein export from the nucleus to the cytoplasm by binding CRM1/exportin 1 (15), a receptor that mediates nuclear export of proteins containing a leucine rich nuclear export signal (NES). LMB blocks the nuclear export of important regulatory proteins such as cyclin B1 (16), mitogen activated protein kinase (MAPK) (17), the catalytic subunit of human telomerase, hTERT (18),

and causes the nuclear accumulation of inactive NF-κB/IκBα complexes (19). The description of an NES in the HDM2 oncoprotein (20), as well as in the p53 protein (21), suggests that the HDM2-directed export of p53 from the nucleus is also mediated by CRM1/exportin (22, 23).

In this study we used LMB to determine if p53 could be stabilized in primary prostatic epithelial cell strains and, if so, whether p53 protein was competent to transcriptionally activate downstream target genes such as $p21^{WAF1/CIP1}$ and HDM2. Treatment with LMB resulted in nuclear accumulation of p53 protein, induction of $p21^{WAF1/CIP1}$ and HDM2, and growth arrest in primary cell strains. LMB-treatment led to apoptotic cell death of a prostate cancer cell line (LNCaP) containing wild-type p53, but had little effect on p53-deficient DU 145 prostate cancer cells. These results suggest that restoration of p53 function in prostatic epithelial cells by LMB may serve as a paradigm for the development of future therapeutic agents for the treatment of prostate cancer.

Materials and Methods

Cell culture. Tissue samples were dissected from radical prostatectomy specimens. None of the patients had received prior chemical, hormonal or radiation therapy. Histological assessment was performed by Dr. John McNeal as previously described (24). Epithelial cells were cultured and characterized as described previously (25). The cell strains used in this study (E-PZ-1 and E-PZ-2) were derived from histologically normal tissue with no evidence of cancer. Prostatic cancer cell lines LNCaP, PC-3 and DU 145 were obtained from the American Type Culture Collection (Rockville, MD). LNCaP and DU 145 cells were cultured in MCDB 105 (Sigma-Aldrich, St Louis, MO) and DME (Gibco-BRL, Grand Island, NY) respectively, containing 10% fetal bovine serum (Gemini Bioproducts, Woodland, CA) and gentamicin. PC-3 cells were cultured in PFMR-4A (25) medium containing 1% fetal bovine serum (Gemini Bioproducts) and gentamicin.

Reagents. Leptomycin B (10 μg/ml stock in ethanol) was a gift from Dr. Minoru Yoshida (University of Tokyo). MG132 and Actinomycin D were obtained from Sigma-Aldrich and Biomol (Plymouth Meeting, PA), respectively.

Immunoblot analysis. Cells were initially washed in ice cold PBS before being scraped off the plate with a rubber policeman. The cells were pelleted and resuspended in UTB buffer (9 M urea, 75 mM Tris-HCl, pH 7.5, 0.15 M 2-mercaptoethanol) and sonicated briefly. The protein concentration was determined by a BioRad assay (Bio Rad, Hercules, CA). Typically, 50 μg of protein were separated on sodium dodecyl sulfate (SDS)-polyacrylamide gels, transferred to PDVF membranes (Osmonics, Westborough, MA) and blocked in phosphate-buffered saline (PBS) with 5% non-fat milk. Proteins were detected with the following antibodies: mouse mAb against p53 (DO-1), polyclonal rabbit anti-$p27^{KIP1}$, polyclonal rabbit anti-$p16^{INK4a}$ and polyclonal

rabbit anti-NFκB (Santa Cruz Biotechnology, Santa Cruz, CA); mouse mAb against $p21^{WAF1/CIP1}$ (Chemicon International Inc., Temecula, CA); and mouse mAb 2A10 to HDM2 [a gift from Dr A. Levine, Princeton University (26)]. Mouse ascites against actin, mouse mAb anti-Rb and anti-keratin 18 were obtained from Sigma-Aldrich, Pharmingen (San Diego, CA) and Biogenex (San Ramon, CA), respectively. Anti species–HRP conjugated secondary antibodies were obtained from Dako and visual detection was performed using the enhanced chemiluminescence (ECL) method (Amersham, Piscataway, NJ). Signals obtained were subjected to desitometric analysis using the UN-SCAN-IT gel digitizing software (Silk Scientific Inc, Orem, UT).

Immunocytochemistry. Cells were grown in chamber slides (Nalge Nunc International, Naperville, IL), fixed with paraformaldehyde, and permeabilized with EtOH. Non-specific binding was blocked with horse serum, and then cells were incubated with primary antibody. After rinsing and incubating with biotinylated secondary antibody (Vector Laboratories, Burlingame, CA), labeling was detected with the ABC reagent (Vector Laboratories) and the chromagen diaminobenzidine. After counterstaining with hematoxylin, the slides were coverslipped and examined microscopically.

Clonal growth assays. Secondary passaged cells were grown to about 50% confluency, then were harvested by trypsinization. Clonal growth assays were initiated by inoculating 500 cells into each 60-mm, collagen-coated dish containing 5 ml of medium. LMB dilutions were made in media and the ethanol concentration was kept constant at 0.01% in control and experimental media. Cells were incubated for either 4 or 24 hr in LMB before being seeded. After incubation in a humidified atmosphere of 5% CO_2/95% air at 37°C for 10 days without feeding, the cells were fixed in 10% formalin and stained with crystal violet (25). An Artek image analyzer (Dynatech, Chantilly, VA) was used to measure the total area of each dish covered by cells,

which is directly proportional to cell number (27). Triplicate dishes were tested for each control and experimental variable, and each experiment was performed twice.

Cell cycle analysis. Cells were harvested with trypsin and fixed by dropwise addition of ice cold 70% EtOH. After 1 hour of fixation, cells were rinsed, then incubated with RNase (50 μg/ml) and stained with propidium iodide (20 μg/ml). Analysis of DNA content was carried out on a FACScan flow cytometer and cell-cycle phase distribution was quantified using Cellfit software.

Northern analysis. Total RNA was extracted from cells with Trizol (Gibco-BRL). After running in agarose gels, the RNA was transferred to Nytran membrane (Schleider and Schnell, Keene, NH) and hybridized with ^{32}P-cDNA probes of full-length human *p53*, *mdm2* (mouse homolog of *hdm2*) and *p21*$^{WAF1/CIP1}$. Equal loading of samples was visualized by staining the 18S rRNA with methylene blue. Blots were visualized and radioactive signals quantitated on a Storm 860 PhosphorImager (Molecular Dynamics, Sunnyvale, CA).

Radiation. Cells at ~ 75% confluency were exposed to γ-irradiation from a ^{137}Cs source at a dose rate of 4 Gray/minute.

Apoptosis. LNCaP and DU 145 cells were inoculated at a density of $2x10^5$ cells/60-mm dish. One day later the medium was changed and cells were treated with various concentrations of LMB (0.2-20μM). Cells treated with diluent (0.1% EtOH) were included as controls. After 24 hr, Hoechst 33342 and propidium iodide (Sigma-Aldrich) were added to the medium at 10 μg/ml and 20 μg/ml, respectively. After incubation for 15 min at 37 C°, 400 cells from each dish were counted using a fluorescent microscope and the proportion of viable and apoptotic cells was determined.

RESULTS

LMB induced accumulation of p53 that localized to the nuclei of primary prostatic cells. We first sought to determine if treatment of primary prostatic epithelial cells with LMB could cause an increase in p53 levels. Western blot analysis using the p53-specific mAb DO-1 demonstrated that p53 protein increased in a time-dependent manner after exposure of primary epithelial cells from the peripheral zone of the prostate (E-PZ-1 cells) to 2 and 20 nM LMB (Figure 1A). The accumulated p53 was found predominantly in nuclei of primary prostatic epithelial cells after 18 hour (hr) of treatment with LMB (2-20 nM) as determined by immunocytochemical analysis (Figure 1B, panels a-d). The abundance and distribution of the nuclear-located retinoblastoma protein, pRb, and the cytoskeletal protein, keratin 18, were not affected by the drug treatment (Figure 1B, panels e-h). These results show that LMB-treatment increased nuclear p53 in prostatic epithelial strains, in accordance with other reports using different cell types (22, 28), without affecting the levels of other proteins not actively exported to the cytoplasm by the CRM1/exportin pathway.

LMB-stabilized p53 activated downstream target gene products. We next investigated the dose-dependency of LMB to stimulate expression of endogenous p53 target genes (*hdm2*, *p21*$^{WAF1/CIP1}$) in primary prostatic epithelial cells (Figure 2). E-PZ-1 cells were incubated with a range of LMB concentrations for 24 hr after which time cell extracts were prepared. A concentration of 1 nM LMB was found to be sufficient to induce p53 accumulation and concomitant increases in HDM2 and p21$^{WAF1/CIP1}$ protein levels (Figure 2). We also found that levels of the p53-regulated pro-apoptotic Bax protein increased with LMB dose in a manner

similar to $p21^{WAF1/CIP1}$ profile (data not shown). No changes in expression of the non- p53-regulated cell cycle inhibitors $p16^{INK4a}$ and $p27^{KIP1}$, or the transcription factor NF-κB, were found after LMB-treatment (Figure 2), suggesting that the elevation of both $p21^{WAF1/CIP1}$ and HDM2 were selective events. Adachi and co-workers (17) have reported that LMB regulates the distribution of p42/44 MAPK (ERK1/2) protein by inhibiting the relocation of nuclear MAPK to the cytoplasm. Their work did not address whether LMB leads to an increase in total MAPK levels, however, we did not detect substantial stabilization of MAPK proteins during our experiments (Figure 2), although it is possible that LMB did cause nuclear accumulation of these proteins. LMB had similar effects on the protein expression of p53 and p53-target genes in the E-PZ-2 primary epithelial cell strain also analyzed (data not shown).

γ-Irradiation did not potentiate LMB-stabilized p53 induction of $p21^{WAF1/CIP1}$. Since LMB enhanced p53 levels in primary cell strains, we next addressed whether irradiation of cells before or after LMB-treatment could further enhance the level and duration of the $p21^{WAF1/CIP1}$ response. Irradiation of cells with LMB-stabilized p53 (after 4hr with LMB) did not increase the extent or duration of $p21^{WAF1/CIP1}$ expression, and irradiation of cells prior to LMB drug treatment also failed to enhance the expression of $p21^{WAF1/CIP1}$ above that of LMB alone (data not shown).

LMB caused p53 accumulation through extension of p53 half-life and increase in mRNA levels. Since western blot analysis with DO-1 demonstrated that p53 protein expression increased in a time-dependent manner after exposure of E-PZ-1 cells to 2 and 20 nM LMB (Figure 2), we next determined the mechanisms involved. Cells were pretreated for 4 hr with 20 nM LMB, 25 μM MG132 or 5 nM Actinomycin D (Act D) and then protein synthesis was

blocked with cycloheximide (40 μM). Cell lysates were prepared after 30, 60 and 120 minutes and subsequently analyzed by western blot for expression of p53. MG132 and Act D treatments were included as controls since p53 is known to be degraded in a ubiquitin-dependent manner by the proteasome, and treatment of cells with the proteasomal inhibitor MG132 leads to increased p53 levels (29). Act D also stimulates p53 accumulation through inhibition of RNA polymerase II at low concentrations (30).

Stabilization of p53 by LMB in primary prostatic epithelial cells was attributable to a post-translational mechanism, as demonstrated by an increase in half-life of the p53 protein (Figure 3A). p53 stabilization also occurred after 4 hr of treatment with MG132 or Act D as expected, whereas irradiation with 8 Gray (Gy) did not upregulate p53 levels (data not shown), as previously reported (14). All three treatments (LMB, MG132 and Act D) stabilized p53 by increasing its half-life to over 1 hr, compared to approximately 30 minutes for p53 in untreated cells.

In addition, Northern blot analysis demonstrated that LMB also increased p53 mRNA levels at 4 and 24 hr after treatment (Figure 3B). In agreement with previous results, irradiation with 6 Gy had little or no affect on the levels of p53 message (14). Induction of $p21^{WAF1/CIP1}$ and *hdm2* transcripts were also detectable after incubation of E-PZ-1 cells with 20 nM LMB at both early (4 hr) and late (24 hr) timepoints (Figure 3B) with $p21^{WAF1/CIP1}$ mRNA levels 3-4 fold above those of the untreated control after 24 hr. Thus, LMB-treatment led to an increase in $p21^{WAF1/CIP1}$ and *hdm2* mRNA due to post-translational stabilization of p53 protein competent in binding and activating the promotors of its target-genes.

LMB-induced p53 expression led to growth arrest and inhibition of clonal growth potential of primary epithelial cells. Considering that $p21^{WAF1/CIP1}$ induction occurred in prostatic epithelial cells after LMB-treatment, we investigated whether these cells underwent cell cycle arrest. Flow cytometric analysis was performed on the E-PZ-1 and E-PZ-2 cell strains that had been incubated in the presence of various concentrations of LMB for 24 hr (Figure 4A). A concentration of 0.5 nM LMB substantially increased the number of cells in G_1 while higher concentrations led to almost 80% of the population arrested in G_1. P53 transcriptional transactivation of the endogenous $p21^{WAF1/CIP1}$ promoter may contribute to the induction of G_1 cell cycle arrest in these cell strains, as the p53-mutant prostate cancer cell line DU 145 (31, 32) did not induce $p21^{WAF1/CIP1}$ or HDM2 or undergo a substantial G_1 arrest in response to LMB (Figure 4B and 5A). LMB-induced growth arrest in prostatic epithelial cells was prolonged, with cells unable to resume proliferation, adopting a senescent-like phenotype as reported by others (28).

In addition, clonal growth assays were performed to assess the proliferative potential of prostatic epithelial cells after exposure to LMB (Figure 4C). E-PZ-1 cells were exposed to various doses of LMB for 4 or 24 hr, then trypsinized and inoculated into medium without LMB. After 10 days, growth was quantified. Treatment with either 2 or 20 nM LMB for 4 hr reduced subsequent clonal growth substantially (to approximately 50% of untreated cells). Cells pretreated with LMB for 24 hr were completely growth inhibited, with little clonal growth at 20 nM. These data would be consistent with the induction of an irreversible growth arrest by LMB at longer time points (33).

LMB-treatment of LNCaP cells caused p53 accumulation and apoptotic cell death. One of the most frequently studied prostatic cancer cell lines is LNCaP, which was derived from a

lymph node metastasis. LNCaP cells contain wild-type p53, which, unlike in primary cells, is rapidly induced after γ-irradiation and can induce $p21^{WAF1/CIP1}$ expression (14). LMB was found to have a potent cytotoxic effect on LNCaP cells, in contrast to primary cells (Figure 5). LNCaP cells treated with LMB induced p53 protein expression at similar doses as in the primary strains, with an associated enhancement of $p21^{WAF1/CIP1}$ expression (Figure 5A) and accumulation in G_1 and G2 phases of the cell cycle (data not shown). However, LNCaP cells underwent dramatic morphologic changes after 24-48 hr of incubation in 2 nM LMB that were indicative of apoptotic cell death (Figure 5B), with the vast majority of cells detached from the culture dish by 48 hr. We used Hoechst/propidium iodide staining to quantitate the level of apoptosis in LNCaP cells after 24 hr in LMB. Doses as low as 0.2 nM LMB were found to cause substantial apoptosis in LNCaP; in contrast, the p53-mutant DU 145 cell line did not undergo significant apoptosis at 20 nM LMB (Figure 5B + C). Upregulation of $p21^{WAF1/CIP1}$ in DU 145 cells was not apparent after treatment with similar concentrations of LMB, suggesting that wild-type p53 function is required for $p21^{WAF1/CIP1}$ expression and/or induction of apoptosis. These data indicate that LNCaP tumor cells are very susceptible to LMB-induced apoptosis that, at least in part, involves p53-dependent mechanisms.

DISCUSSION

Targeting the activation of p53 in tumors that contain the wild-type gene is a promising strategy for future cancer therapies. Commonly used chemotherapeutic agents, which in many cases act by inducing DNA damage, activate cellular pathways that inhibit proliferation and lead to growth arrest or programmed cell death/apoptosis. Although most prostate cancers contain wild-type p53 and proliferate slowly, radiation and chemotherapeutic strategies used to control this disease are relatively ineffective. Previous work performed in this laboratory demonstrated that p53 stabilization and p53-dependent activation of the $p21^{WAF1/CIP1}$ promoter did not occur after γ-irradiation of prostatic epithelial cells or after treatment with DNA damaging drugs (14).

We therefore tested an alternative approach that was previously shown to upregulate p53 in rat (33) and human (28) primary fibroblasts. Reactivation of p53 in prostate cells is an attractive goal as p53 plays a central role in the 1) regulation of genes involved in growth arrest, such as $p21^{WAF1/CIP1}$ and the growth arrest and DNA damage-inducible protein 45 (GADD45), 2) repression of genes associated with survival, i.e., bcl-2, fos (34), and 3) activation of pro-apoptotic genes (fas/apo1, bax and IGF-BP3).

Our analysis of the effect of the nuclear export inhibitor LMB on the expression of p53 in prostatic epithelial cells demonstrated, in agreement with previous reports using other cell types, 1) nuclear accumulation of p53, 2) post-translational stabilization of the p53 protein and 3) induction of specific downstream target genes of p53 (22, 23). We demonstrated induction of $p21^{WAF1/CIP1}$ and HDM2 at both the protein and mRNA level, due to transcriptionally active p53 located in the nuclei of the prostatic epithelial cells. These primary prostatic epithelial cells also underwent growth arrest and eventually adopted a senescent-like phenotype, as reported by

Smart and co-workers (1999). We also tested the possibility that irradiation in combination with LMB could further influence the activity of p53 in prostatic epithelial cells. By inducing p53 stabilization, through LMB-inhibition of nucleocytoplasmic shuttling for 4 hr, and subsequently causing DNA damage by γ-irradiating primary prostatic cells, it was hypothesized that the activity of p53 would be amplified by the DNA damage signal transduction cascade. However, we found no difference in the level of induction or duration of $p21^{WAF1/CIP1}$ or HDM2 proteins when cells were 1) irradiated before or 2) irradiated after LMB addition compared to non-irradiated, LMB-treated cells.

In contrast to the elevation of $p21^{WAF1/CIP1}$, Bax and HDM2, no induction of the GADD45 protein was found after LMB-treatment (data not shown), suggesting that LMB does not elicit a DNA damage response in prostatic epithelial cells. Alternatively, lack of GADD45 induction may be due in part to a primary defect in the DNA damage-sensing machinery that is responsible for activating the p53-signaling cascade. However, it has recently been reported that overexpression of p53 in the absence of a DNA damage signal is insufficient to activate GADD45 (35). Further studies are required to determine if exposure to both LMB and γ-irradiation alters the expression of p53 target genes, such as *Bax* and *GADD45*, in both normal and cancer-derived primary epithelial strains.

Since we demonstrated that LMB inhibited cell cycle progression of prostatic epithelial cells through a G_1 phase cell cycle block, we investigated the responses of prostate tumor-derived cell lines to LMB. The DU 145 prostate cancer cell line does not express wild-type p53, did not upregulate $p21^{WAF1/CIP1}$ and did not undergo a substantial growth arrest in response to LMB. In contrast, LNCaP cells, which contain a wild-type p53 gene, exhibited increased accumulation of p53 protein in response to LMB, with a concomitant increase in $p21^{WAF1/CIP1}$.

Interestingly, low concentrations of LMB (i.e. 2nM) were sufficient to induce a profound cytotoxic effect after 24-48hr. Cell death by apoptosis was not manifested in the p53-mutant cancer cell lines, DU 145 and PC-3, up to 48hr after LMB treatment. Although further work is required, our data indicates that LMB-treatment of advanced prostate tumor-derived results in p53-dependent apoptosis and not p53-dependent growth arrest. Preliminary work with primary epithelial cancer strains has demonstrated that p53 can indeed be stabilized by similar concentrations of LMB that elevate p53 levels in normal epithelial cells. It will be interesting to determine if this upregulated p53 leads to a profound growth arrest or the induction of apoptosis in these cancer-derived cells. Thus, if primary cancer strains display a differential sensitivity to LMB than their normal counterparts then the activation of p53 in an LMB-like fashion could have possible therapeutic applications for the treatment of both primary and metastatic prostate cancer.

The importance of the regulatory mechanisms that influence protein export from the nucleus has recently been emphasized by the finding that $p14^{ARF1}$ (murine $p19^{ARF1}$), identified as an activator of p53 activity, functions as an inhibitor of nuclear export (36). $p14^{ARF1}$ interacts with HDM2, inhibits HDM2-mediated ubiquitination of p53 and causes an increased turnover of HDM2 (37, 38). Since LMB stabilized transcriptionally active p53 in prostatic epithelial cells through inhibition of CRM1-dependent nuclear export, it may be feasible in the future to develop small molecular drugs with low toxicity that specifically inhibit the nuclear export of p53. This would be an effective therapeutic strategy for the treatment of cancers in which p53 is wild-type but aberrantly regulated, as is the case in prostate cancer.

ACKNOWLEDGMENTS. We thank Dr Susannah Green for help with the flow cytometry analysis.

REFERENCES

1. Landis, S. H., Murray, T., Bolden, S., and Wingo, P. A. Cancer statistics, 1999 [see comments], CA Cancer J Clin. *49:* 8-31, 1, 1999.
2. McNeal, J. E. Origin and development of carcinoma in the prostate, Cancer. *23:* 24-34, 1969.
3. Abbas, F. and Scardino, P. T. The natural history of clinical prostate carcinoma, Cancer. *80:* 827-33, 1997.
4. Effert, P. J., McCoy, R. H., Walther, P. J., and Liu, E. T. p53 gene alterations in human prostate carcinoma, J Urol. *150:* 257-61, 1993.
5. el-Deiry, W. S., Tokino, T., Velculescu, V. E., Levy, D. B., Parsons, R., Trent, J. M., Lin, D., Mercer, W. E., Kinzler, K. W., and Vogelstein, B. WAF1, a potential mediator of p53 tumor suppression, Cell. *75:* 817-25, 1993.
6. Giaccia, A. J. and Kastan, M. B. The complexity of p53 modulation: emerging patterns from divergent signals, Genes Dev. *12:* 2973-83, 1998.
7. Jimenez, G. S., Khan, S. H., Stommel, J. M., and Wahl, G. M. p53 regulation by post-translational modification and nuclear retention in response to diverse stresses, Oncogene. *18:* 7656-65, 1999.
8. Colman, M. S., Afshari, C. A., and Barrett, J. C. Regulation of p53 stability and activity in response to genotoxic stress, Mutat Res. *462:* 179-88, 2000.
9. Wu, X., Bayle, J. H., Olson, D., and Levine, A. J. The p53-mdm-2 autoregulatory feedback loop, Genes Dev. *7:* 1126-32, 1993.

10. Oliner, J. D., Kinzler, K. W., Meltzer, P. S., George, D. L., and Vogelstein, B. Amplification of a gene encoding a p53-associated protein in human sarcomas [see comments], Nature. *358:* 80-3, 1992.

11. Honda, R., Tanaka, H., and Yasuda, H. Oncoprotein MDM2 is a ubiquitin ligase E3 for tumor suppressor p53, FEBS Lett. *420:* 25-7, 1997.

12. Haupt, Y., Maya, R., Kazaz, A., and Oren, M. Mdm2 promotes the rapid degradation of p53, Nature. *387:* 296-9, 1997.

13. Kubbutat, M. H., Jones, S. N., and Vousden, K. H. Regulation of p53 stability by Mdm2, Nature. *387:* 299-303, 1997.

14. Girinsky, T., Koumenis, C., Graeber, T. G., Peehl, D. M., and Giaccia, A. J. Attenuated response of p53 and p21 in primary cultures of human prostatic epithelial cells exposed to DNA-damaging agents, Cancer Res. *55:* 3726-31, 1995.

15. Kudo, N., Matsumori, N., Taoka, H., Fujiwara, D., Schreiner, E. P., Wolff, B., Yoshida, M., and Horinouchi, S. Leptomycin B inactivates CRM1/exportin 1 by covalent modification at a cysteine residue in the central conserved region, Proc Natl Acad Sci U S A. *96:* 9112-7, 1999.

16. Toyoshima, F., Moriguchi, T., Wada, A., Fukuda, M., and Nishida, E. Nuclear export of cyclin B1 and its possible role in the DNA damage- induced G2 checkpoint, Embo J. *17:* 2728-35, 1998.

17. Adachi, M., Fukuda, M., and Nishida, E. Nuclear export of MAP kinase (ERK) involves a MAP kinase kinase (MEK)- dependent active transport mechanism, J Cell Biol. *148:* 849-56, 2000.

18. Seimiya, H., Sawada, H., Muramatsu, Y., Shimizu, M., Ohko, K., Yamane, K., and Tsuruo, T. Involvement of 14-3-3 proteins in nuclear localization of telomerase, Embo J. *19:* 2652-61, 2000.

19. Huang, T. T., Kudo, N., Yoshida, M., and Miyamoto, S. A nuclear export signal in the N-terminal regulatory domain of IkappaBalpha controls cytoplasmic localization of inactive NF- kappaB/IkappaBalpha complexes, Proc Natl Acad Sci U S A. *97:* 1014-9, 2000.

20. Roth, J., Dobbelstein, M., Freedman, D. A., Shenk, T., and Levine, A. J. Nucleo-cytoplasmic shuttling of the hdm2 oncoprotein regulates the levels of the p53 protein via a pathway used by the human immunodeficiency virus rev protein, Embo J. *17:* 554-64, 1998.

21. Stommel, J. M., Marchenko, N. D., Jimenez, G. S., Moll, U. M., Hope, T. J., and Wahl, G. M. A leucine-rich nuclear export signal in the p53 tetramerization domain: regulation of subcellular localization and p53 activity by NES masking, Embo J. *18:* 1660-72, 1999.

22. Freedman, D. A. and Levine, A. J. Nuclear export is required for degradation of endogenous p53 by MDM2 and human papillomavirus E6, Mol Cell Biol. *18:* 7288-93, 1998.

23. Lain, S., Midgley, C., Sparks, A., Lane, E. B., and Lane, D. P. An inhibitor of nuclear export activates the p53 response and induces the localization of HDM2 and p53 to U1A-positive nuclear bodies associated with the PODs, Exp Cell Res. *248:* 457-72, 1999.

24. Schmid, H. P. and McNeal, J. E. An abbreviated standard procedure for accurate tumor volume estimation in prostate cancer, Am J Surg Pathol. *16:* 184-91, 1992.

25. Peehl, D. M. Culture of human prostatic epithelial cells. *In:* R. I. Freshney (ed.) Culture of Epithelial Cells, pp. 159-180. New York, NY: Wiley- Liss, Inc., 1992.

26. Chen, J., Marechal, V., and Levine, A. J. Mapping of the p53 and mdm-2 interaction domains, Mol Cell Biol. *13:* 4107-14, 1993.

27. Tsao, M. C., Walthall, B. J., and Ham, R. G. Clonal growth of normal human epidermal keratinocytes in a defined medium, J Cell Physiol. *110:* 219-29, 1982.

28. Smart, P., Lane, E. B., Lane, D. P., Midgley, C., Vojtesek, B., and Lain, S. Effects on normal fibroblasts and neuroblastoma cells of the activation of the p53 response by the nuclear export inhibitor leptomycin B, Oncogene. *18:* 7378-86, 1999.

29. Maki, C. G., Huibregtse, J. M., and Howley, P. M. In vivo ubiquitination and proteasome-mediated degradation of p53 (1), Cancer Res. *56:* 2649-54, 1996.

30. Ljungman, M., Zhang, F., Chen, F., Rainbow, A. J., and McKay, B. C. Inhibition of RNA polymerase II as a trigger for the p53 response, Oncogene. *18:* 583-92, 1999.

31. Chi, S. G., deVere White, R. W., Meyers, F. J., Siders, D. B., Lee, F., and Gumerlock, P. H. p53 in prostate cancer: frequent expressed transition mutations, J Natl Cancer Inst. *86:* 926-33, 1994.

32. Isaacs, W. B., Carter, B. S., and Ewing, C. M. Wild-type p53 suppresses growth of human prostate cancer cells containing mutant p53 alleles, Cancer Res. *51:* 4716-20, 1991.

33. Yoshida, M., Nishikawa, M., Nishi, K., Abe, K., Horinouchi, S., and Beppu, T. Effects of leptomycin B on the cell cycle of fibroblasts and fission yeast cells, Exp Cell Res. *187:* 150-6, 1990.

34. Ginsberg, D., Mechta, F., Yaniv, M., and Oren, M. Wild-type p53 can down-modulate the activity of various promoters, Proc Natl Acad Sci U S A. *88:* 9979-83, 1991.

35. Xiao, G., Chicas, A., Olivier, M., Taya, Y., Tyagi, S., Kramer, F. R., and Bargonetti, J. A DNA damage signal is required for p53 to activate gadd45, Cancer Res. *60:* 1711-9, 2000.

36. Zhang, Y. and Xiong, Y. Mutations in human ARF exon 2 disrupt its nucleolar localization and impair its ability to block nuclear export of MDM2 and p53, Mol Cell. *3:* 579-91, 1999.

37. Pomerantz, J., Schreiber-Agus, N., Liegeois, N. J., Silverman, A., Alland, L., Chin, L., Potes, J., Chen, K., Orlow, I., Lee, H. W., Cordon-Cardo, C., and DePinho, R. A. The Ink4a tumor suppressor gene product, p19Arf, interacts with MDM2 and neutralizes MDM2's inhibition of p53, Cell. *92:* 713-23, 1998.

38. Zhang, Y., Xiong, Y., and Yarbrough, W. G. ARF promotes MDM2 degradation and stabilizes p53: ARF-INK4a locus deletion impairs both the Rb and p53 tumor suppression pathways, Cell. *92:* 725-34, 1998.

separated by SDS-PAGE. After blotting and incubation with the DO-1 mAb specific for p53, ECL signals were subjected to desitometric analysis using the UN-SCAN-IT gel digitizing software. (B) Western blot analysis of p53 levels in E-PZ-1 cells 4 hours after treatment with 6 Gy γ–irradiation, 25μM MG132 or 20 nM LMB. P53 was detected by the DO-1 mAb. (C) Northern blot analysis of E-PZ-1 cells treated with either 6 Gy γ–irradiation or 20 nM LMB. Cells were treated as described and harvested at the indicated times. Total RNA was isolated and subjected to agarose gel electrophoresis. After blotting, full length p53, mdm2 and $p21^{WAF1/CIP1}$ cDNA probes were radiolabeled and used to probe the blot. Blots were visualized and radioactive signals quantitated on a Storm 860 PhosphorImager. This experiment was performed, with similar results being obtained, on two occasions.

Figure 4: LMB induced G_1 cell cycle arrest and loss of growth potential of primary epithelial cell strains. One million cells of E-PZ-1 (A) and the DU 145 cancer line (B) were treated with various doses of LMB for 24 hr before cells were trypsinized and fixed. Cells were stained with 20 μg/ml propidium iodide and analyzed with a FACScan flow cytometer. Cell-cycle phase distribution was quantified using CellQuest and Modfit software (Becton Dickinson). (C) Inhibition of clonal growth by LMB. Cell strain E-PZ-1 was treated with LMB for 4 and 24 hr. Five hundred cells were then seeded in fresh LMB-free medium and allowed to grow for 10 days before staining and counting. Growth in absence of LMB was set at 100%. Each point represents the average of duplicate experiments, with three dishes per point in each experiment, ± SEM. Similar results were obtained with the E-PZ-2 strain.

Figure 5: Effect of LMB on prostate cancer cell lines. (A) 2 and 20 nM LMB induced expression of p53 and $p21^{WAF1/CIP1}$ in LNCaP cells but not in mutant-p53 containing DU 145 cells. DU 145 cells were harvested at 4, 8 and 24 hr after exposure to LMB and the primary prostate strain E-PZ-2 was included as a control. A short ECL exposure was used to display the p53 signal from DU 145. DO-1 reactive p53 was present as a doublet in LNCaP cell, as previously observed in a number of different cell lines. (B) Morphological characteristics of LNCaP and DU 145 cancer cell lines after 48 hr exposure to LMB. Semi-confluent populations of each cell line were grown with or without LMB for 48 hr and examined microscopically. LNCaP cells- Panel (a) untreated control and (b) 2 nM LMB. DU 145 cells- Panel (c) untreated cells and (d) 20 nM LMB. (C) The amount of apoptosis induced in LNCaP and DU 145 cells by 24hr incubation with various doses of LMB was quantified by Hoechst 33258/propidium iodide staining of nuclear DNA. Nuclear morphology was examined and the number of cells with normal and abnormal nuclei was noted for each treatment. Data presented represents the mean (+/- SEM) of 3 separate experiments.

A

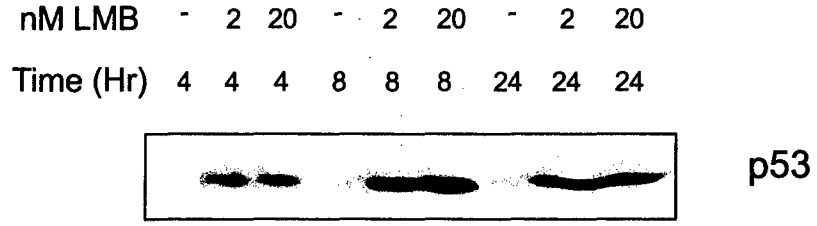

B

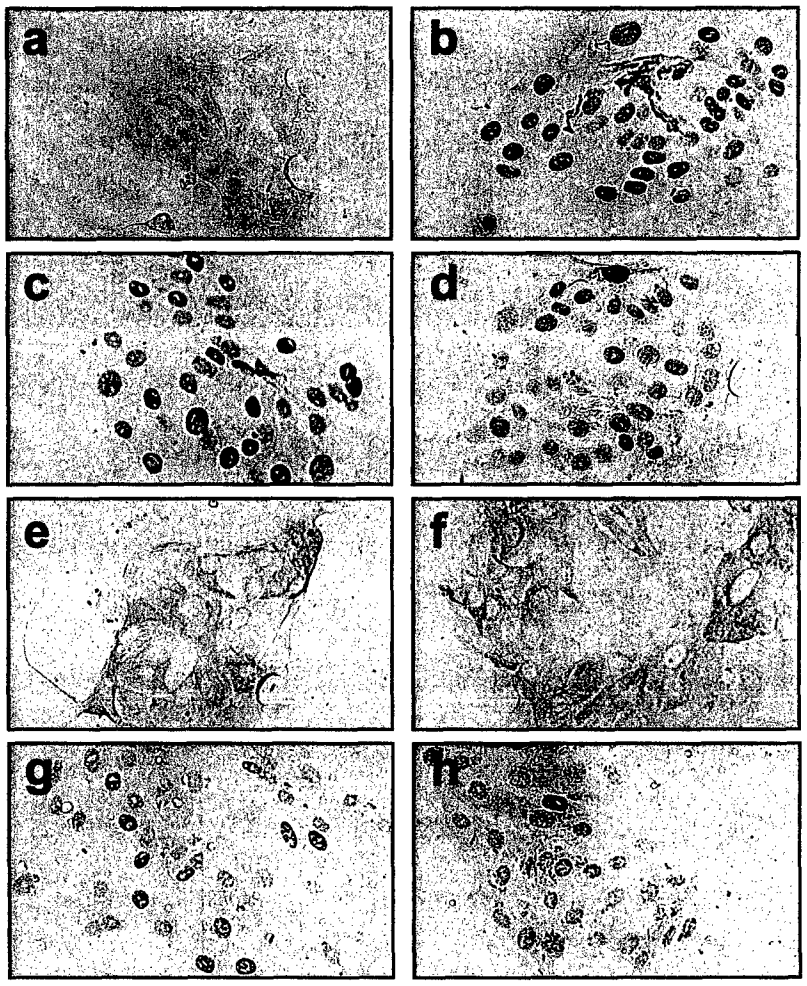

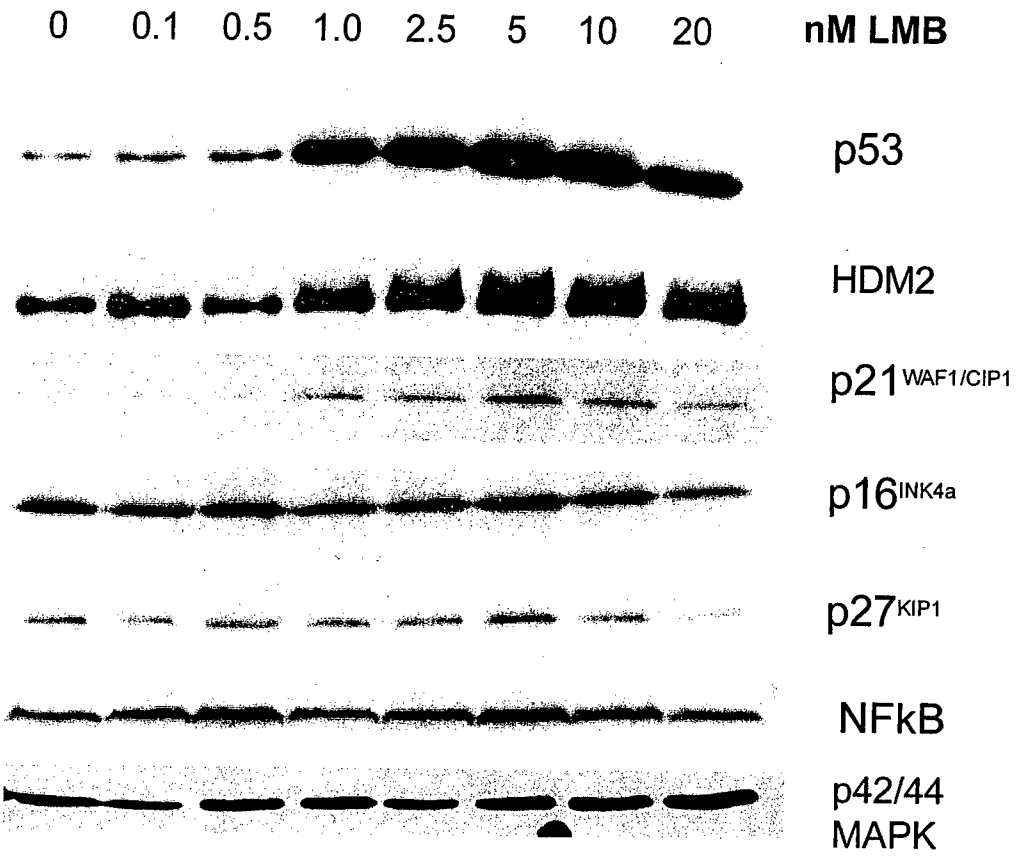
0
0.1
0.5
1.0
2.5
5
10
20
nM LMB
p53
HDM2
p21WAF1/CIP1
p16INK4a
p27KIP1
NFkB
p42/44
MAPK

A

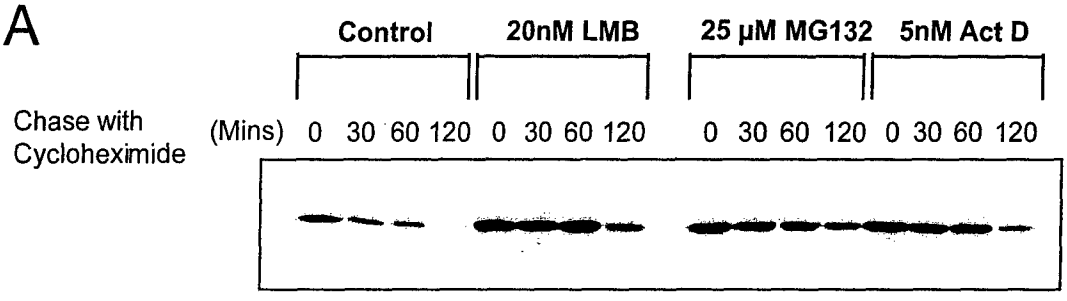
Control
20nM LMB
25 µM MG132
5nM Act D
Chase with Cycloheximide
(Mins) 0 30 60 120 0 30 60 120 0 30 60 120 0 30 60 120

B

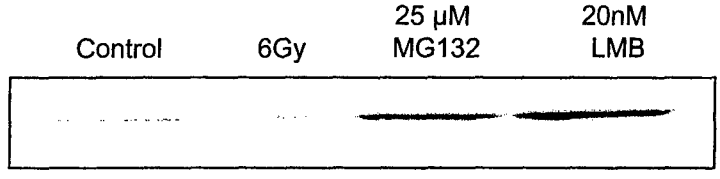
Control
6Gy
25 µM MG132
20nM LMB

C

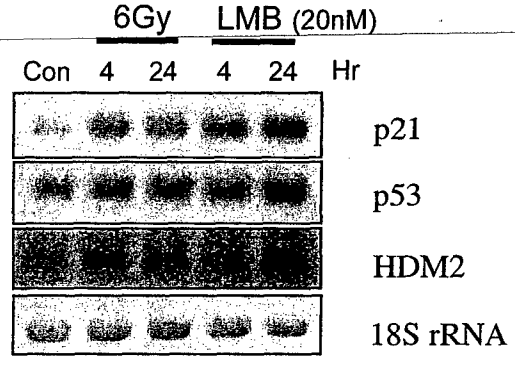
6Gy
LMB (20nM)
Con 4 24 4 24 Hr
p21
p53
HDM2
18S rRNA

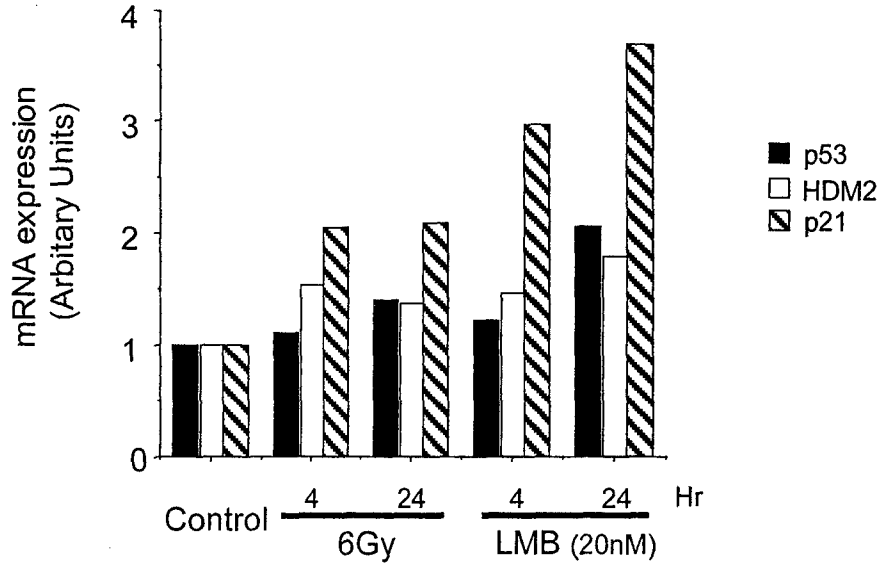
mRNA expression (Arbitary Units)
0
1
2
3
4
p53
HDM2
p21
Control
4 24
6Gy
4 24
LMB (20nM)
Hr

A

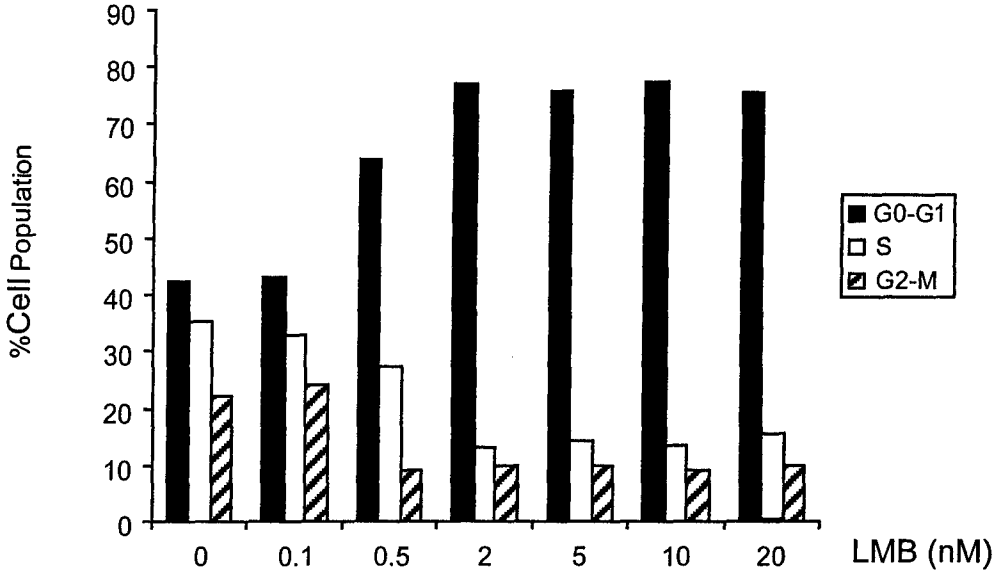
90
80
70
60
50
40
30
20
10
0
%Cell Population
G0-G1
S
G2-M
0
0.1
0.5
2
5
10
20
LMB (nM)

B

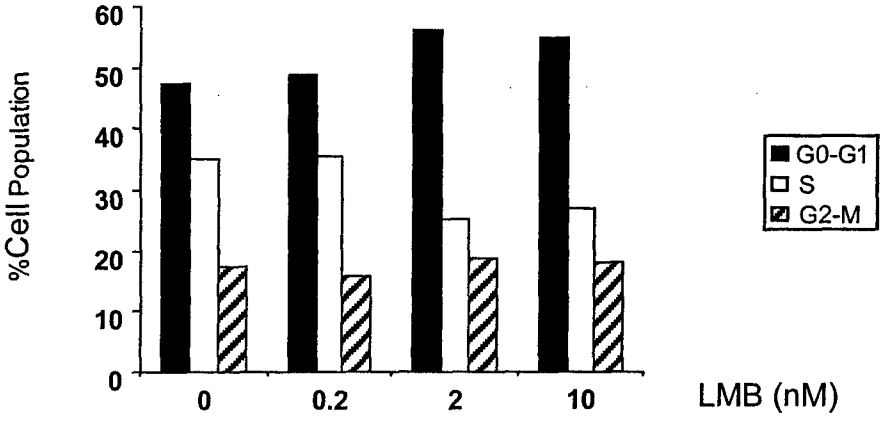
60
50
40
30
20
10
0
%Cell Population
G0-G1
S
G2-M
0
0.2
2
10
LMB (nM)

C

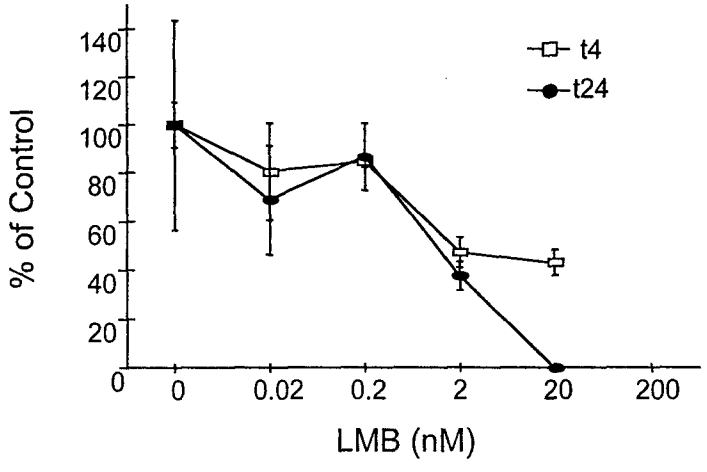
140
120
100
80
60
40
20
0
% of Control
t4
t24
0
0.02
0.2
2
20
200
LMB (nM)

A

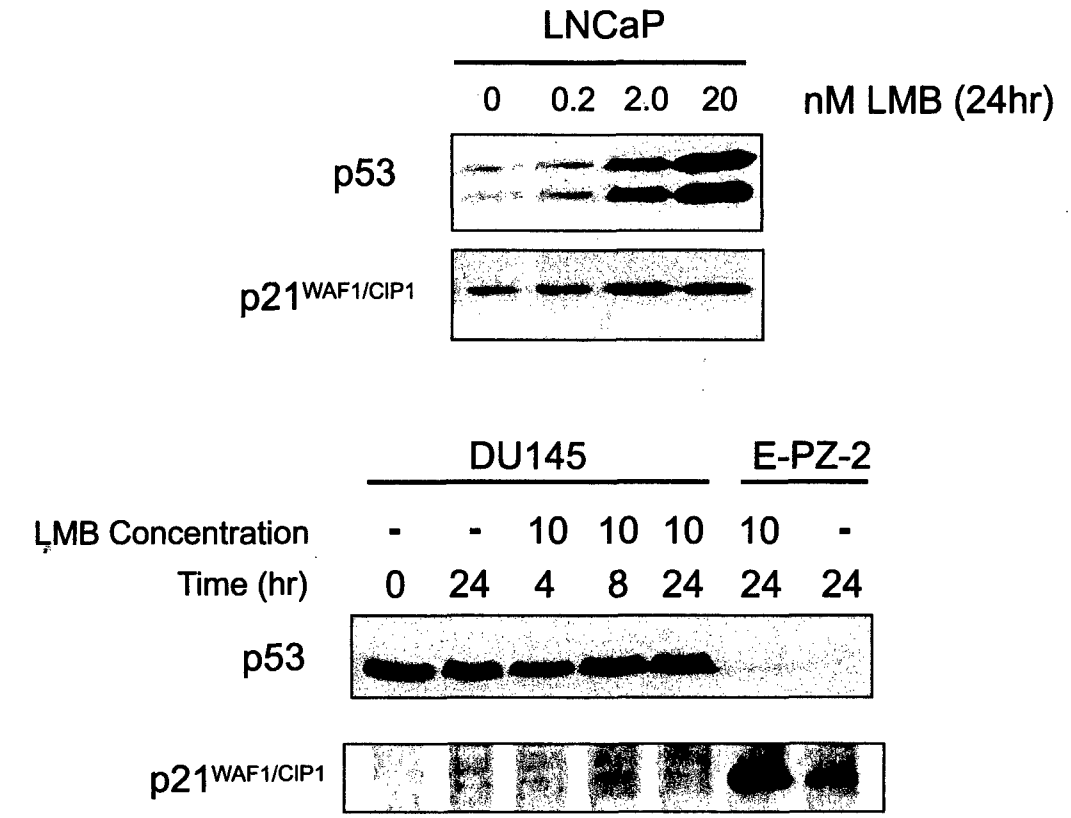
LNCaP
0 0.2 2.0 20
nM LMB (24hr)
p53
p21WAF1/CIP1
DU145
E-PZ-2
LMB Concentration
- - 10 10 10 10 -
Time (hr)
0 24 4 8 24 24 24
p53
p21WAF1/CIP1

B

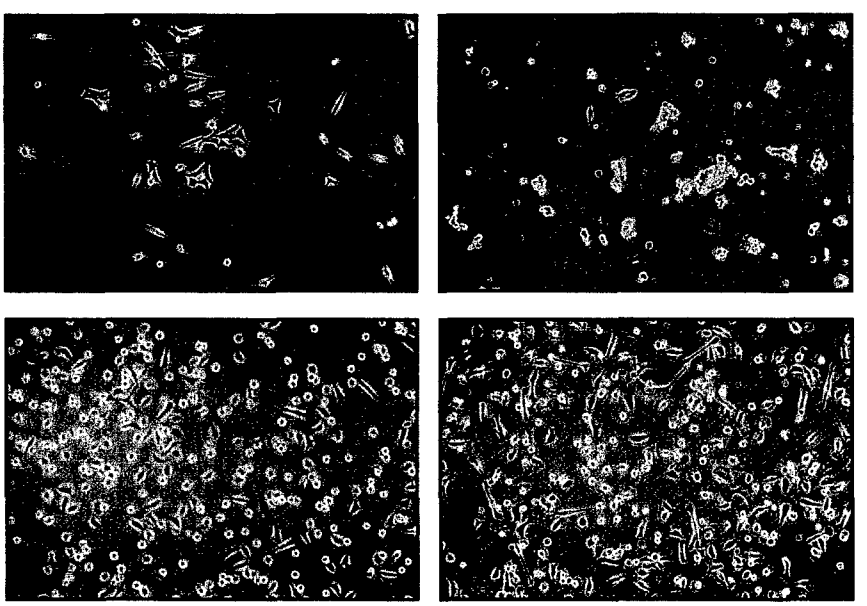

C

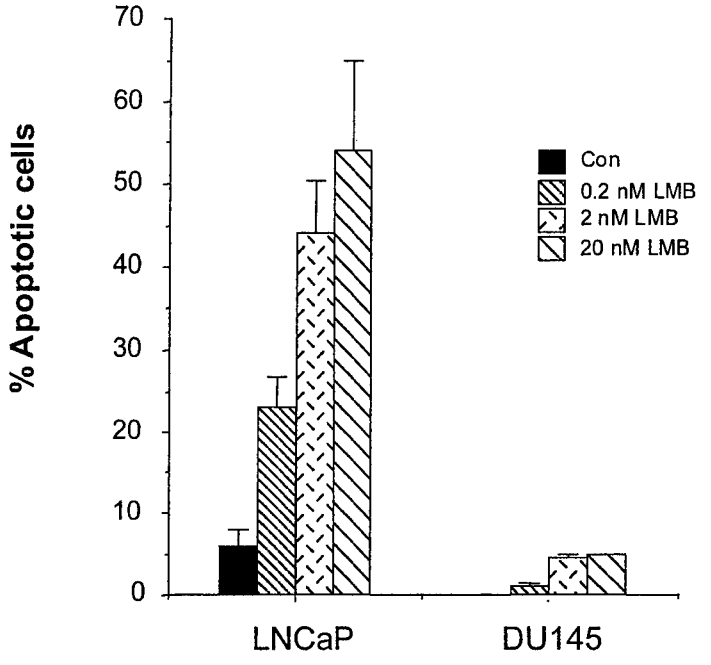
% Apoptotic cells
70
60
50
40
30
20
10
0
Con
0.2 nM LMB
2 nM LMB
20 nM LMB
LNCaP
DU145

Cancer Research

American Association for Cancer Research
Public Ledger Building • Suite 826
150 South Independence Mall West
Philadelphia, PA 19106-3483
Telephone: (215) 440-9300 • Fax: (215) 440-9354

Frank J. Rauscher, III, Ph.D., Editor-in-Chief
Margaret Foti, Ph.D., Managing Editor

July 3, 2001

Dr. Donna M. Peehl
Stanford University School of Medicine
Department of Urology
Room S275
Stanford, CA 94305-5118

RE: MS No. CAN-0814-1
"Leptomycin B Stabilizes and Activates p53 in Primary Prostatic Epithelial Cells and Induces . . ."

Dear Dr. Peehl:

The Editors have completed examination of your above-referenced manuscript. We regret to inform you that it is not acceptable for publication in *Cancer Research*.

Decisions rendered on *Cancer Research* submissions are based on the Editor-in-Chief's overall assessment of all of the information obtained on a manuscript during the review process. In addition to reviewers' comments, such factors as the Associate Editor's recommendation and the priority scores assigned the work are taken into consideration. Only those manuscripts that meet stringent requirements of high scientific quality and significance, originality, and priority can be accepted. Unfortunately, in light of all of the information at the Editor's disposal on this manuscript, he feels that your submission does not meet all of these criteria and, therefore, cannot be accepted.

We regret that we could not render a more favorable decision on your manuscript, but we appreciate the opportunity to review your work, and we would welcome future submissions from you for our consideration.

Sincerely yours,

EDITORIAL BOARD

Margaret Foti /kr

Margaret Foti, Ph.D.
Managing Editor

MF:jr
Enclosures

Reviewer #1

Summary—This paper describes the effects of LMB, an inhibitor of CRM-1 based nuclear export, on induction of p53 responses, cell cycle, and viability of a variety of prostate cancer cell lines. The data confirm previous analyses of other lines that LMB can induce nuclear accumulation of p53, and can activate downstream targets. At certain concentrations and times, LMB can induce cell cycle arrest or apoptosis. LMB was not shown to have such effects in several p53-deficient prostate tumor cell lines, leading to the suggestion that development of p53-specific LMB-type agents might be of therapeutic utility.

Critique: This study recapitulates prior studies in other cell lines, and comes to similar conclusions about the ability of LMB to increase p53 abundance and generate p53 transcriptional and biological responses. Therefore, the only thing that can be said to be really new has to do with the particular cell lines. Although the authors do not state it explicitly, there is a suggestion that the effects of LMB may be dependent on cell lines containing a wild type p53. This inference is based on comparisons of p53 wt and p53-deficient cell lines. Of course, the p53 deficient cell lines are genetically distinct from the p53 wt cell lines, and this, not the p53 status, could cause the difference in LMB response. Clearly, the authors need to inactivate p53 in the p53wt lines, and then assess the effects of LMB, to make such a point. If the authors could show that the effects of LMB on cell viability were dependent on p53, this would significantly add to the strength of the paper. As LMB inhibits the nuclear export of all proteins that require CRM-1 for export. However, the finding that LMB nor only induces p53 nuclear accumulation, but also results in activation of a p53 stress response including enhanced transcription of p21, induction of BAX, apoptosis or senescent-like arrest suggest that LMB IS capable of inducing a damage response, despite the assertion to the contrary because GADD45 is not induced.

Other points:

1. It appears that 20nM LMB results in decreased abundance of p21 and p27. How reproducible was this result? It seems that a good internal standard is needed. What about actin, and some densitometric quantification?

2. The half-life measurement lacks appropriate internal control and quantification, making I difficult to draw a firm conclusion. Why doesn't 6Gy induce p53 in these cells? Are they ARF-?

3. The cell cycle analysis of the p53-deficient prostate cell line in Fig. 4Bshows no apparent change with LMB. However, could this just be a reflection of a dose-response difference since only 10nM LMB was used and the full effect on the p53+ line was observed at about 2nM? Also, if the cells grow at different rates, perhaps a different treatment time needs to be explored.

4. The paper refers to the requirement for MDM2 to export p53 from the nucleus. This is a highly debated point. Indeed, both p53 and MDM2 have NESs, and both were found to be quite weak. Thus, MDM2 will do well to get itself out of the nucleus, let alone cart p53 along with it. Others have shown that the p53 NES is required for its export, whereas MDM2 is not required for p53 nuclear export, except perhaps via ubiquitin mediated destabilization of the p53 tetramer to expose the p53 NES. However, this is still a matter of debate. The authors also finish the discussion with comments on ARF assisting in unclear exit of both MDM2 and p53. This has been shown to be an artifact of expressing ARF at supraphysiologic levels. The authors should endeavor to cite the relevant literature more carefully.

The suggestion to use LMB for therapy has been made before, and specifically by D. Lane with regard to p53 activation. However, it is my understanding that this drug is extremely toxic, and hence would be unlikely to engender a useful therapeutic index.

Reviewer #2

In their manuscript entitled "Leptomycin B Stabilizes and Activates p53 in Primary Prostatic Epithelial Cells and Induces Apoptosis in the LNCaP Cell Line" Lecane et al describe a series of experiments in which they demonstrate stabilization and downstream activities of p53 induced by leptomycin B (LMB) in primary prostatic epithelial cells and in selected prostate cancer cell lines. This is a well written paper in which the authors initially demonstrate that LMB treatment can lead to the stabilization of p53 protein in prostatic epithelial cells and that this in turn leads to transcriptional activation of p21 and HDM2 and growth arrest in primary prostate epithelial cell strains. These experiments, although not conceptually novel, generalize the effects of LMB to primary prostatic epithelial cells. The authors do contribute some new information by carefully documenting that LMB treatment significantly increases p53 half-life and by demonstrating that LMB induces p53 mRNA levels. The authors also demonstrate that relatively low concentrations of LMB can induce cell cycle arrest and apoptosis in LNCaP cells which contain wild-type p53, but not in DU145 prostate cancer cells in which p53 is mutated. This apparently new information shows the capacity of LMB to induce cell death in a specific prostate cancer cell line *in vitro*. Although there is some new and interesting information contributed in the manuscript regarding the mechanism of action of LMB vis-a-vis p53 stabilization and downstream effects, the most interesting contribution, i.e., induction of apoptosis in LNCaP cells, is not further investigated in regard to characterizing the apoptotic response at the molecular level, possibly in direct comparison with primary prostate cancer cell strains which do not undergo apoptosis. Thus, the most interesting novel observation in this paper is limited to a superficial analysis.

Another concern is the lack of discussion regarding the occurrence of p53 mutations in prostate cancer. The authors imply that p53 mutations are, in general, very limited in prostate cancer and thus LMB could be used to activate endogenous p53 contained within prostate cancer cells. However, the authors do not mention or discuss the extensive literature regarding selection for p53 mutations in metastatic prostate cancer. Data from numerous laboratories have documented that mutation frequencies in soft tissue and bone metastases occur at frequencies of approximately 30% and 70%, respectively. Therefore, p53 mutations in metastatic prostate cancer are common and could present a serious obstacle in regard to efficacy of systemically delivered LMB-like molecules.

DEPARTMENT OF THE ARMY
US ARMY MEDICAL RESEARCH AND MATERIEL COMMAND
504 SCOTT STREET
FORT DETRICK, MARYLAND 21702-5012

REPLY TO
ATTENTION OF:

MCMR-RMI-S (70-1y) 26 Nov 02

MEMORANDUM FOR Administrator, Defense Technical Information Center (DTIC-OCA), 8725 John J. Kingman Road, Fort Belvoir, VA 22060-6218

SUBJECT: Request Change in Distribution Statement

1. The U.S. Army Medical Research and Materiel Command has reexamined the need for the limitation assigned to technical reports written for this Command. Request the limited distribution statement for the enclosed accession numbers be changed to "Approved for public release; distribution unlimited." These reports should be released to the National Technical Information Service.

2. Point of contact for this request is Ms. Kristin Morrow at DSN 343-7327 or by e-mail at Kristin.Morrow@det.amedd.army.mil.

FOR THE COMMANDER:

Encl

PHYLLIS M. RINEHART
Deputy Chief of Staff for
Information Management

ADB263708
ADB257291
ADB262612
ADB266082
ADB282187
ADB263424
ADB267958
ADB282194
ADB261109
ADB274630
ADB244697
ADB282244
ADB265964
ADB248605
ADB278762
ADB264450
ADB279621
ADB261475
ADB279568
ADB262568
ADB266387
ADB279633
ADB266646
ADB258871
ADB266038
ADB258945
ADB278624